Coherent comb-matter interaction

TICIJANA BAN

Institute of Physics, Zagreb, Croatia


ITALY
SLOVENIA
Ljubljana
230 km
Zagreb
HUNGARY
Trieste
Udine
Maribor
Cakovec
Varazdin
Koprivnica
Kaposvár
Pécs
Karlovac
Sisak
Osijek
Vukovar
Novi Sad
Rijeka
Pula
Zadar
Split
Dubrovnik
Sarajevo
BOSNIA AND HERZEGOVINA
SERBIA
MONTENEGRO
ALBANIA
Adriatic Sea
CROATIA
National capital
Town, village
Major airport
International boundary
Highway
Road
Railroad
© Nations Online Project

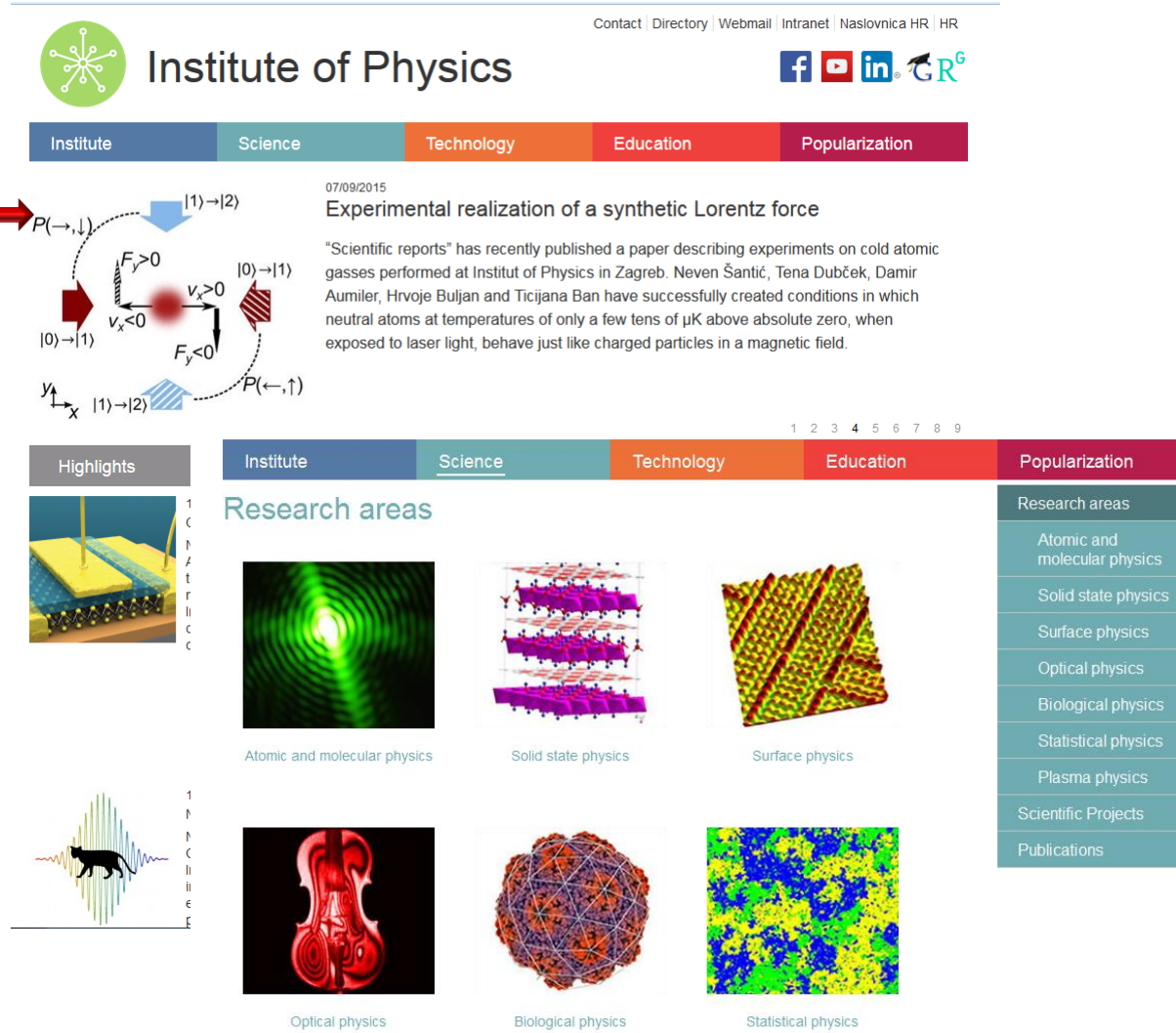
Contact | Directory | Webmail | Intranet | Naslovnica HR | HR
Institute of Physics
Institute
Science
Technology
Education
Popularization
07/09/2015
Experimental realization of a synthetic Lorentz force
"Scientific reports" has recently published a paper describing experiments on cold atomic gasses performed at Institut of Physics in Zagreb. Neven Šantić, Tena Dubček, Damir Aumiler, Hrvoje Buljan and Ticijana Ban have successfully created conditions in which neutral atoms at temperatures of only a few tens of μK above absolute zero, when exposed to laser light, behave just like charged particles in a magnetic field.
1 2 3 4 5 6 7 8 9
Highlights
Research areas
Atomic and molecular physics
Solid state physics
Surface physics
Optical physics
Biological physics
Statistical physics
Plasma physics
Scientific Projects
Publications

Outlook

Part I

1. Time- and frequency-domain description of mode-locked lasers
2. The density-matrix formalism (2-levels and multi-level atom)
3. Accumulation of populations and coherences – model
4. Coherent population trapping (CPT) - model

killing you with theory

Part II

1. Experimental demonstration of the coherence accumulation effects induced by FC with applications – **room temperature vapour**
2. Experimental demonstration of the coherence accumulation effects induced by FC– **cold atoms**
3. Frequency-comb-induced radiative force

make you happy with experiment

PART I

Why fs lasers ?

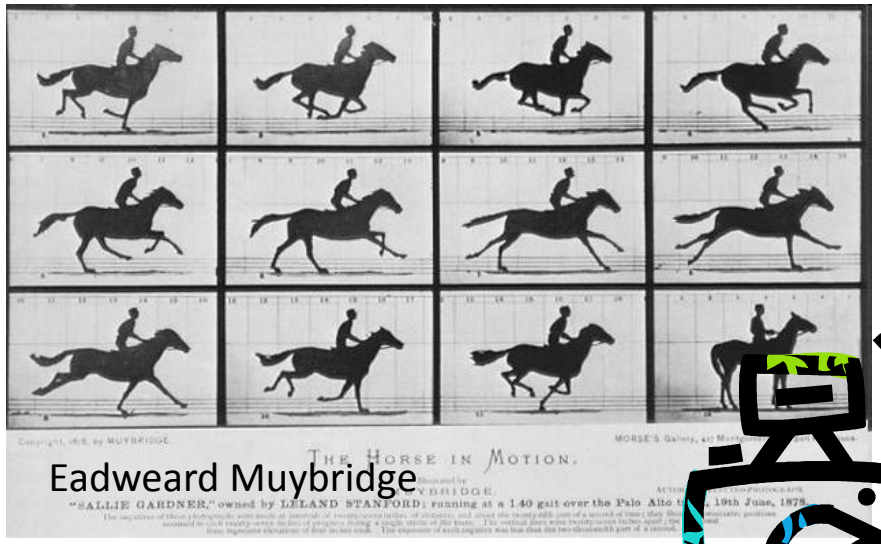

Eadweard Muybridge

- on a logarithmic time scale **one minute is approximately half-way between 10 fs and the age of the universe**
- taking the speed of light in vacuum into account, a **10 fs light pulse can be considered as a 3µm** thick slice of light whereas a light pulse of one second spans approximately the distance between earth and moon
- **the fastest molecular vibrations in nature have an oscillation time of about 10 fs**

To monitor time dynamics !!!

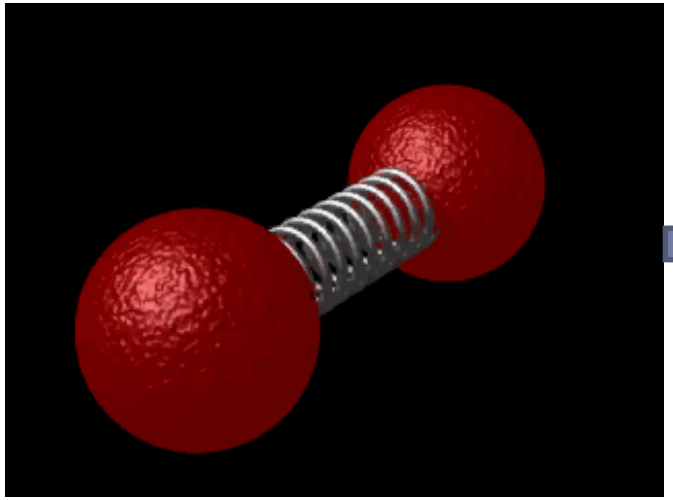

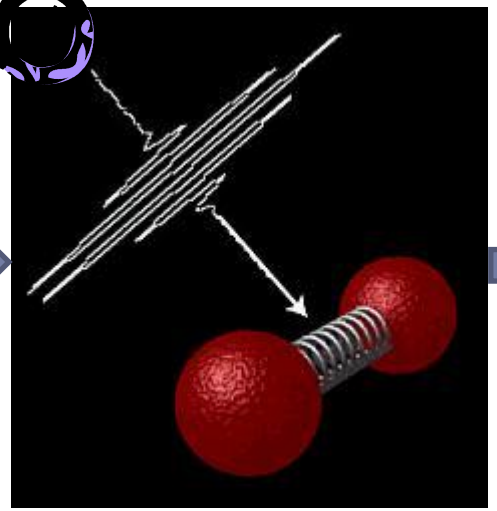

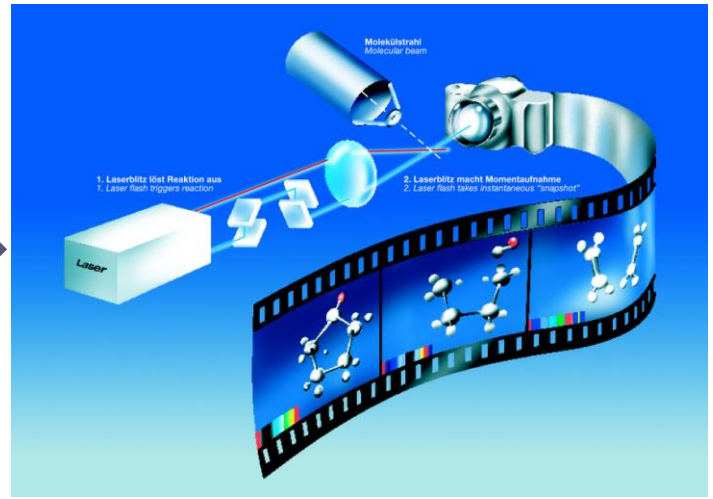

http://www.sciencedaily.com/releases/2008/10/081030144622.htm

Mode-locked lasers generate femtosecond pulses

Single pulse

The temporal and spectral characteristic of the field are related to each other through Fourier transforms.

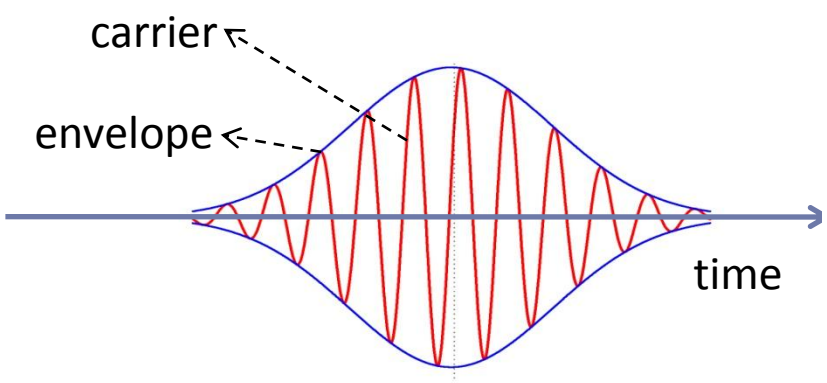

Time domain

$$E(t) = \frac{1}{2\pi} \int_{-\infty}^{\infty} \tilde{E}(\omega) e^{i\omega t} \, d\omega$$

Fourier inversion theorem

$$\tilde{E}(\omega) = \int_{-\infty}^{\infty} E(t) e^{-i\omega t} \, dt$$

Frequency domain

$$\Delta \nu_p \cdot \Delta \tau_p \geq c_B$$

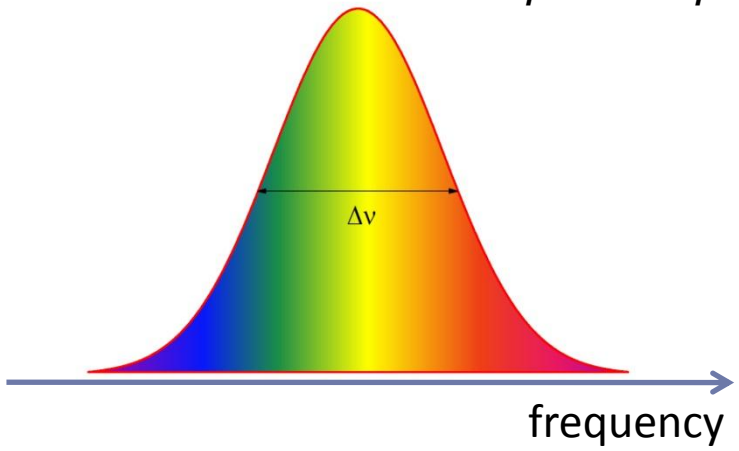

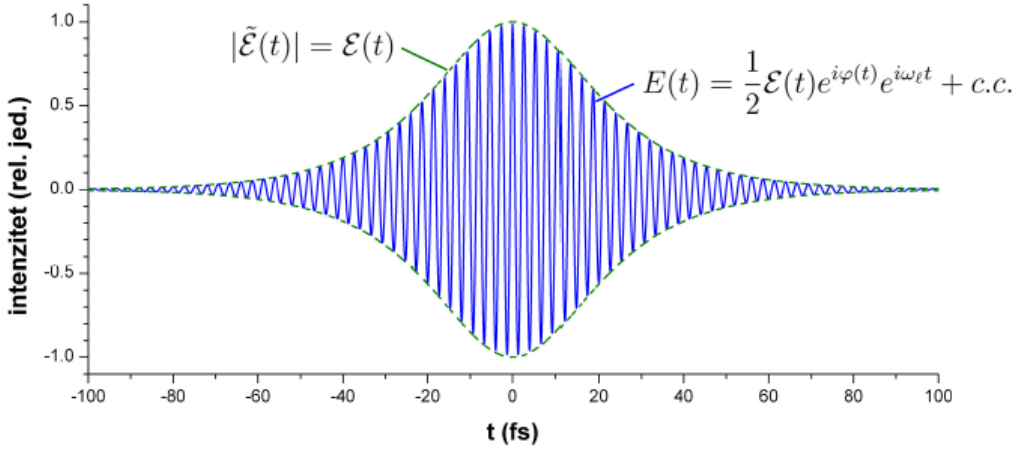

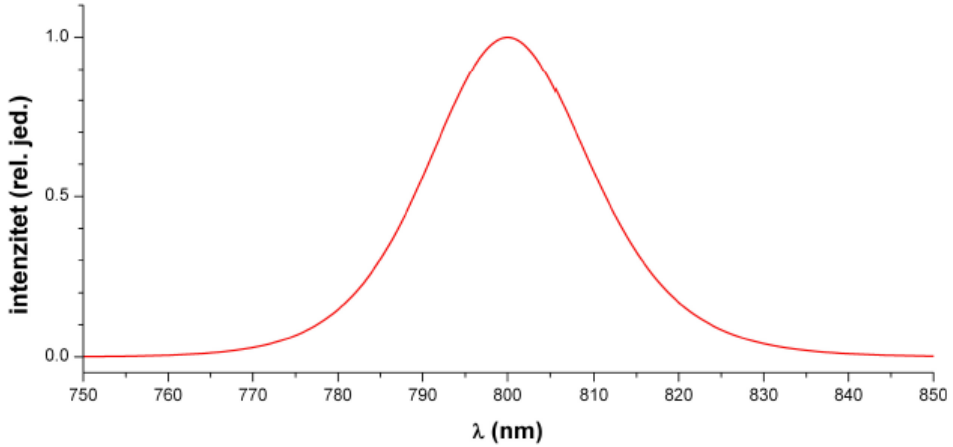

Fourier-limited 10fs pulse from Ti:sapphire oscillator generate spectra of approximatelly 40 THz.

Temporal and spectral intensity profiles of various pulse shape

Table 12.1 Temporal and spectral intensity profiles and time bandwidth products ($\Delta\nu\Delta t \geq K$) of various pulse shape $\Delta\nu$ and Δt are FWHM quantities of the corresponding intensity profiles. The ratio $\Delta t_{\mathrm{intAC}}/\Delta t$, where $\Delta t_{\mathrm{intAC}}$ is tl FWHM of the intensity autocorrelation with respect to background (Sect. 12.3.2), is also given. In the following form las employed in the calculations we set $\omega_0 = 0$ for simplicity.

Gaussian:	$E^+(t) = \frac{E_0}{2} e^{-2\ln 2(\frac{t}{\Delta t})^2}$	$\tilde{E}^+(\omega) = \frac{E_0 \Delta t}{2}\sqrt{\frac{\pi}{2\ln 2}} e^{-\frac{\Delta t^2}{8\ln 2}\omega^2}$,
Sech:	$E^+(t) = \frac{E_0}{2}\mathrm{sech}\left[2\ln\left(1+\sqrt{2}\right)\frac{t}{\Delta t}\right]$	$\tilde{E}^+(\omega) = E_0 \Delta t \frac{\pi}{4\ln\left(1+\sqrt{2}\right)} \times \mathrm{sech}\left(\frac{\pi \Delta t}{4\ln\left(1+\sqrt{2}\right)}\omega\right)$,
Rect:	$E^+(t) = \frac{E_0}{2} \quad t \in \left[-\frac{\Delta t}{2}, \frac{\Delta t}{2}\right]$, 0 elsewhere	$\tilde{E}^+(\omega) = \frac{E_0 \Delta t}{2}\mathrm{sinc}\left(\frac{\Delta t}{2}\omega\right)$,
Single sided Exp.:	$E^+(t) = \frac{E_0}{2} e^{-\frac{\ln 2}{2}\frac{t}{\Delta t}} \quad t \in [0, \infty]$, 0 elsewhere	$\tilde{E}^+(\omega) = \frac{E_0 \Delta t}{2i\Delta t\,\omega + \ln 2}$,
Symmetric Exp.:	$E^+(t) = \frac{E_0}{2} e^{-\ln 2 \frac{t}{\Delta t}}$	$\tilde{E}^+(\omega) = \frac{E_0 \Delta t \ln 2}{\Delta t^2 \omega^2 + (\ln 2)^2}$.

Shape	$I(t)$	$I(\omega)$	$\Delta\nu \cdot \Delta t$	$\Delta t_{\mathrm{intAC}}/\Delta t$
Gaussian	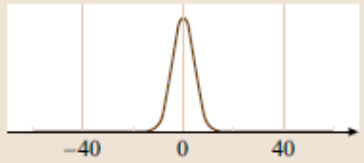	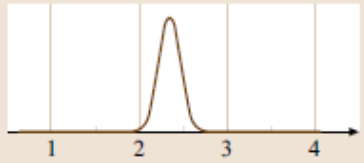	0.441	1.414
Hyperbolic sechant	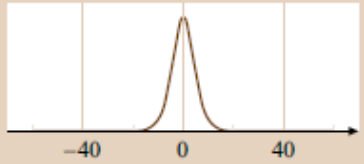	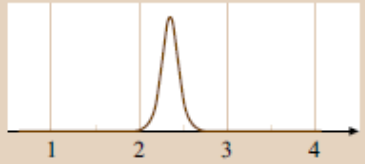	0.315	1.543
Square	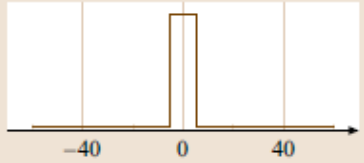	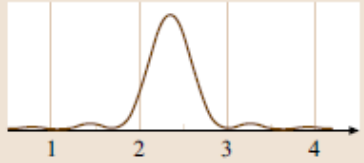	0.886	1.000
Single sided exponential	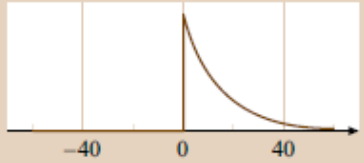	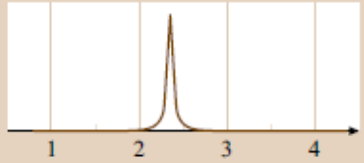	0.110	2.000
Symmetric exponential	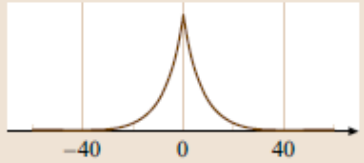	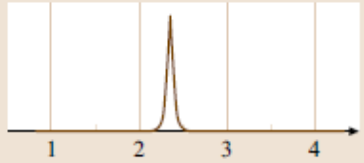	0.142	2.421

Mode – locking: technique for the generation of ultrashort pulses

Electric field of M longitudinal cavity modes :

$$\omega_m = 2\pi\nu_m = \omega_\ell + 2\pi m\Delta \qquad \Delta = \nu_{m+1} - \nu_m = c/(2nL)$$

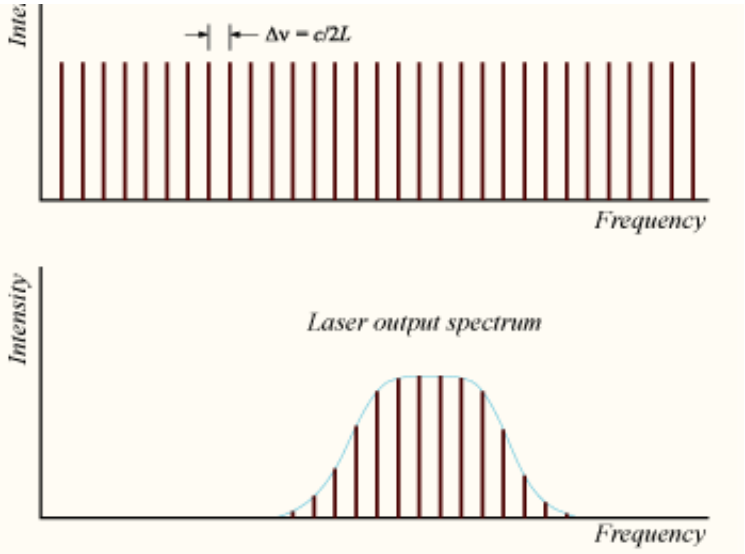

Mode – locking: technique for the generation of ultrashort pulses

$$\tilde{E}^+(t) = \frac{1}{2}\tilde{\mathcal{E}}(t)e^{i\omega_\ell t} = \frac{1}{2}\mathcal{E}_0 e^{i\omega_\ell t} \sum_{m=-(M-1)/2}^{m=(M-1)/2} e^{i(2m\pi\Delta t+\phi_m)}$$

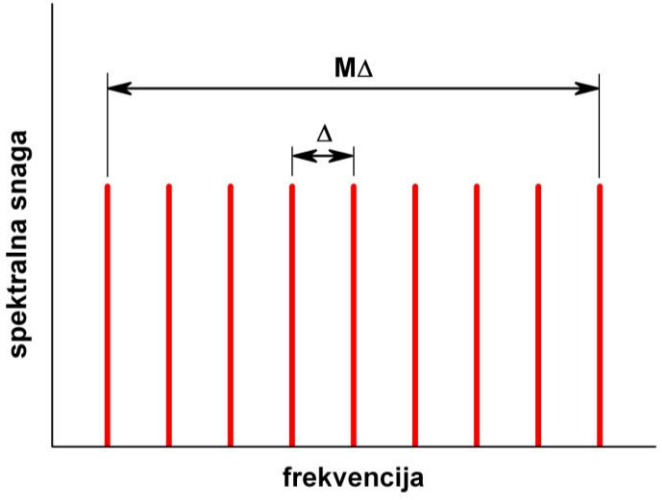

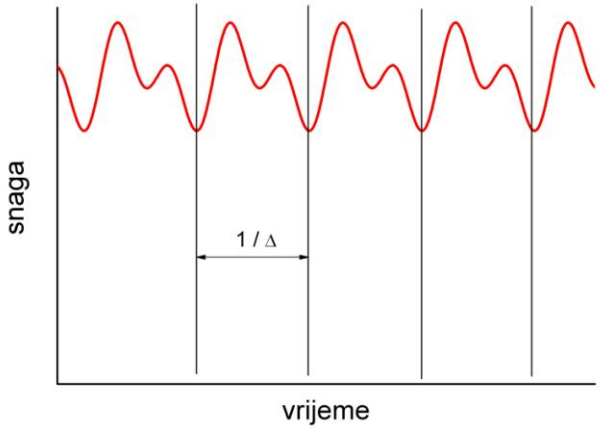

Random phase ϕ_m

- quasi continuous emission

Fixed phase relationship between the modes of laser`s cavity

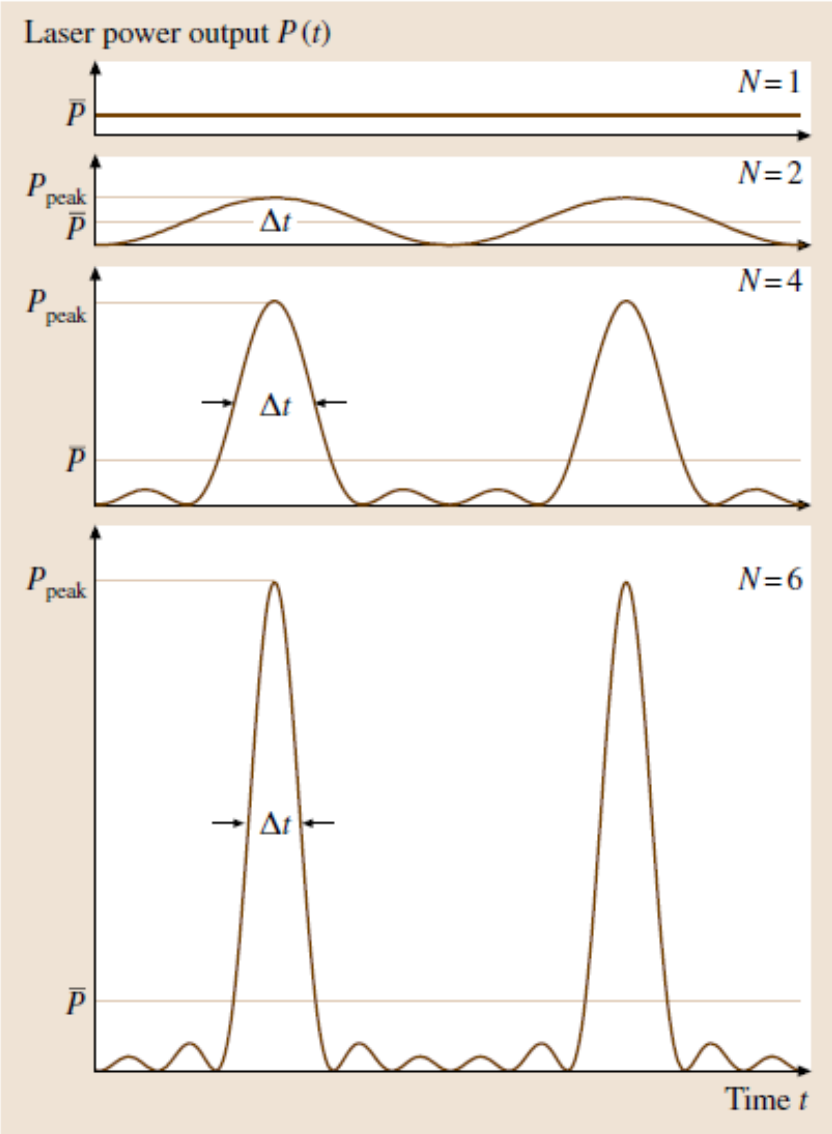

$$\tilde{E}^{+}(t) = \frac{1}{2}\tilde{\mathcal{E}}(t)e^{i\omega_\ell t} = \frac{1}{2}\mathcal{E}_0 e^{i\phi_0} e^{i\omega_\ell t}\frac{\sin(M\pi\Delta t)}{\sin(\pi\Delta t)}$$

- The power is emitted in the form of a train of pulses with a period corresponding to the cavity round-trip time $T_{RT} = 1/\delta\nu$.
- The **peak power P_{Peak} increases quadratically with the number N** of modes locked together: $P_{Peak} = N^2 P_0$.
- The **FWHM pulse duration Δt decreases linearly with the number N** of modes locked together or equivalent is approximately the inverse of the gain bandwidth Δν:

$\Delta t \approx T_{RT} / N = 1 / N\delta\nu = 1/ \Delta\nu$.

M. Wollenhaupt, A. Assion, T. Baumert, Short and Ultrashort Laser Pulses, Springer Handbook of Lasers and Optics pp 1047-1094, 2012.

Output power for different conditions of mode-locking

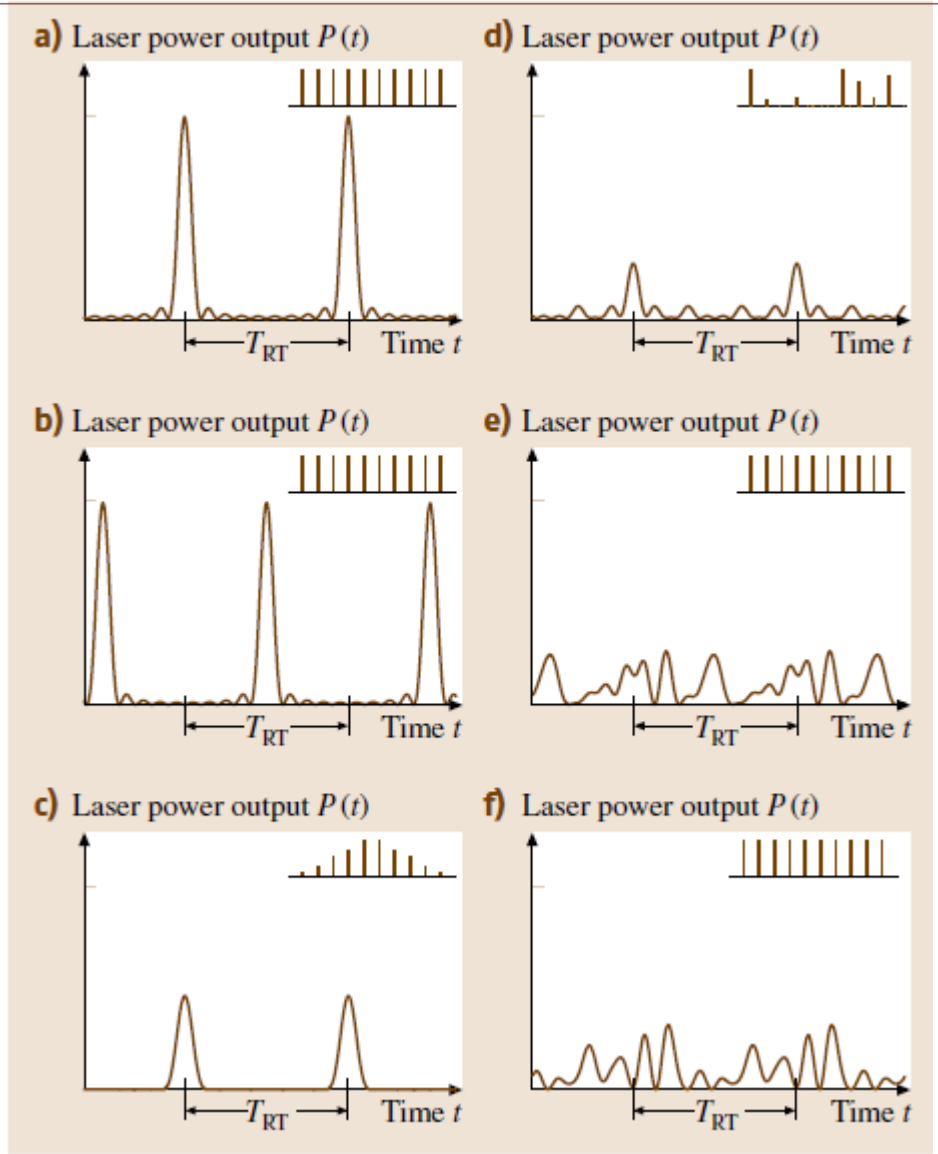

Fig. 12.22a–f Output power for 10 equally spaced modes with different relative amplitudes (as indicated in the *insets*) and phase angles (T_{RT} is the round-trip time): **(a)** linear phase relation $\varphi_n = n\alpha$ amongst the modes (i. e., a constant phase relation between two adjacent modes) with $\alpha = 0$, **(b)** linear phase relation $\varphi_n = n\alpha$ with $\alpha = \pi$, **(c)** Gaussian spectrum with five modes at FWHM and linear phase relation with $\alpha = 0$, **(d)** random spectrum and linear phase relation with $\alpha = 0$, **(e)** constant spectrum and random phase, **(f)** constant spectrum and different random phase

M. Wollenhaupt, A. Assion, T. Baumert, Short and Ultrashort Laser Pulses, Springer Handbook of Lasers and Optics pp 1047-1094, 2012.

From single pulse to multiple pulses: multipulse interference

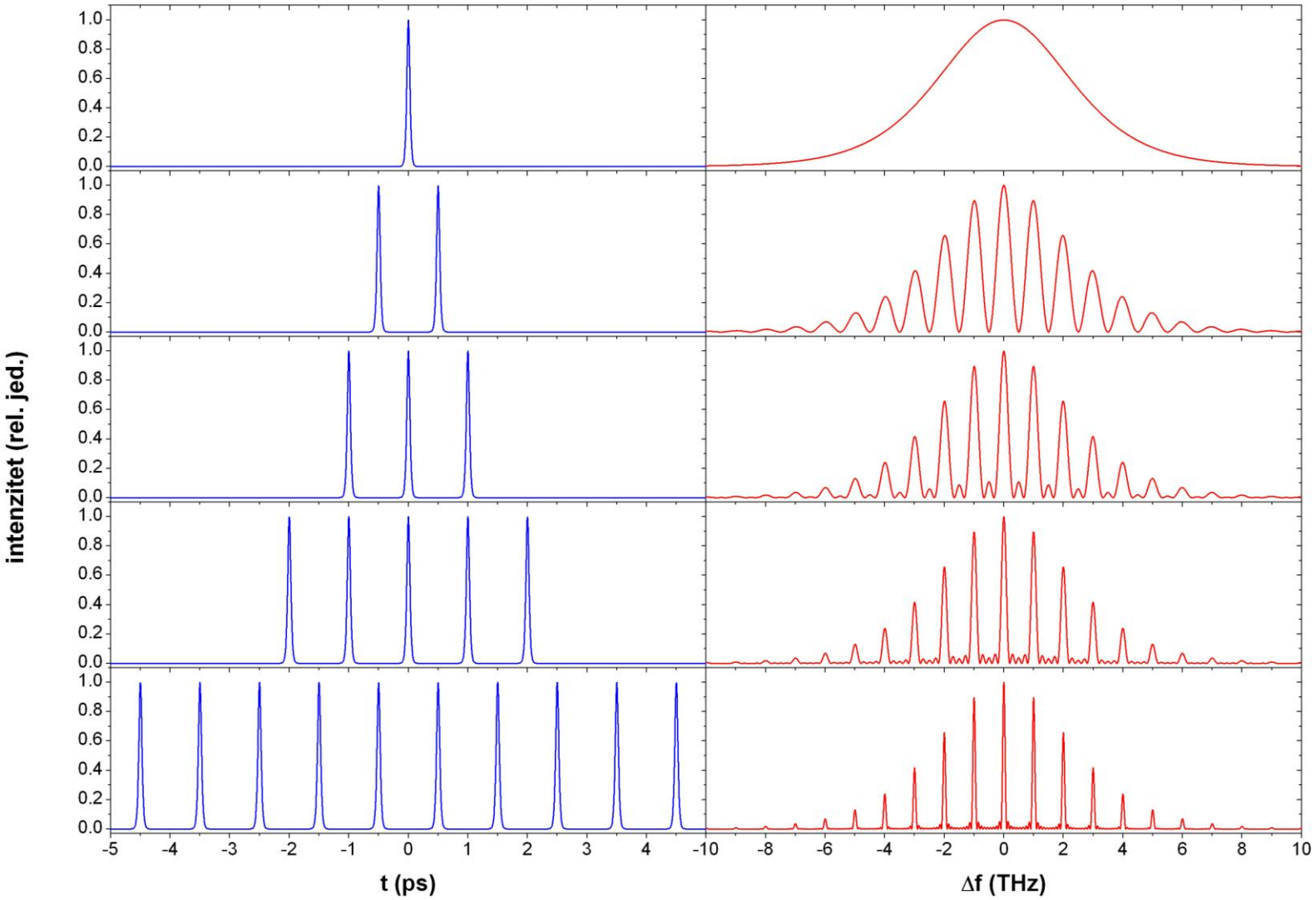

Pulse train in time domain = frequency comb in the frequency domain

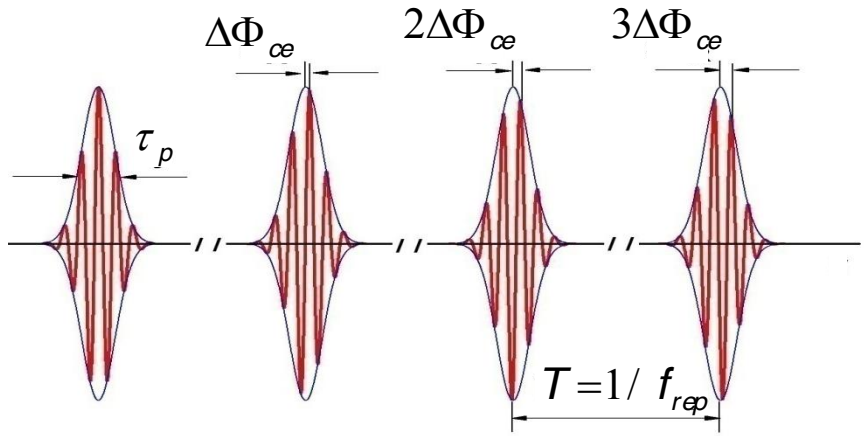

Pulse train in the time domain

Frequency comb in the frequency domain

Frequency combs provide **narrow lines**
over a **wide** (hundreds of terahertz) **spectral bandwidth !**

Measuring and controling comb modes

Time domain

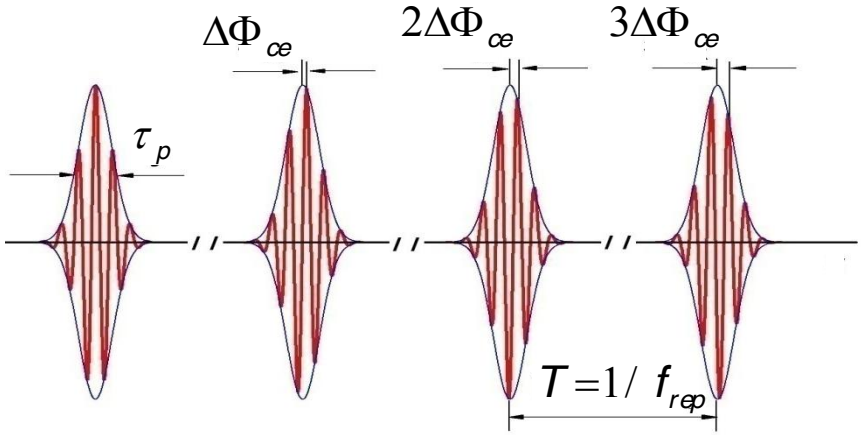

$$E_T(t) = \sum_{n=0}^{\infty}\left[\varepsilon(t-nT)e^{jn\Delta\Phi_{ce}}\right]e^{j\omega_L t}$$

$$\Phi_{ce} = \left(\frac{1}{v_g} - \frac{1}{v_p}\right) l\,\omega \bmod 2\pi$$

Individual comb lines – narrow as a the line of a cw laser.
Regular spacing over the entire bandwidth (better than 1 part in 10^18).
Comb line on the oposite end of the spectrum show negligible phase difference.

Frequency domain

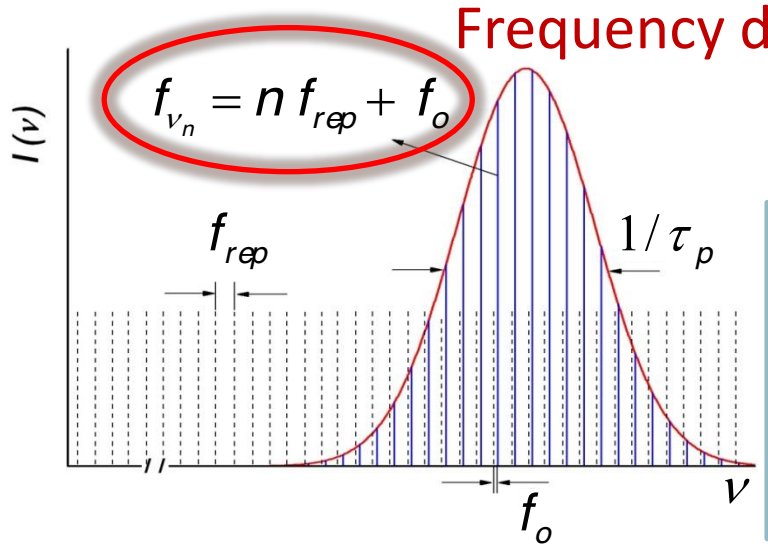

$$f_{rep} = 1/T$$

$$f_o = \frac{1}{2\pi} f_{rep}\Delta\Phi_{ce}$$

By measuring and controlling frep and f0 (rf frequencies) it is possible to control the frequencies of all comb modes (optical frequencies) !

Measuring light

First experiments – FC are used only as rulers and not to directly interrogate the atoms.

fs Comb-Measured Optical Frequencies

• Ca	657 nm	Schnatz – PTB	PRL 1 Jan '96
• C_2H_2	1.5 μm	Nakagawa - NRLM	JOSA-B Dec '96
• Sr^+	674 nm	Bernard – NRC	PRL 19 Apr '99
• In^+	236 nm	v. Zanthier - MPQ	Opt.Comm. Aug'99
• H	243 nm	Reichert - MPQ	PRL 10 Apr '00
• Rb	778 nm	D. Jones - JILA	Science 28 Apr 00
• I_2	532 nm	Diddams - JILA	PRL 29 May '00
• H	243 nm	Niering - MPQ	PRL 12 June '00
• Yb^+	467 nm	Roberts - NPL	PRA 7 July '00
• In^+	236 nm	v. Zanthier – MPQ	Opt. Lett. 1 Dec.'00
• Ca	657 nm	Stenger – PTB	PRA 17 Jan '01
• Hg^+	282 nm	Udem – NIST	PRL 28 May '01
• Ca	657 nm	Udem – NIST	PRL 28 May '01
• Yb^+	435 nm	Stenger – PTB	Opt. Lett.15 Oct '01

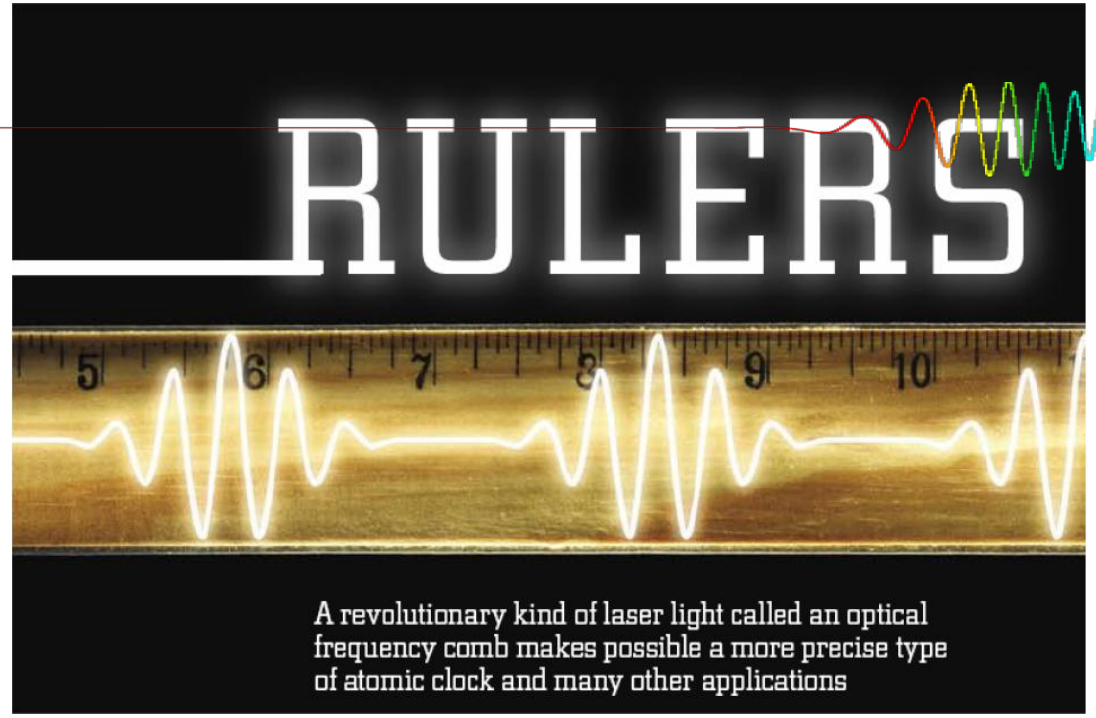

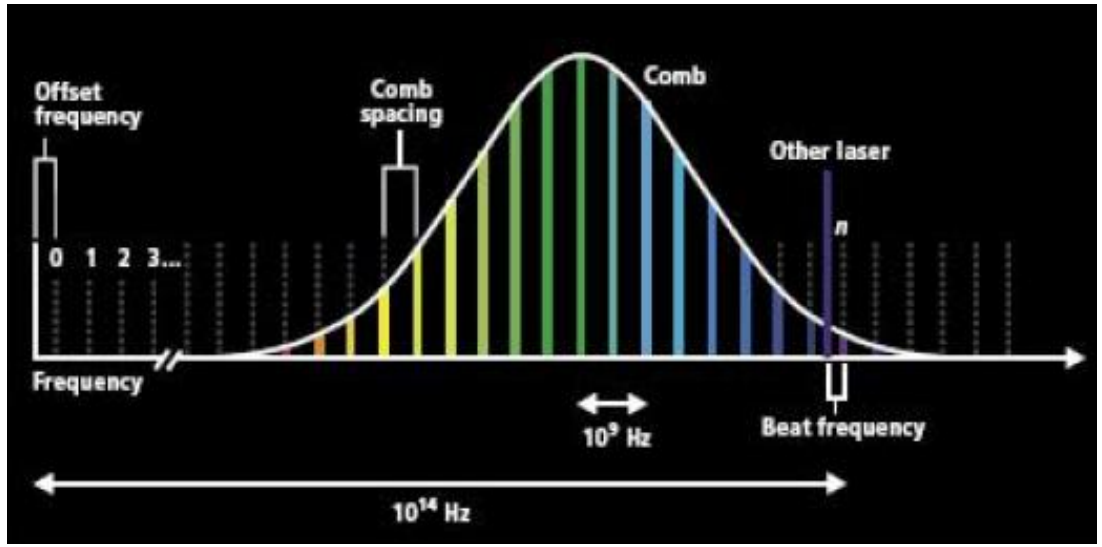

S. Cundiff, j. Ye, J. Hall, Scientific American, April 2008.

Applications of frequency combs

FC combines the advantage of incoherent broadband continua and tunable cw lasers !

May be coupled to an enhanced cavity with high efficiency !

Its spectral coverage may be extendend to regions not not directly attainable from laser sources!

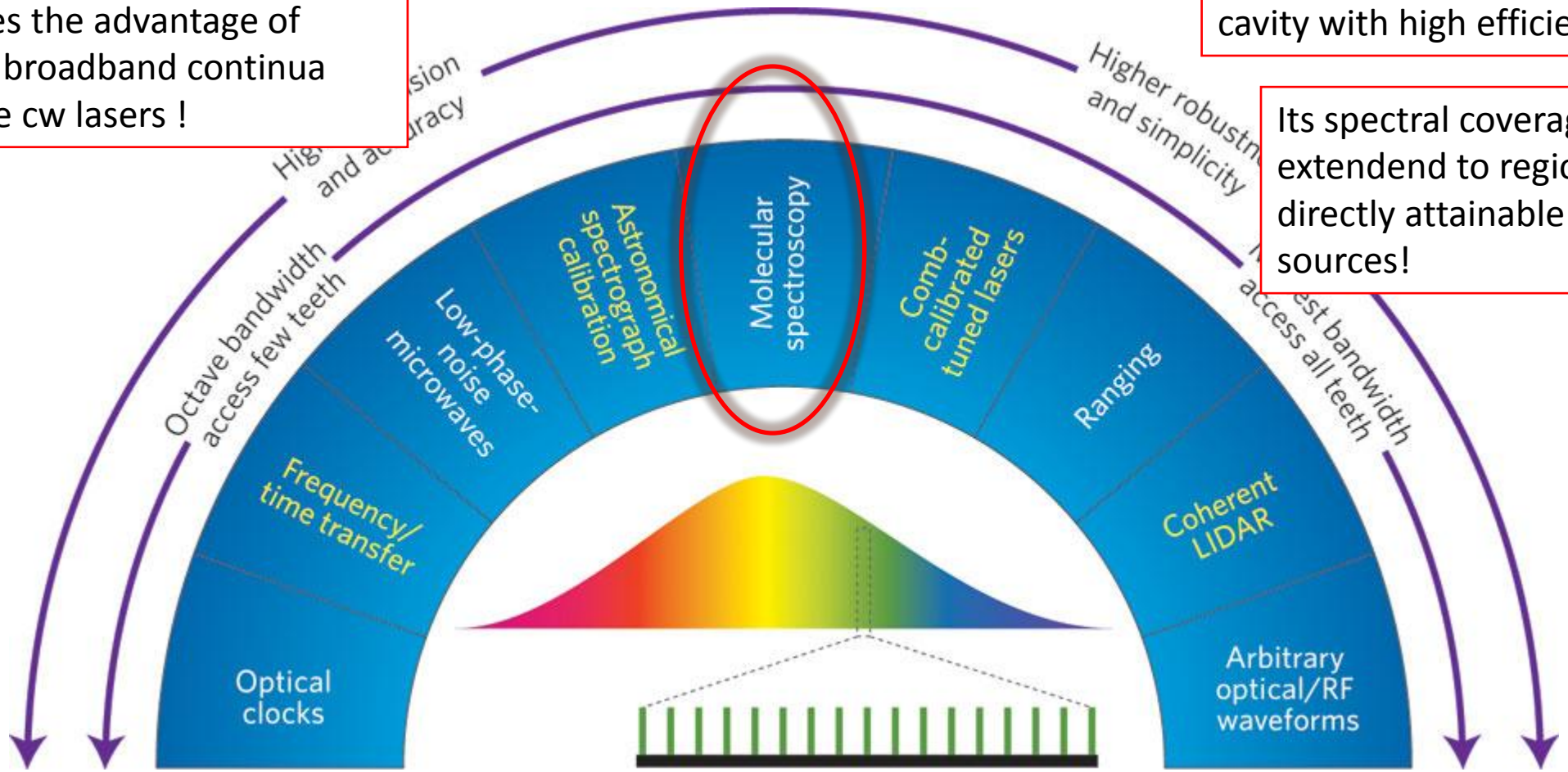

NR Newbury, Nature Photonics **5**, 186 (2011).

Direct frequency comb spectroscopy (DFCS)

DFCS involves using light from a comb of appropriate structure to directly interrogate atomic levels and to study time dependent quantum coherence.

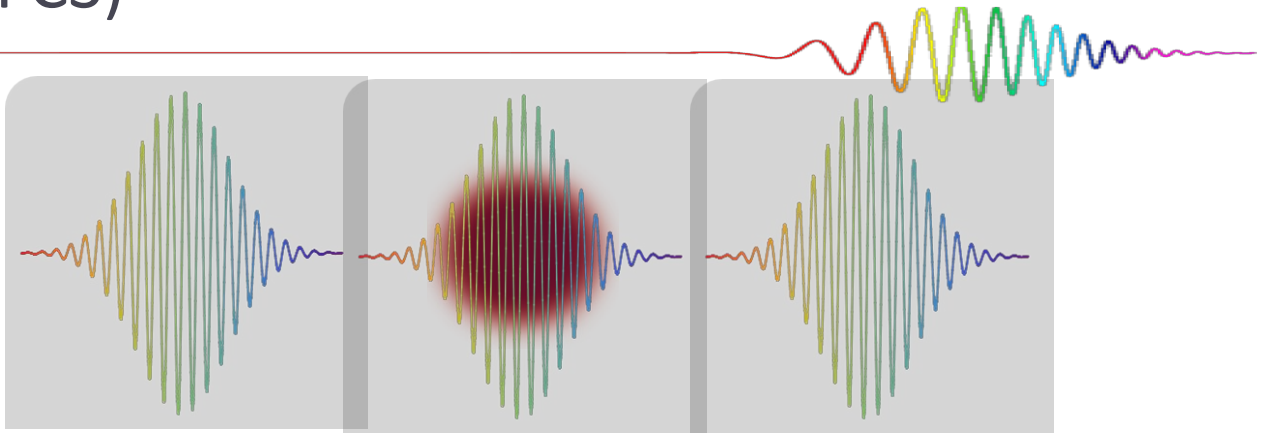

BRIDGING THE FIELDS OF HIGH-RESOLUTION SPECTROSCOPY AND ULTRAFAST SCIENCE

- Multiple atomic states may be simultaneously and directly excited and subsequent dynamics may be probed
- Simultaneously satisfy two-photon as well as one photon condition
- Determination of absolute frequencies for atomic transition anywhere within comb bandwidth
- The entire transition spectrum can be efficiently retrieved by a quick scan of the frep

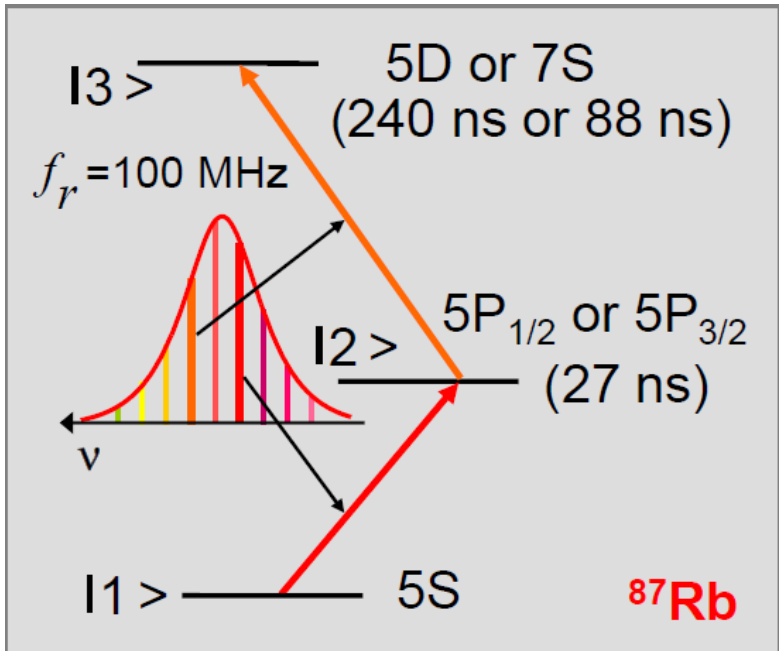

Basic concepts of QM description of an atom

In QM all information about a system in a pure state *s* is stored in the wavefunctio $\psi_s(\mathbf{r},t)$

The time-dependent Schrödinger equation

$$i\hbar\frac{\partial\psi_s(\mathbf{r},t)}{\partial t} = \hat{H}\psi_s(\mathbf{r},t) \rightarrow i\hbar\frac{d}{dt}C_m^s(t) = \sum_n H_{mn}C_n^s(t)$$

$$\hat{H} = \hat{H}_0 + \hat{V}(t)$$

$$\hat{H}_0 u_n(\mathbf{r}) = E_n u_n(\mathbf{r})$$

$$\psi_s(\mathbf{r},t) = \sum_n C_n^s(t)u_n(\mathbf{r})$$

$$H_{mn} = \int u_m^*(\mathbf{r})\hat{H}u_n(\mathbf{r})d^3r$$

total Hamiltonian = free Hamiltonian + interaction energy

eigenfunctions of the free Hamiltonian form a complete set $\int u_m^*(\mathbf{r})u_n(\mathbf{r})\,d^3r = \delta_{mn}$

The expansion coefficient $C^s_n(t)$ gives the probability amplitude that the atom, which is known to be in state *s*, is in energy eigenstate *n* at time t .

The time evolution of $\psi_s(\mathbf{r},t)$ can be specified in terms of the time evolution of each of the expansion coefficient $C^s_n(t)$.

$$i\hbar\sum_n \frac{dC_n^s(t)}{dt}u_n(\mathbf{r}) = \sum_n C_n^s(t)\hat{H}u_n(\mathbf{r})$$

multiply each side from the left by $u_m^*(\mathbf{r})$ and integrate over all space

$$H_{mn} = \int u_m^*(\mathbf{r})\hat{H}u_n(\mathbf{r})\,d^3r$$

$$i\hbar\frac{d}{dt}C_m^s(t) = \sum_n H_{mn}C_n^s(t)$$

$$i\hbar \frac{d}{dt} C_m^s(t) = \sum_n H_{mn} C_n^s(t)$$

EQ entirely equivalent to the Schrödinger equation, but written in terms of the probability amplitudes $C^s_n(t)$.

In experiment – **expetation values** of a set of QM operators
Observable A is associated with the Hermitian operator $\hat{A}$

$$\langle A \rangle = \int \psi_s^* \hat{A} \psi_s d^3 r$$

Dirac notation

$$\langle A \rangle = \langle \psi_s | \hat{A} | \psi_s \rangle = \langle s | \hat{A} | s \rangle$$

$$\langle A \rangle = \sum_{mn} C_m^{s*} C_n^s A_{mn}$$

R. W. Boyd, *Nonlinear Optics Academic Press, San Diego,* 2003.

Matrix element of operator A: $A_{mn} = \langle u_m | \hat{A} | u_n \rangle = \int u_m^* \hat{A} u_n \, d^3 r$

known initial state and the Hamiltonian operator for the system → a complete description of the time evolution of the system and of all of its observable properties.

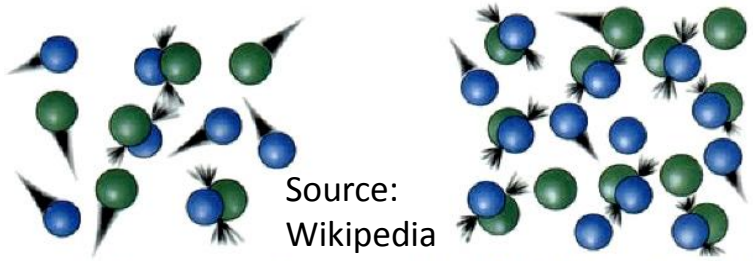

Source: Wikipedia

Low concentration = Few collisions High concentration = More collisions

the state of the system is not known in a precise manner

→ **the initial state of each atom is not known**

↓

Use **density matrix formalism** to describe the system in a statistical sense.

The density matrix formalism

The state of the system can be described by the density operator $\boldsymbol{\rho}$ $\longrightarrow$ $\rho_{nm} = \sum_s p(s) C_m^{s*} C_n^s$

the probability that the system is in the state *s*

statistical mixtures – consequence of incomplete preparation of the system, or partial detection of the final state (spontaneous emission, collisions,...)

- diagonal elements $\boldsymbol{\rho_{mm}}$ –
  the probabilities for the atom to be in state ***m*** – between 0 and 1
- off-diagonal elements $\boldsymbol{\rho_{mn}}$ –
  coherences between states ***m*** and ***n***
  will be nonzero only if the system is in a coherent superposition of energy eigenstate n and m.
  depend on the phase difference between C_m and C_n

- eliminates the arbitary overall phase
- establish a more direct connection with observables
- powerful method for doing calculations
- it can handle pure states as well as mixed states
- it can treat effects such as collisional broadening

$$\overline{\langle A \rangle} = \sum_{nm} \rho_{nm} A_{mn} = \sum_n (\hat{\rho}\,\hat{A})_{nn} \equiv \mathrm{tr}(\hat{\rho}\,\hat{A})$$

the expectation value of any observable quantity can be determined straightforwardly in terms of the density matrix

$$\frac{d\rho_{nm}}{dt} = \sum_s \frac{dp(s)}{dt} C_m^{s*} C_n^s + \sum_s p(s) \left(C_m^{s*} \frac{dC_n^s}{dt} + \frac{dC_m^{s*}}{dt} C_n^s \right) \longrightarrow \frac{d\rho_{nm}}{dt} = \sum_s p(s) \frac{i}{\hbar} \sum_\nu (\rho_{n\nu} H_{\nu m} - H_{n\nu} \rho_{\nu m})$$

Time evolution of the density operator

$$\boxed{\frac{d\rho_{nm}}{dt} = \frac{i}{\hbar} (\hat{\rho}\,\hat{H} - \hat{H}\,\hat{\rho})_{nm} = \frac{-i}{\hbar} [\hat{H}, \hat{\rho}]_{nm}}$$

Optical Bloch equations (OBE)

DMF - describes how the density matrix evolves in time as the result of interactions that are included in the Hamiltonian. However there are certain interactions (for example collisions between atoms) that cannot conveniently be included in a Hamiltonian description. Such interactions can lead to a change in the state of the system, and hence to a nonvanishing value of dp(s)/dt . We include such effects in the formalism by **adding phenomenological damping terms to the equation of motion**.

TIME EVOLUTION OF THE COHERENCES

$$\frac{d\rho_{nm}}{dt} = \frac{-i}{\hbar}[\hat{H},\hat{\rho}]_{nm} - \gamma_{nm}\rho_{nm}, \qquad n \neq m,$$

TIME EVOLUTION OF THE POPULATIONS

$$\frac{d\rho_{nn}}{dt} = \frac{-i}{\hbar}[\hat{H},\hat{\rho}]_{nn} + \sum_{E_m>E_n} \Gamma_{nm}\rho_{mm} - \sum_{E_m<E_n} \Gamma_{mn}\rho_{nn}$$

DECAY OF THE EXCITED STATE POPULATIONS

$$\Gamma_n = \sum_{n'\,(E_{n'}<E_n)} \Gamma_{n'n} \qquad \tau_n = 1/\Gamma_n$$

DECAY OF THE COHERENCES

$$\gamma_{nm} = \tfrac{1}{2}(\Gamma_n + \Gamma_m) + \gamma_{nm}^{(\mathrm{col})}$$

the dipole dephasing rate due to processes (such as elastic collisions) that are not associated with the transfer of population

$\hat{H} = \hat{H}_0 + \hat{H}_{int}$ total hamiltonian

$(H_{int})_{nm} = -\mu_{nm}E(t)$ interaction of the atom

μ_{nm} dipole moment of the ellectronically allowed transition $(F_g \rightarrow F_g, F_g \pm 1)$

slowly varing envelopes

$$\mathcal{E}(t) = E(t)e^{-i\omega_L t} \qquad \sigma_{nm} = \rho_{nm}e^{-i\omega_L t}$$

Two-level atom: example

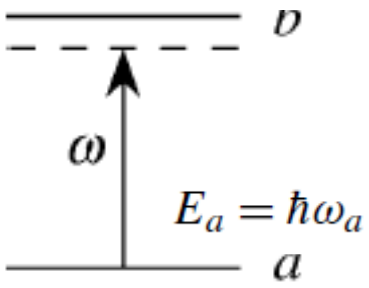

The wavefunction describing state s $\psi_s(\mathbf{r}, t) = C_a^s(t)u_a(\mathbf{r}) + C_b^s(t)u_b(\mathbf{r})$

$$\begin{bmatrix} \rho_{aa} & \rho_{ab} \\ \rho_{ba} & \rho_{bb} \end{bmatrix} = \begin{bmatrix} \overline{C_a C_a^*} & \overline{C_a C_b^*} \\ \overline{C_b C_a^*} & \overline{C_b C_b^*} \end{bmatrix}$$

the density matrix describing the atom

$$\rho_{ba} = \rho_{ab}^*$$

$$\hat{\mu} \Rightarrow \begin{bmatrix} 0 & \mu_{ab} \\ \mu_{ba} & 0 \end{bmatrix}$$

the matrix representation of the dipole moment operator

$$\langle \hat{\mu} \rangle = \mathrm{tr}(\hat{\rho}\hat{\mu}) \qquad \mu_{ij} = \mu_{ji}^* = -e\langle i|\hat{z}|j\rangle \qquad \hat{\rho}\hat{\mu} \Rightarrow \begin{bmatrix} \rho_{aa} & \rho_{ab} \\ \rho_{ba} & \rho_{bb} \end{bmatrix}\begin{bmatrix} 0 & \mu_{ab} \\ \mu_{ba} & 0 \end{bmatrix} = \begin{bmatrix} \rho_{ab}\mu_{ba} & \rho_{aa}\mu_{ab} \\ \rho_{bb}\mu_{ba} & \rho_{ba}\mu_{ab} \end{bmatrix}$$

$$\boxed{\overline{\langle \mu \rangle} = \mathrm{tr}(\hat{\rho}\hat{\mu}) = \rho_{ab}\mu_{ba} + \rho_{ba}\mu_{ab}}$$

the expectation value of the dipole moment depend upon the off-diagonal elements of the density matrix

$$\hat{H} = \hat{H}_0 + \hat{V}(t) \xrightarrow{\text{electric dipole approximation}} \hat{V}(t) = -\hat{\mu}\tilde{E}(t)$$

$$V_{ba} = V_{ab}^* = -\mu_{ba}\tilde{E}(t)$$

$\downarrow$ diagonal matrix

$$H_{0,nm} = E_n \delta_{nm}$$

Equations of motion

$$\dot{\rho}_{nm} = \frac{-i}{\hbar}[\hat{H}, \hat{\rho}]_{nm} = \frac{-i}{\hbar}[(\hat{H}\hat{\rho})_{nm} - (\hat{\rho}\hat{H})_{nm}]$$

$$\dot{\rho}_{nm} = -i\omega_{nm}\rho_{nm} - \frac{i}{\hbar}\sum_{\nu}(V_{n\nu}\rho_{\nu m} - \rho_{n\nu}V_{\nu m})$$

$$\omega_{nm} = (E_n - E_m)/\hbar$$

$$\dot{\rho}_{ba} = -i\omega_{ba}\rho_{ba} + \frac{i}{\hbar}V_{ba}(\rho_{bb} - \rho_{aa}),$$

$$\dot{\rho}_{bb} = \frac{i}{\hbar}(V_{ba}\rho_{ab} - \rho_{ba}V_{ab}),$$

$$\dot{\rho}_{aa} = \frac{i}{\hbar}(V_{ab}\rho_{ba} - \rho_{ab}V_{ba}).$$

Absence of relaxation

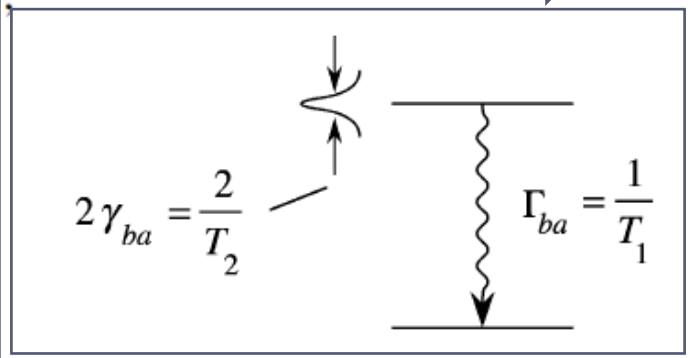

$$\dot{\rho}_{ba} = -\left(i\omega_{ba} + \frac{1}{T_2}\right)\rho_{ba} + \frac{i}{\hbar}V_{ba}(\rho_{bb} - \rho_{aa}),$$

$$\dot{\rho}_{bb} = \frac{-\rho_{bb}}{T_1} - \frac{i}{\hbar}(V_{ba}\rho_{ab} - \rho_{ba}V_{ab}),$$

$$\dot{\rho}_{aa} = \frac{\rho_{bb}}{T_1} + \frac{i}{\hbar}(V_{ba}\rho_{ab} - \rho_{ba}V_{ab}).$$

Closed system with spontaneous emission

$$\dot{\rho}_{bb} + \dot{\rho}_{aa} = 0 \qquad \rho_{aa} + \rho_{bb} = 1$$

$$[\rho_{bb}(t) - \rho_{aa}(t)] = (\rho_{bb} - \rho_{aa})^{(\mathrm{eq})} + \{[\rho_{bb}(0) - \rho_{aa}(0)] - (\rho_{bb} - \rho_{aa})^{(\mathrm{eq})}\}e^{-t/T_1}.$$

Population inversion relaxes from its initial value to its equilibrium value in a time of the order of T_1. For this reason, T_1 is called the population relaxation time.

$$\rho_{ba}(t) = \rho_{ba}(0)e^{-(i\omega_{ba}+1/T_2)t}$$

$$\langle\tilde{\mu}(t)\rangle = \mu_{ab}\rho_{ba}(t) + \mu_{ba}\rho_{ab}(t) = \mu_{ab}\rho_{ba}(0)e^{-(i\omega_{ba}+1/T_2)t} + \mathrm{c.c.}$$

$$= [\mu_{ab}\rho_{ba}(0)e^{-i\omega_{ba}t} + \mathrm{c.c.}]e^{-t/T_2}.$$

For an undriven atom, the dipole moment oscillates at frequency ω_{ba} and decays to zero in the characteristic time T_2, which is known as the dipole dephasing time.

$$\frac{1}{T_2} = \frac{1}{2T_1} + \gamma_c \qquad \gamma_c = C_s N + C_f N_f$$

Pressure broadening

Steady-State Response of a Two-Level Atom to a Monochromatic Field

$$\hat{V} = -\hat{\mu}\tilde{E}(t) = -\hat{\mu}\left(Ee^{-i\omega t} + E^* e^{i\omega t}\right)$$

$$V_{ba} = -\mu_{ba}\left(Ee^{-i\omega t} + E^* e^{i\omega t}\right)$$

cannot be solved exactly

$$\rho_{ba}(t) = \rho_{ba}(0)e^{-(i\omega_{ba}+1/T_2)t}$$

RWA $V_{ba} = -\mu_{ba} E e^{-i\omega t}$

$$\tilde{P}(t) = N\langle\tilde{\mu}\rangle = N\,\mathrm{Tr}\left(\hat{\tilde{\rho}}\hat{\tilde{\mu}}\right) = N(\mu_{ab}\rho_{ba} + \mu_{ba}\rho_{ab})$$

$$\tilde{P}(t) = Pe^{-i\omega t} + \text{c.c.}$$ **Polarization**

$$P = \epsilon_0 \chi E$$

Susceptibility

$$\chi = \frac{N|\mu_{ba}|^2(\rho_{bb} - \rho_{aa})}{\epsilon_0\hbar(\omega - \omega_{ba} + i/T_2)}$$

Absorption

$$\alpha = \frac{2\omega}{c}\,\mathrm{Im}\,n = \frac{2\omega}{c}\,\mathrm{Im}\left[(1+\chi)^{1/2}\right]$$

$$\alpha = \frac{\omega}{c}\,\mathrm{Im}\,\chi$$

$$\Omega = 2|\mu_{ba}||E|/\hbar$$ **Rabi frequency**

$$\Delta = \omega - \omega_{ba}$$

dispersive lineshape

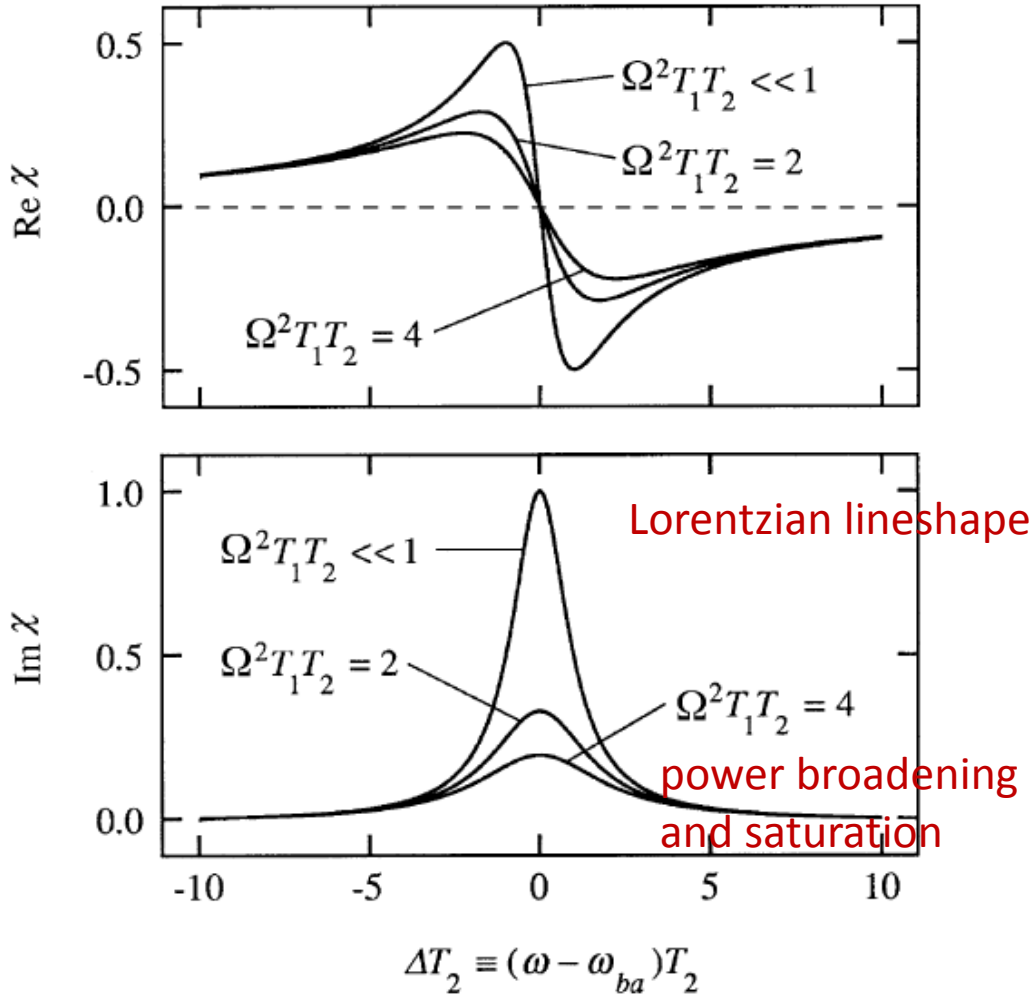

Lorentzian lineshape

power broadening and saturation

Interaction of two-level atoms with a **train of fs pulses**

- resonant excitation of atoms
- room-temperature atoms (inhomogeneous broadening)
- atomic relaxation times > pulse repetition period

OBE

$$\frac{\partial \rho_{22}}{\partial t} = \left[\mathrm{i} \frac{\mu_{12} \mathscr{E}^*(t)}{\hbar} \sigma_{12} + \mathrm{c.c.} \right] - \frac{\rho_{22}}{T_1},$$

$$\frac{\partial \sigma_{12}}{\partial t} = \mathrm{i}\delta\sigma_{12} + \mathrm{i} \frac{\mu_{12} \mathscr{E}(t)}{\hbar} (2\rho_{22} - 1) - \frac{\sigma_{12}}{T_2}$$

$$\mathscr{E}(t) = E(t) \mathrm{e}^{-\mathrm{i}\omega_\mathrm{L} t}$$

Direct integration

ACCUMULATION OF POPULATION AND COHERENCE

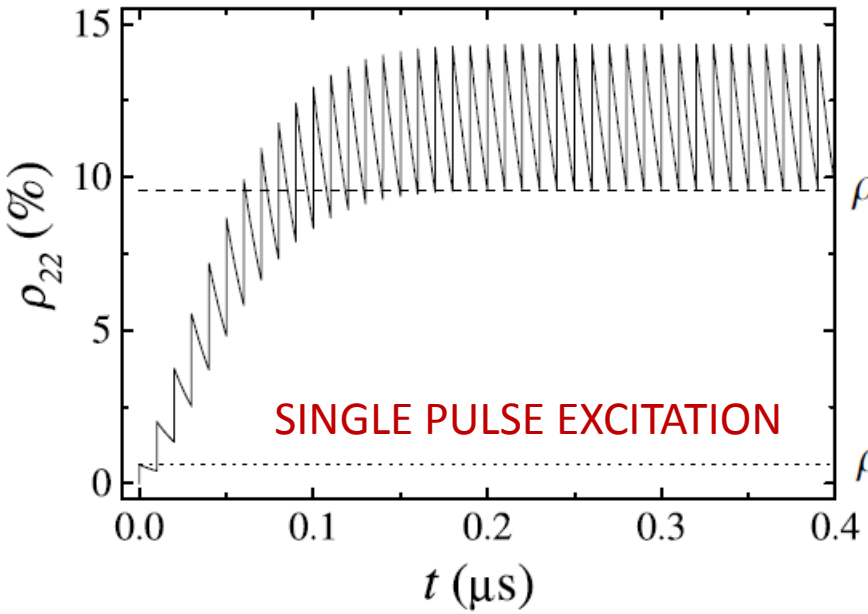

$$\rho_{22}^{\mathrm{f}} = \gamma_\mathrm{c} \rho_{22}^{\mathrm{s}}$$

$$\gamma_\mathrm{c} = 15.5$$

$$\rho_{22}^{\mathrm{s}} = \sin^2(\theta/2)$$

PULSE TRAIN ELECTRIC FIELD

$$E_T(t) = \sum_{n=0}^{\infty} E(t - nT_\mathrm{R}) \mathrm{e}^{\mathrm{i}n\Delta\Psi}$$

$$= \left[\sum_{n=0}^{\infty} \mathscr{E}(t - nT_\mathrm{R}) \mathrm{e}^{\mathrm{i}n\Phi_\mathrm{R}} \right] \mathrm{e}^{\mathrm{i}\omega_\mathrm{L} t}$$

$$= \mathscr{E}_\mathrm{T}(t) \mathrm{e}^{\mathrm{i}\omega_\mathrm{L} t}.$$

PULSE AREA

$$\theta = \frac{2\mu_{12}}{\hbar} \int_{-\infty}^{\infty} \mathscr{E}(t)\, \mathrm{d}t$$

The coherence excited by one pulse adds to the coherence excited by the previous pulse, leading to the strong enhancement of population.

This enhancement can be understood as a constructive interference, since the time-delayed phases acquired by the coherence with the succession of pulses are analogous to the time-delayed phases that result in the interference in a multiple slit experiment

*D. Felinto, C.A.C. Bosco, L.H. Acioli, S.S. Vianna: Optics Communications **215** (2003) 69–73*

Time dynamics of a multilevel system excited by a train of fs pulses

OBE $\widehat{H}_{int} = -\mu_{kl} E_T(t)|k\rangle\langle l|$ $\quad E_T(t) = \left[\sum_{n=0}^{N} \mathcal{E}(t - nT_R)e^{in\Phi_R}\right] e^{i\omega_\ell t} = \mathcal{E}_T(t)e^{i\omega_\ell t}$

FOUR-LEVELS

$$
\begin{aligned}
\frac{d\rho_{11}}{dt} &= \left(-\frac{i\mu_{13}\mathcal{E}_T^*(t)}{\hbar}\sigma_{13} - \frac{i\mu_{14}\mathcal{E}_T^*(t)}{\hbar}\sigma_{14} + \text{c.c.}\right) + \Gamma_{13}\rho_{33} + \Gamma_{14}\rho_{44} + \Pi(\rho_{22} - \rho_{11}),\\
\frac{d\rho_{22}}{dt} &= \left(-\frac{i\mu_{23}\mathcal{E}_T^*(t)}{\hbar}\sigma_{23} - \frac{i\mu_{24}\mathcal{E}_T^*(t)}{\hbar}\sigma_{24} + \text{c.c.}\right) + \Gamma_{23}\rho_{33} + \Gamma_{24}\rho_{44} - \Pi(\rho_{22} - \rho_{11}),\\
\frac{d\rho_{33}}{dt} &= \left(\frac{i\mu_{13}\mathcal{E}_T^*(t)}{\hbar}\sigma_{13} + \frac{i\mu_{23}\mathcal{E}_T^*(t)}{\hbar}\sigma_{23} + \text{c.c.}\right) - (\Gamma_{13} + \Gamma_{23})\rho_{33} + \Pi(\rho_{44} - \rho_{33}),\\
\frac{d\rho_{44}}{dt} &= \left(\frac{i\mu_{14}\mathcal{E}_T^*(t)}{\hbar}\sigma_{14} + \frac{i\mu_{24}\mathcal{E}_T^*(t)}{\hbar}\sigma_{24} + \text{c.c.}\right) - (\Gamma_{14} + \Gamma_{24})\rho_{44} - \Pi(\rho_{44} - \rho_{33}),\\
\frac{d\sigma_{12}}{dt} &= i\delta_{12}\sigma_{12} + \frac{i\mathcal{E}_T(t)}{\hbar}(\mu_{13}\sigma_{23}^* + \mu_{14}\sigma_{24}^*) - \frac{i\mathcal{E}_T^*(t)}{\hbar}(\mu_{23}\sigma_{13} + \mu_{24}\sigma_{14}) - \gamma_{12}\sigma_{12},\\
\frac{d\sigma_{13}}{dt} &= i\delta_{13}\sigma_{13} + \frac{i\mu_{13}\mathcal{E}_T(t)}{\hbar}(\rho_{33} - \rho_{11}) + \frac{i\mathcal{E}_T(t)}{\hbar}(\mu_{14}\sigma_{34}^* - \mu_{23}\sigma_{12}) - \gamma_{13}\sigma_{13},\\
\frac{d\sigma_{14}}{dt} &= i\delta_{14}\sigma_{14} + \frac{i\mu_{14}\mathcal{E}_T(t)}{\hbar}(\rho_{44} - \rho_{11}) + \frac{i\mathcal{E}_T(t)}{\hbar}(\mu_{13}\sigma_{34} - \mu_{24}\sigma_{12}) - \gamma_{14}\sigma_{14},\\
\frac{d\sigma_{23}}{dt} &= i\delta_{23}\sigma_{23} + \frac{i\mu_{23}\mathcal{E}_T(t)}{\hbar}(\rho_{33} - \rho_{22}) + \frac{i\mathcal{E}_T(t)}{\hbar}(\mu_{24}\sigma_{34}^* - \mu_{13}\sigma_{12}^*) - \gamma_{23}\sigma_{23},\\
\frac{d\sigma_{24}}{dt} &= i\delta_{24}\sigma_{24} + \frac{i\mu_{24}\mathcal{E}_T(t)}{\hbar}(\rho_{44} - \rho_{22}) + \frac{i\mathcal{E}_T(t)}{\hbar}(\mu_{23}\sigma_{34} - \mu_{14}\sigma_{12}^*) - \gamma_{24}\sigma_{24},\\
\frac{d\sigma_{34}}{dt} &= i\delta_{34}\sigma_{34} + \frac{i\mathcal{E}_T^*(t)}{\hbar}(\mu_{13}\sigma_{14} + \mu_{23}\sigma_{24}) - \frac{i\mathcal{E}_T(t)}{\hbar}(\mu_{14}\sigma_{13}^* + \mu_{24}\sigma_{23}^*) - \gamma_{24}\sigma_{24}.
\end{aligned}
$$

$$
\begin{aligned}
\sigma_{12} &= \rho_{12},\\
\sigma_{13} &= \rho_{13}e^{-i\omega_\ell t},\\
\sigma_{14} &= \rho_{14}e^{-i\omega_\ell t},\\
\sigma_{23} &= \rho_{23}e^{-i\omega_\ell t},\\
\sigma_{24} &= \rho_{24}e^{-i\omega_\ell t},\\
\sigma_{34} &= \rho_{34},
\end{aligned}
$$

$$
\begin{aligned}
\gamma_{12} &= \Pi,\\
\gamma_{13} &= \gamma_{23} = \frac{1}{2}(\Gamma_{13} + \Gamma_{23}) + \Pi,\\
\gamma_{14} &= \gamma_{24} = \frac{1}{2}(\Gamma_{14} + \Gamma_{24}) + \Pi,\\
\gamma_{34} &= \frac{1}{2}(\Gamma_{13} + \Gamma_{23} + \Gamma_{14} + \Gamma_{24}) + \Pi.
\end{aligned}
$$

$$
\begin{aligned}
\delta_{12} &= \omega_2,\\
\delta_{13} &= \omega_3 - \omega_\ell,\\
\delta_{14} &= \omega_4 - \omega_\ell,\\
\delta_{23} &= \omega_3 - \omega_2 - \omega_\ell,\\
\delta_{24} &= \omega_4 - \omega_2 - \omega_\ell,\\
\delta_{34} &= \omega_4 - \omega_3,
\end{aligned}
$$

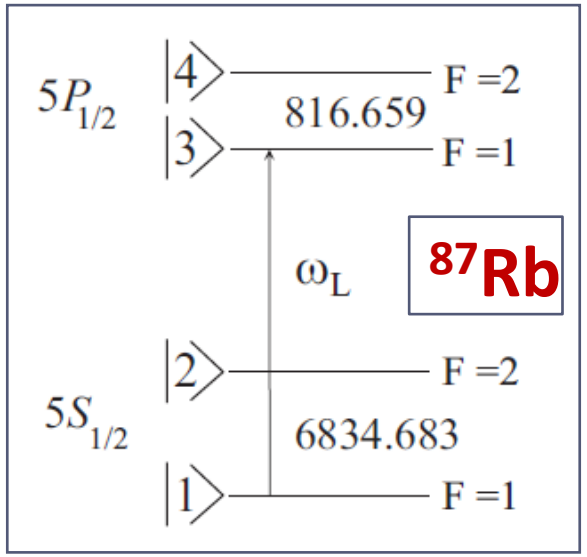

10 coupled differential equations

For one velocity group ☺

Doppler-broadened atomic transitions

- Doppler broadening (~500 MHz for Rb at room temperature)
  $\gg$ homogeneous broadening (~6 MHz for Rb)
- different velocity groups of atoms "see" different laser frequencies
- different atomic groups – different excitation process
- atomic transition frequency ω_{ge} is modified into $\omega'_{ge} = \omega_{ge} + \vec{k} \cdot \vec{v}$

$\vec{k}$ is laser wavevector
$\vec{v}$ is the atomic velocity

$$
\begin{aligned}
\delta_{12} &= \omega_2, \\
\delta_{13} &= \omega_3 + \vec{k} \cdot \vec{v} - \omega_\ell, \\
\delta_{14} &= \omega_4 + \vec{k} \cdot \vec{v} - \omega_\ell, \\
\delta_{23} &= \omega_3 - \omega_2 + \vec{k} \cdot \vec{v} - \omega_\ell, \\
\delta_{24} &= \omega_4 - \omega_2 + \vec{k} \cdot \vec{v} - \omega_\ell, \\
\delta_{34} &= \omega_4 - \omega_3.
\end{aligned}
$$

The system of OBE needs to be solved individually for all velocity group of atoms!

OBE provides a complete description of the temporal evolution of the atomic system, but this procedure becomes very demanding and time consuming even in the case of four-level atomic system excited by a large number of pulses.

An iterative analytic solution to the optical Bloch equations

The iterative solution circumvents the use of time consuming numerical procedures and can be used as a practical tool in future investigations.

Numerical solution vs iterative analytical solution

D. Aumiler, T. Ban, and G. Pichler; PRA 79, 063403 (2009).

Integration of OBE under approximations:

- The pulse is very short compared to all atomic relaxation times
- The pulse is very short compared to the laser repetition period
- fs pulse electric field is weak enough to keep only the lowest-order term in perturbative series

Iterative solution assumptions:

- the state of the system before (n+1)th pulse is a function of the state before nth pulse
- pulses have a small area
- the excitation occurs in the quasi impulsive regime
- pulse duration is much smaller than the population relaxation times, coherence relaxation times and pulse repetition period

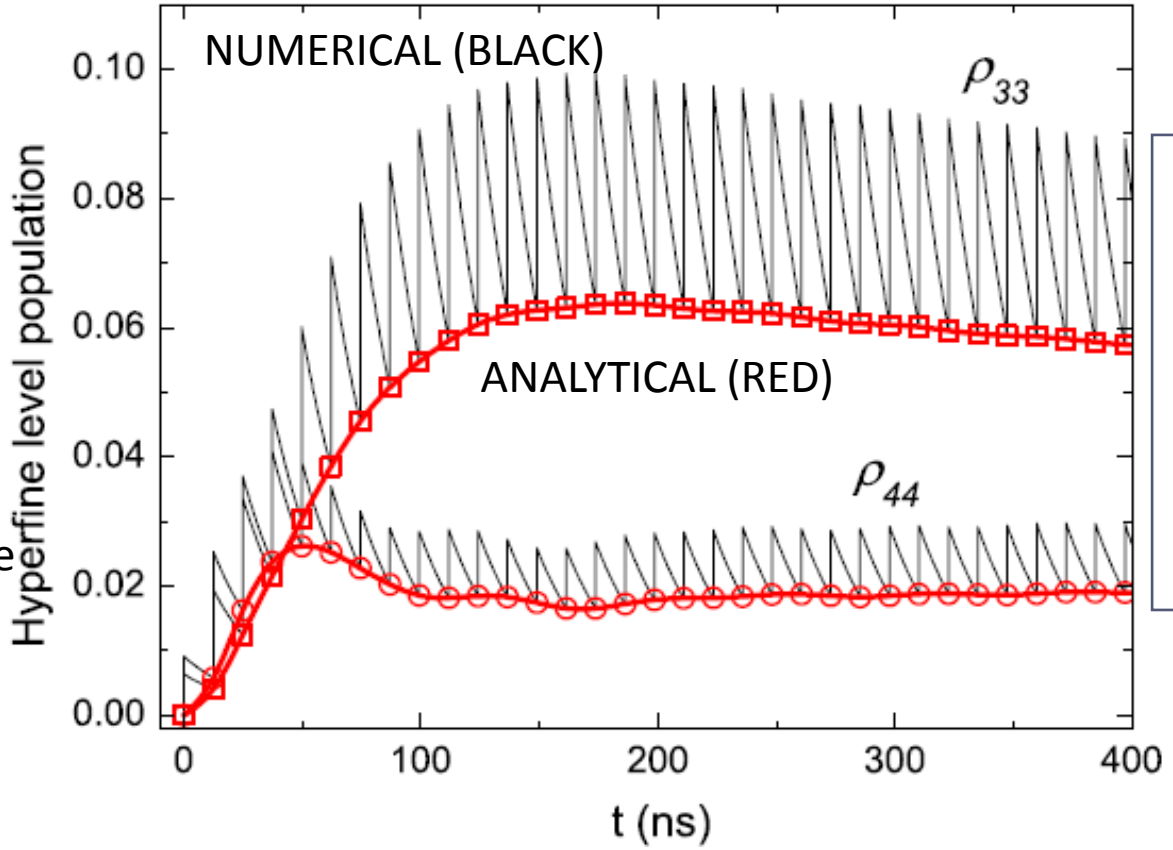

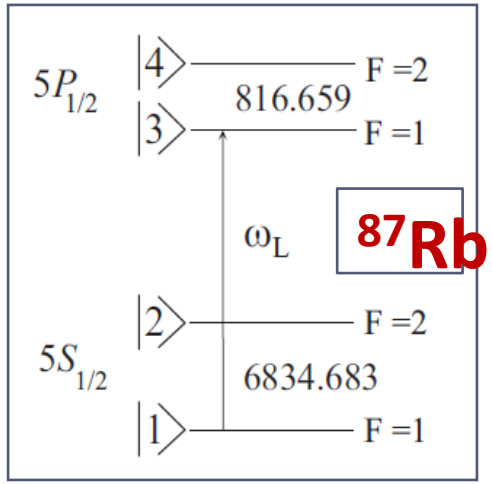

Iterative analytic solution enables fast and accurate calculation of the system time evolution circumventing the use of time-consuming numerical procedures.

Level populations as a function of atomic velocity

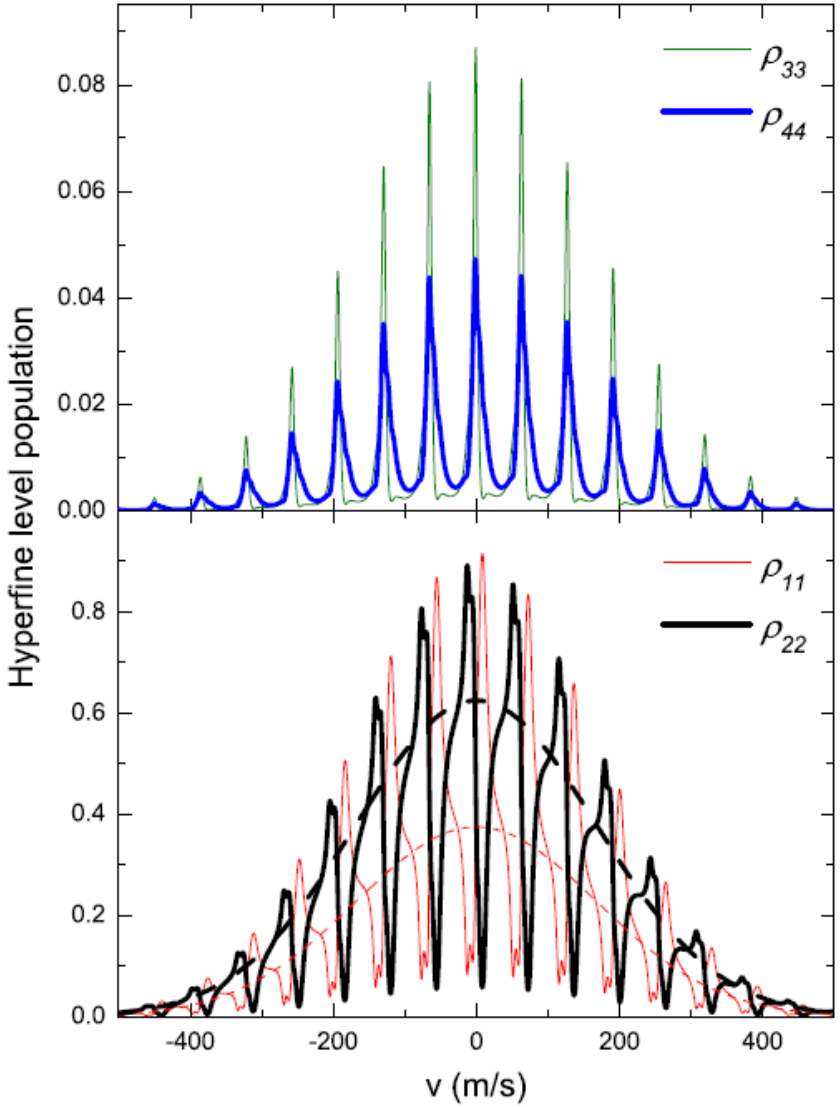

Excited level population as a function of the number of excitation pulses.

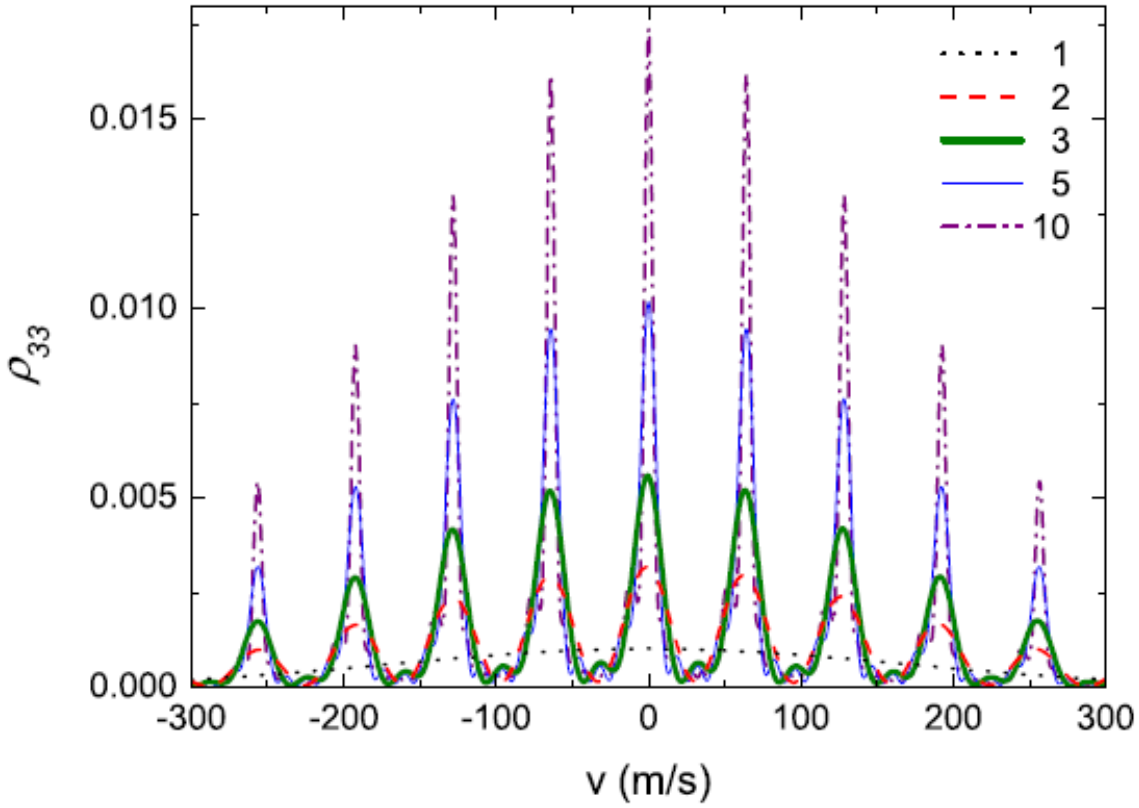

Mapping of the Optical Frequency Comb to the Atom Velocity Comb

Excited level population as a function of the field peak amplitude.

Level populations as a function of the excitation pulse repetition frequency.

TIME

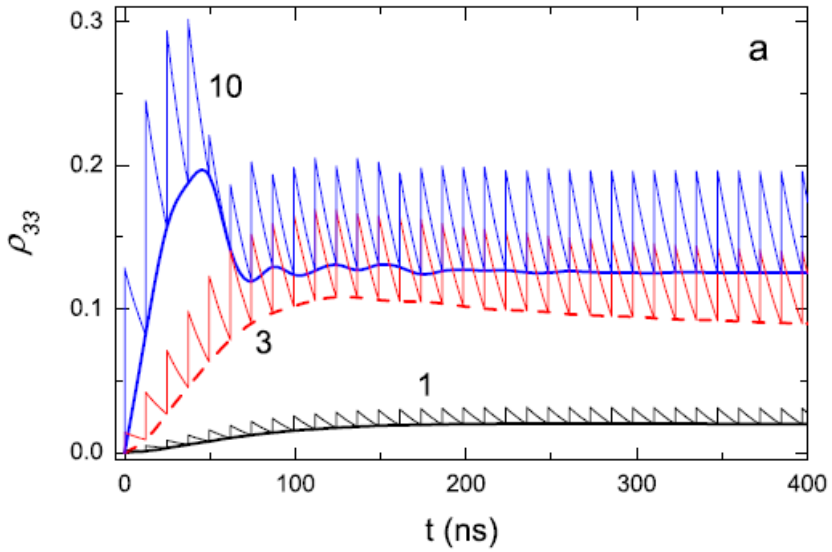

FREQUENCY

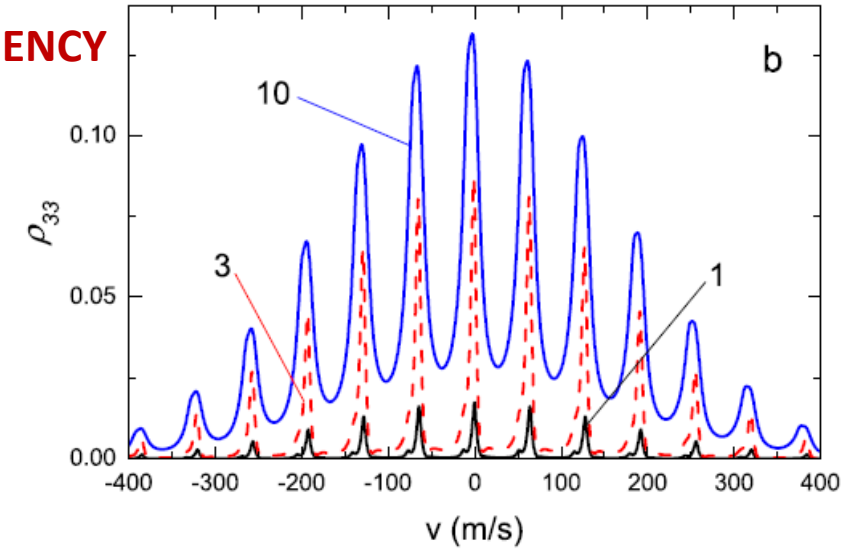

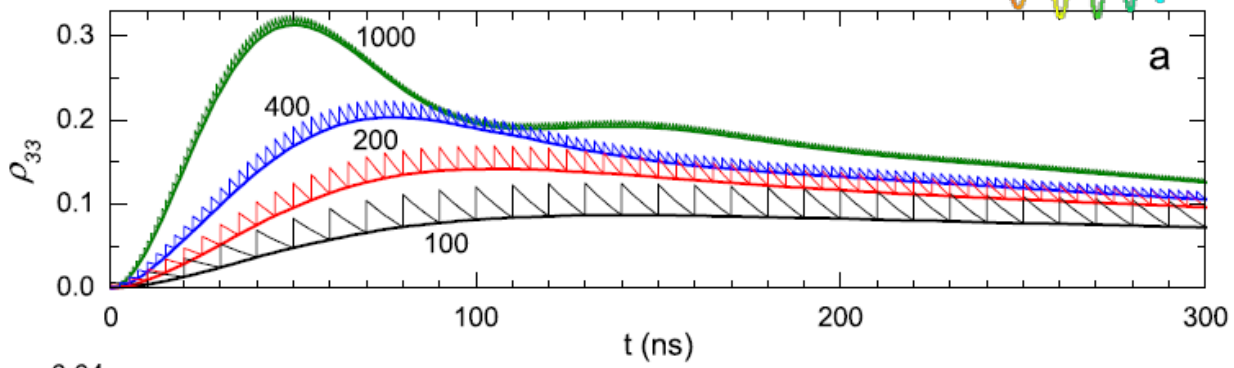

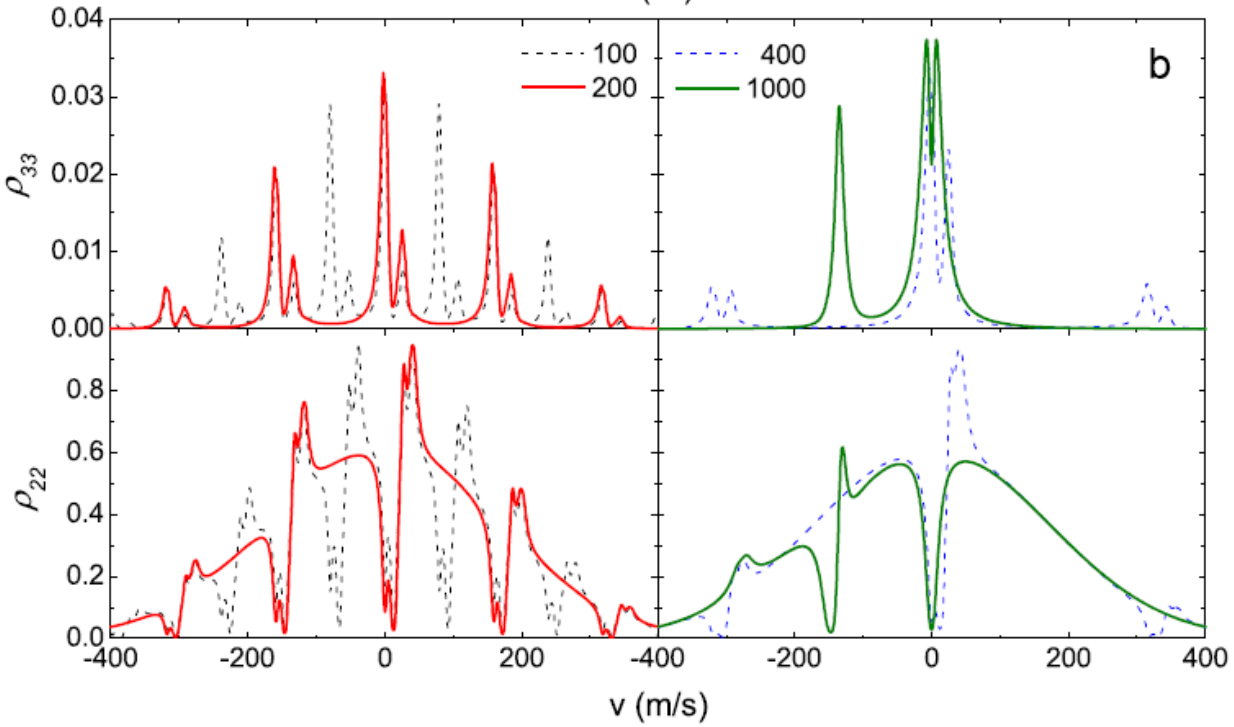

Electromagnetically induced transparency EIT

The strength of the interaction between light and atoms is a function of the wavelength or frequency of light. When the light frequency matches the frequency of a particular atomic transition, a resonance condition occurs and the optical response of the medium is greatly enhanced. Light propagation is then accompanied by strong absorption and dispersion.

Speed of light in cold Na atoms
17 m / s = 61.2 km / h

destructive quantum interference of two possible pathways

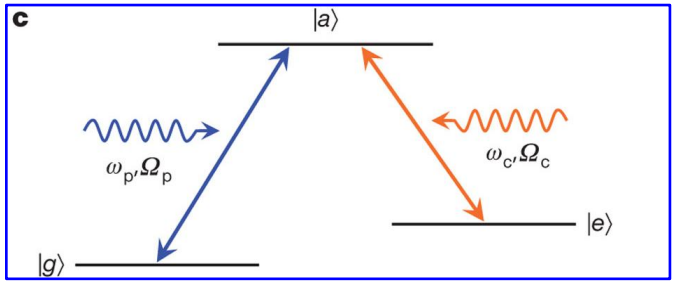

Λ-type excitation scheme

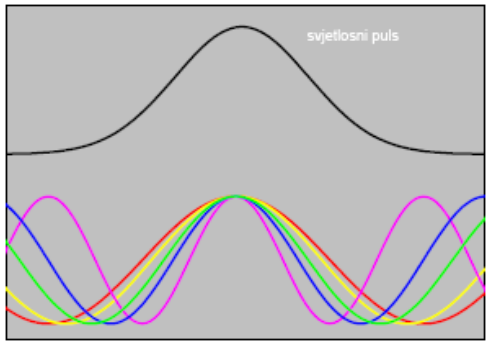

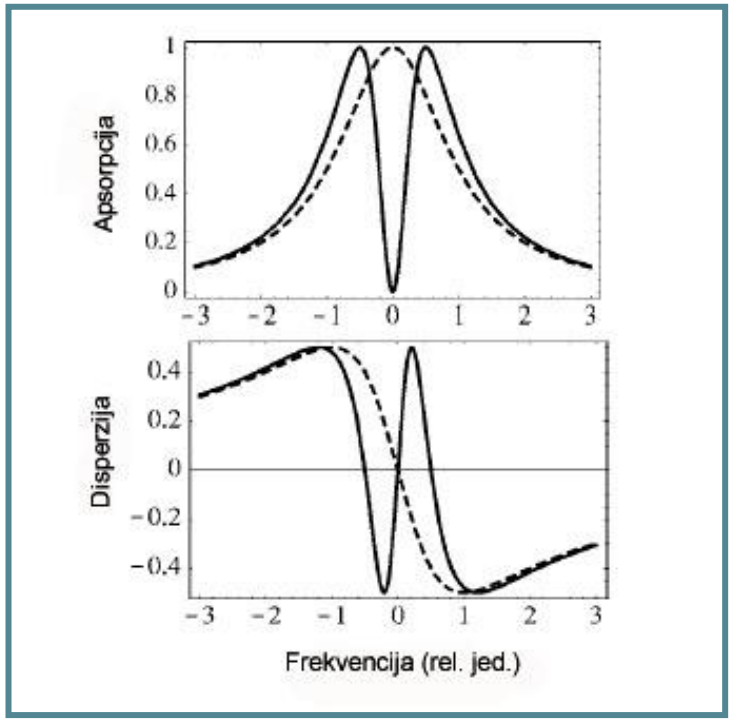

$$v_g = \frac{c}{n(\omega) + \omega \frac{dn(\omega)}{d\omega}} = \frac{c}{n_g}$$

Nonlinear optics, storage light, quantum memory, ...

Coherence population trapping (CPT) induced by the FC excitation

Coherent preparation of the quantum states of atoms by laser light.

Quantum interference in the amplitudes of optical transitions.

Modification of the optical properties of a medium.

D. Aumiler, PRA A 82, 055402 (2010).

- EIT - atomic medium is made transparent to a resonant probe field
- The two excitation laser fields create destructive interference between excitation pathways
- Dark superposition state is formed, with the population reduced in the upper state and trapped within the two ground states

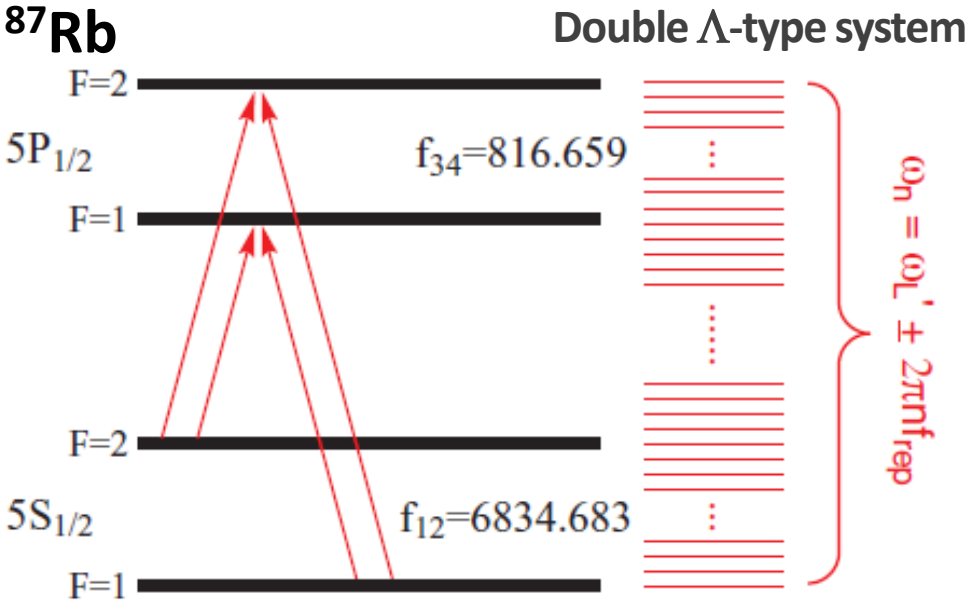

$$|D\rangle = (|1\rangle - |2\rangle)/\sqrt{2}$$

$$|B\rangle = (|1\rangle + |2\rangle)/\sqrt{2}$$

Dark state, a linear combination of the ground-state levels which is decoupled from the excitation pulses.

- pulse repetition frequency *frep* is a subharmonic of the hyperfine splitting of the ground state, $\omega_{12} = 2\pi f_{12}$
- for the case of room-temperature vapor a double Λ-type excitation scheme can be achieved

Dark state fomation

Accumulation of coherence between the ground-state hyperfine levels.

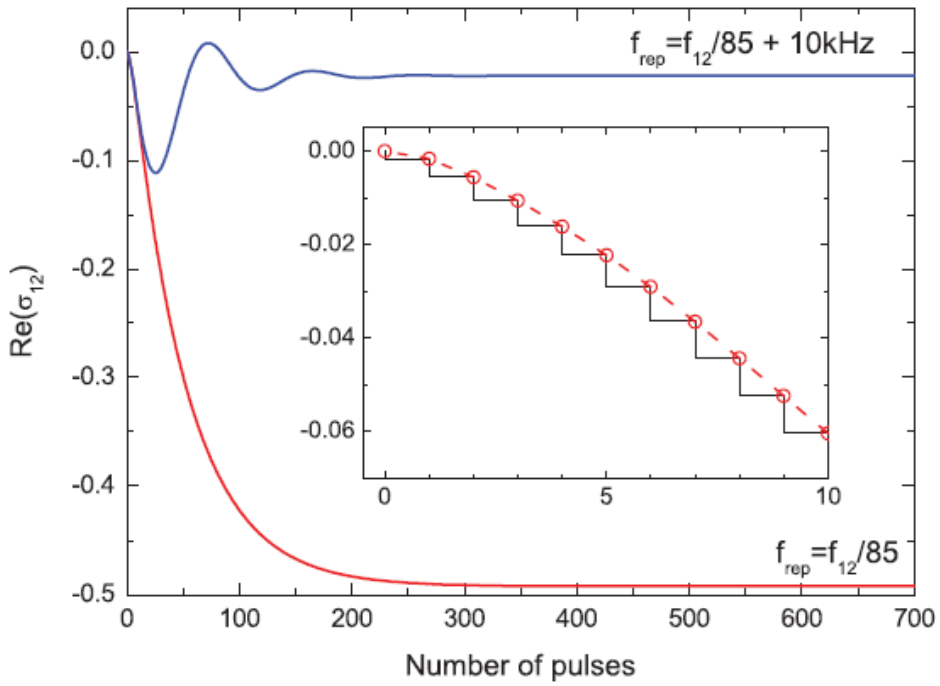

Excited-state populations, averaged over the atomic velocity, as a function of pulse repetition frequency.

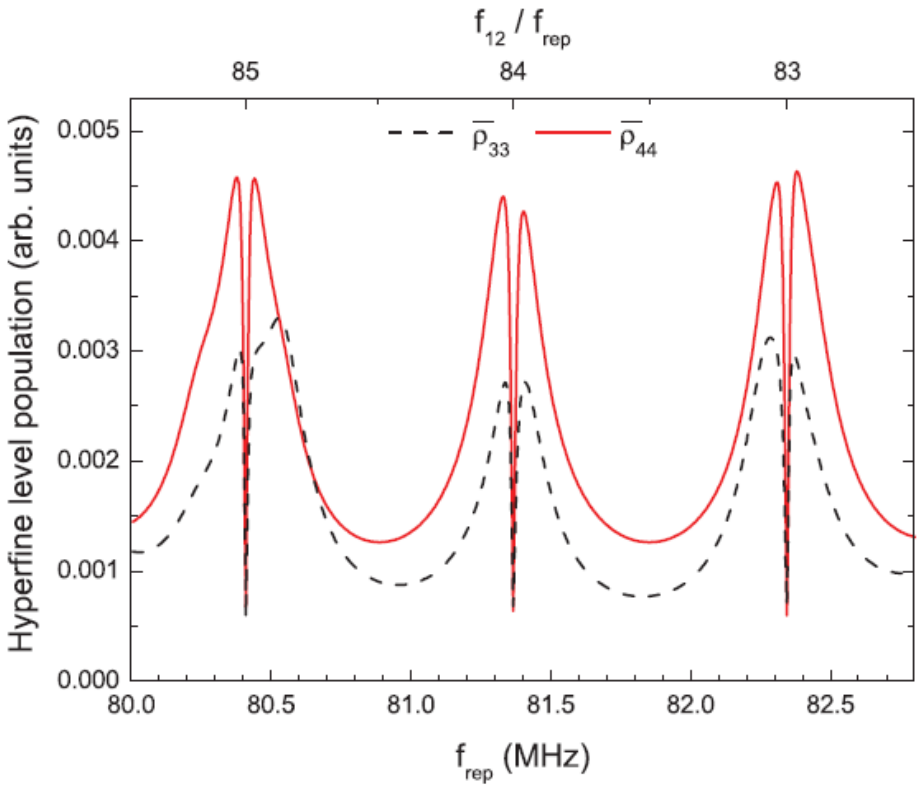

Coherent accumulation of excitation leads to the complete population transfer to the dark state. Simultaneously, the population of the excited state goes toward zero, the pulses are no longer absorbed, and EIT takes place.

Dark state population

Stationary dark state population vs. f_{rep}

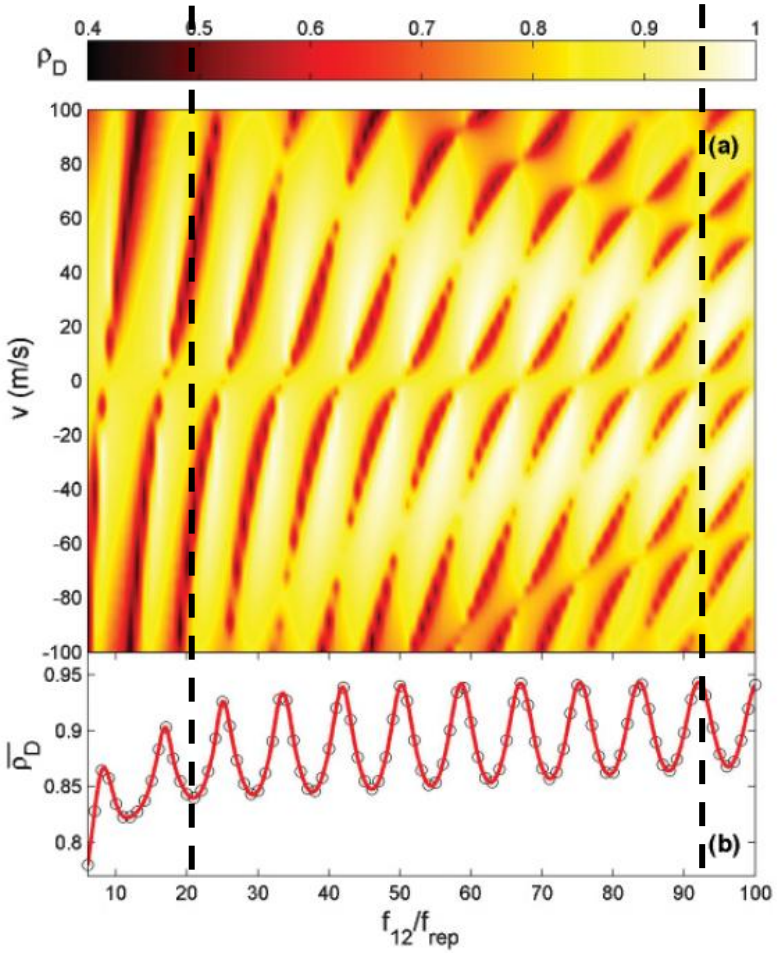

Maxima:

A double Λ--type excitation scheme is achieved for a particular velocity group of atoms,
frep is simultaneously a subharmonic of the ground- and excited-state hyperfine splitting
(f12/92 ≈ f34/11).

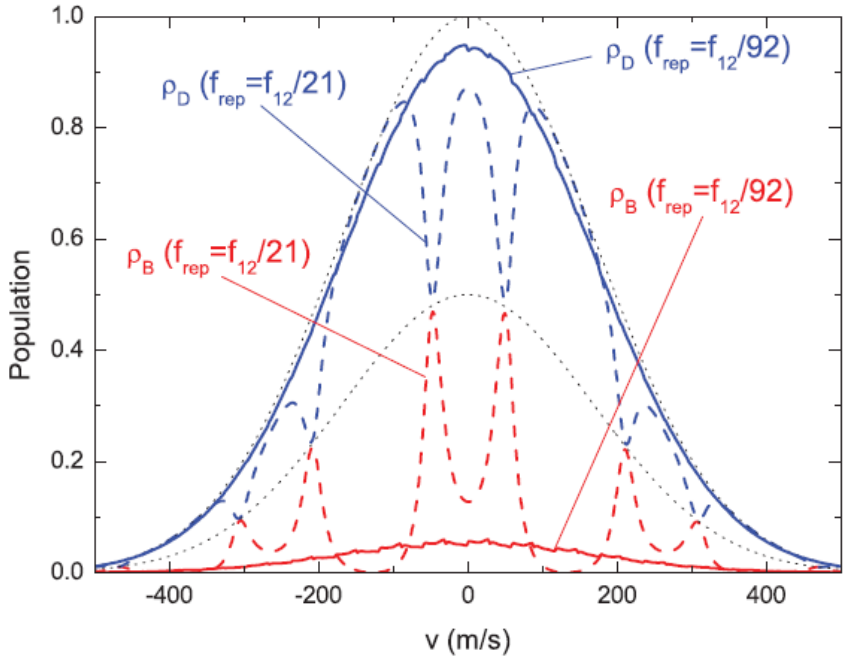

Time dynamics of the dark state population

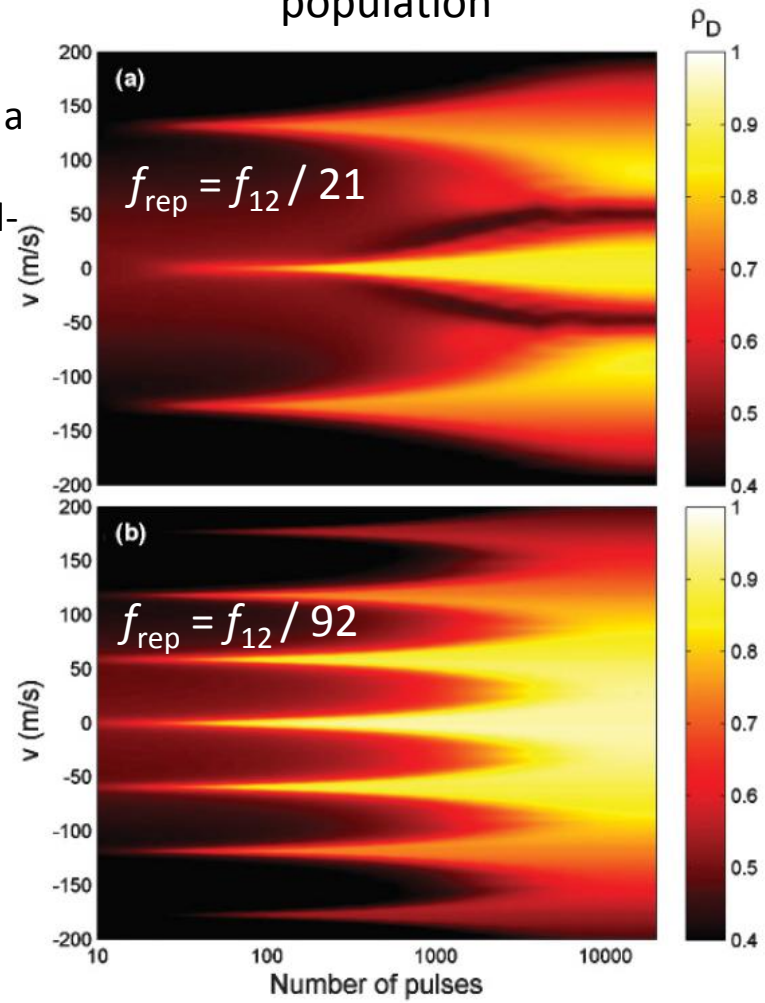

PART II – Experimental demonstration of the coherence accumulation effects induced by FC

Detection of coherence accumulation effects

We need a system with atomic relaxation time longe than the pulse repetition period.

Rb atoms: lifetime of the first excited state ~30 ns

Tsunami fs mode-locked laser: frep=80 MHz (Trep ~ 12 ns)

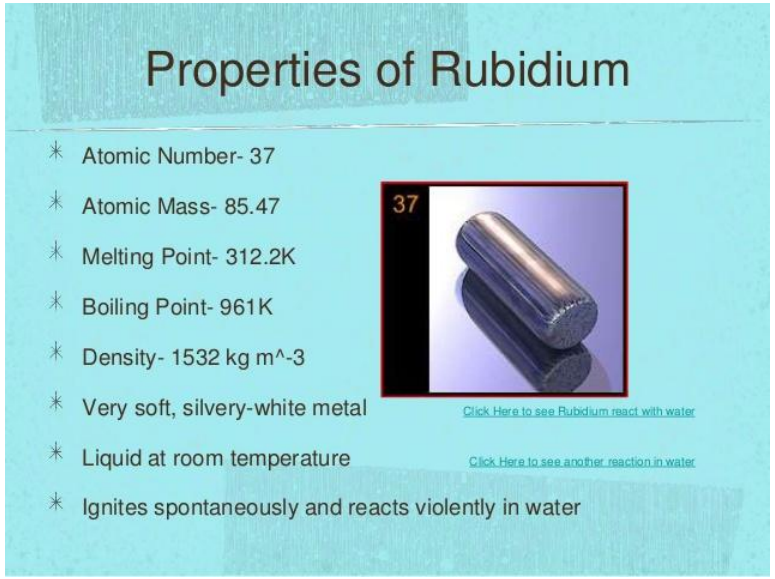

EXCITATION

resonant fs pulse train excitation of rubidium atoms

DETECTION

weak cw scanning probe laser

- probe absorption → ground state population

In the weak field approximation and linear absorption regime, the measured optical thickness is directly proportional to the ground state populations.

Experiment

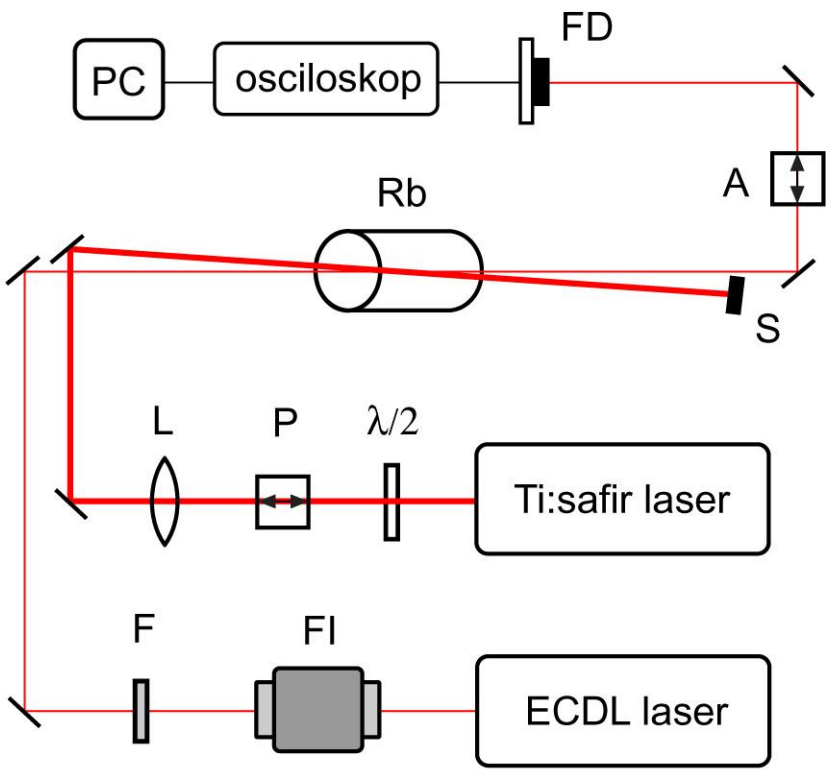

Experimental setup
FI–Faraday isolator, F–filter, λ/2–λ/2 plate, P–polarizer, L–lens, S–beam stoper, A–analizer, FD–photodiode.

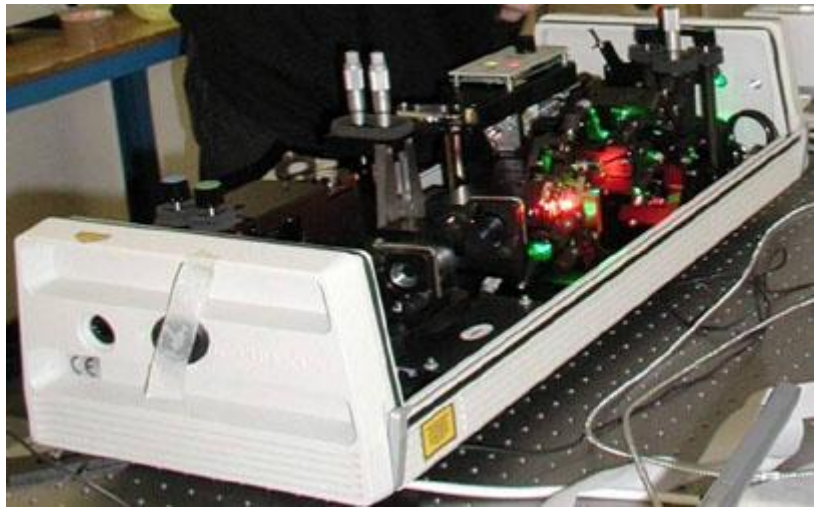

Tsunami fs laser

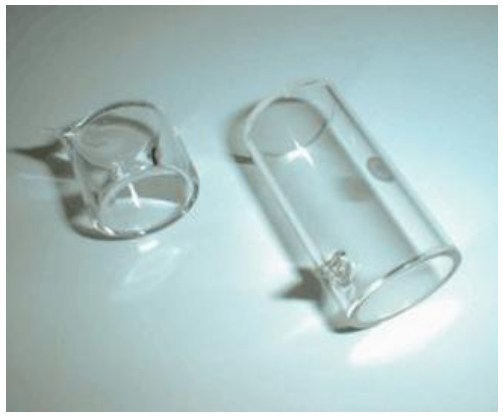

Rb cell

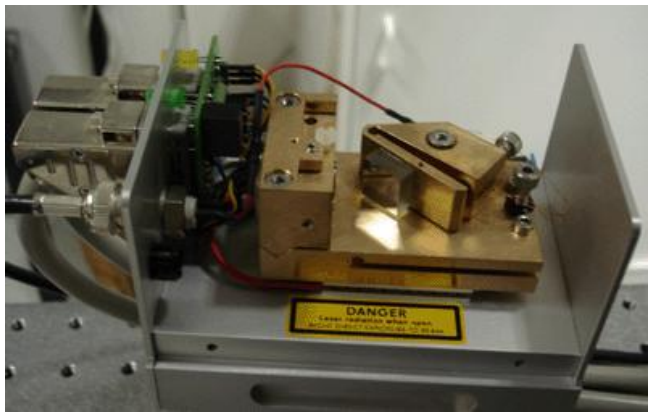

External cavity diode laser

Rubidium atom

Natural rubidium is a mix of two isotopes.

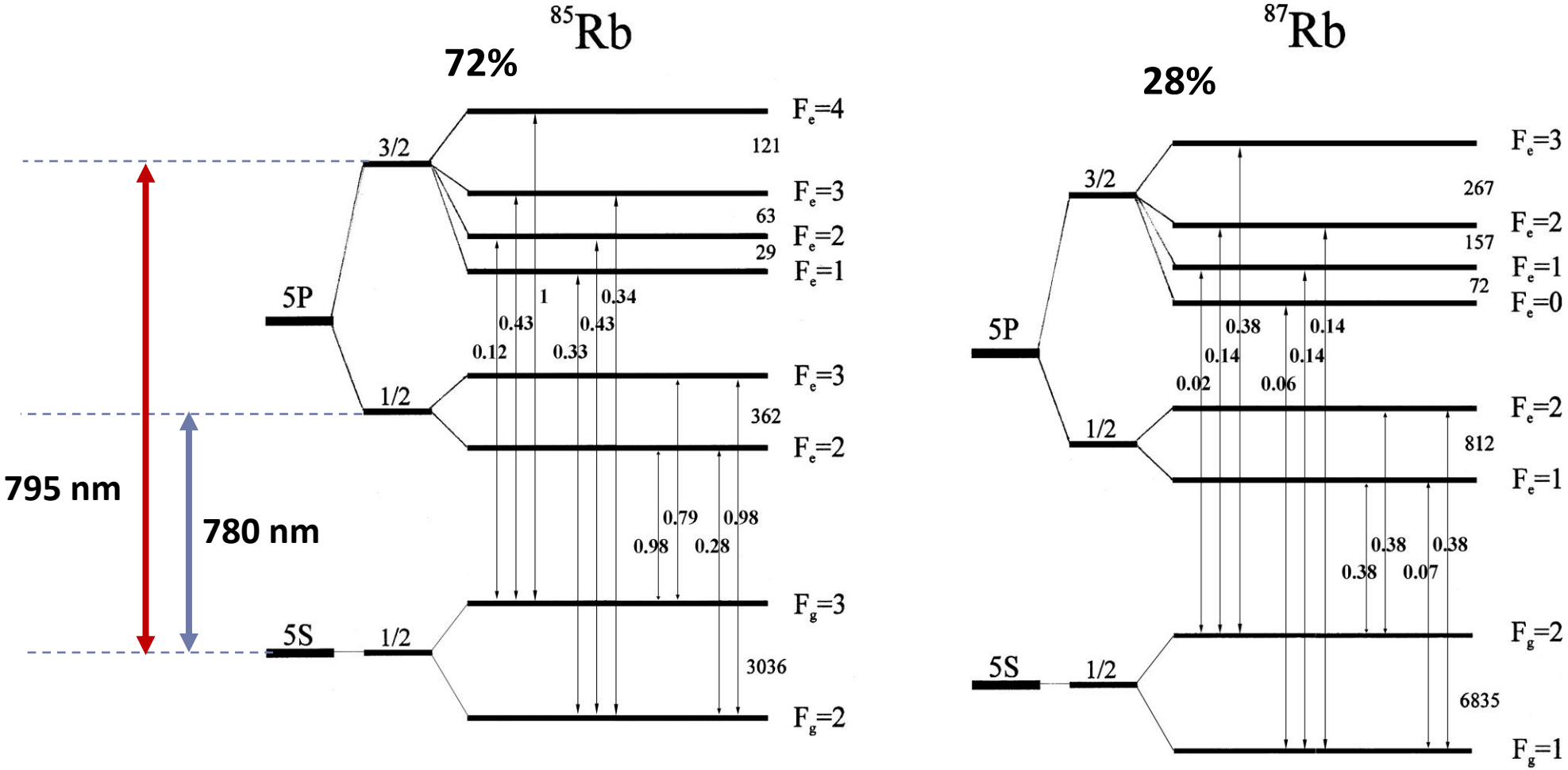

Hyperfine energy levels scheme with the corresponding relative transition probabilities.

Absorption spectum of Rb D_2 $5S_{1/2}$-$5P_{3/2}$ resonance line

fs laser induced changes in the absorption spectra

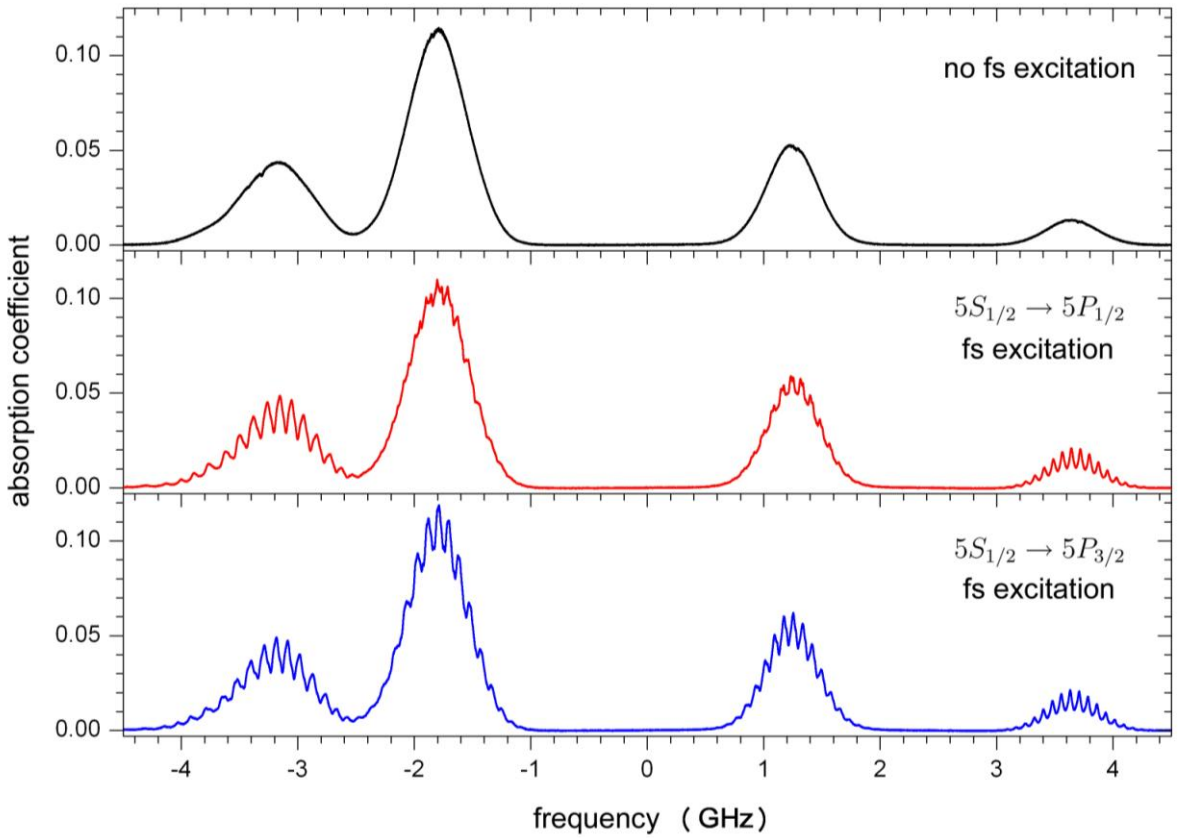

Hyperfine resolution absorption spectra of Rb D_2 $5S_{1/2}$ - $5P_{3/2}$ resonance line @ 780 nm

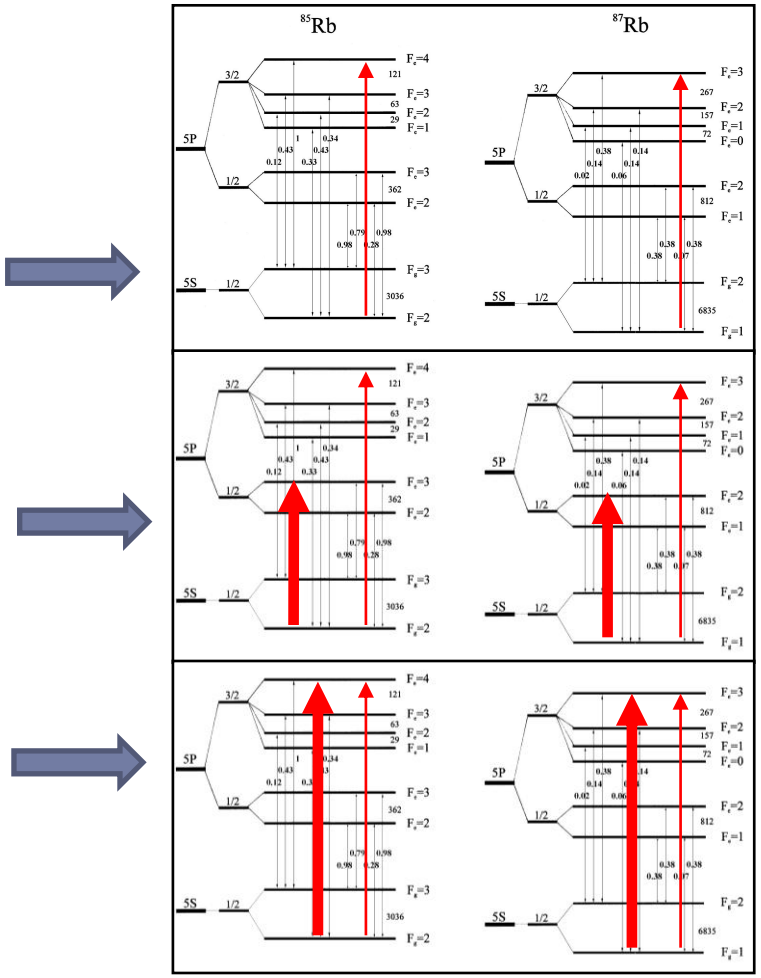

Excitation scheme
fs laser + probe laser

D. Aumiler, T. Ban, H. Skenderović, and G. Pichler; PRL 95, 233001 (2005).

T. Ban, D. Aumiler, H. Skenderović, and G. Pichler; PRA 73, 043407 (2006).

Fs laser power and wavelength dependence

Relative modulation intensity dependence ...

on averaged fs laser power

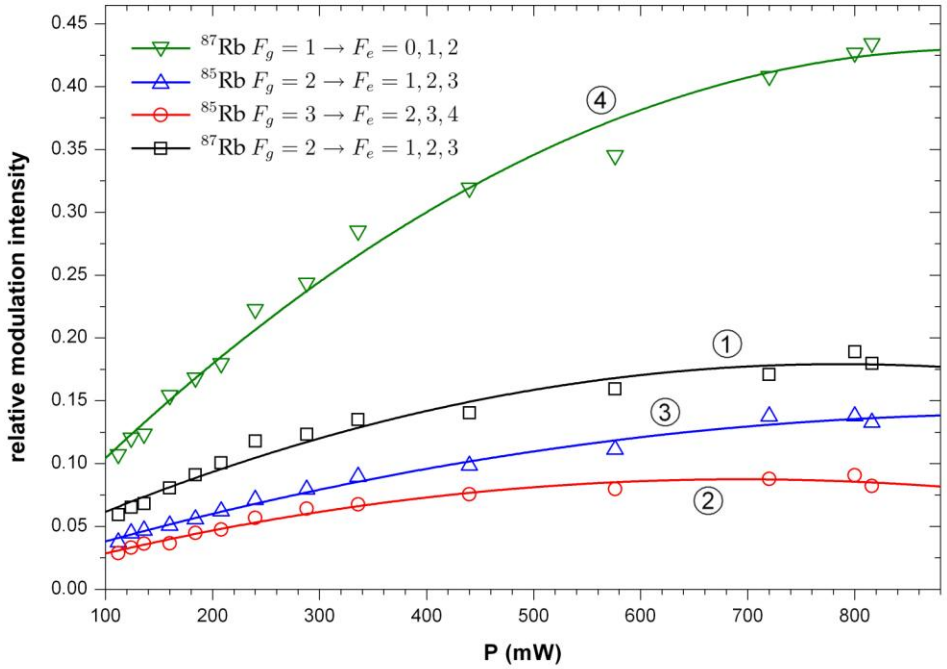

on fs laser central wavelength

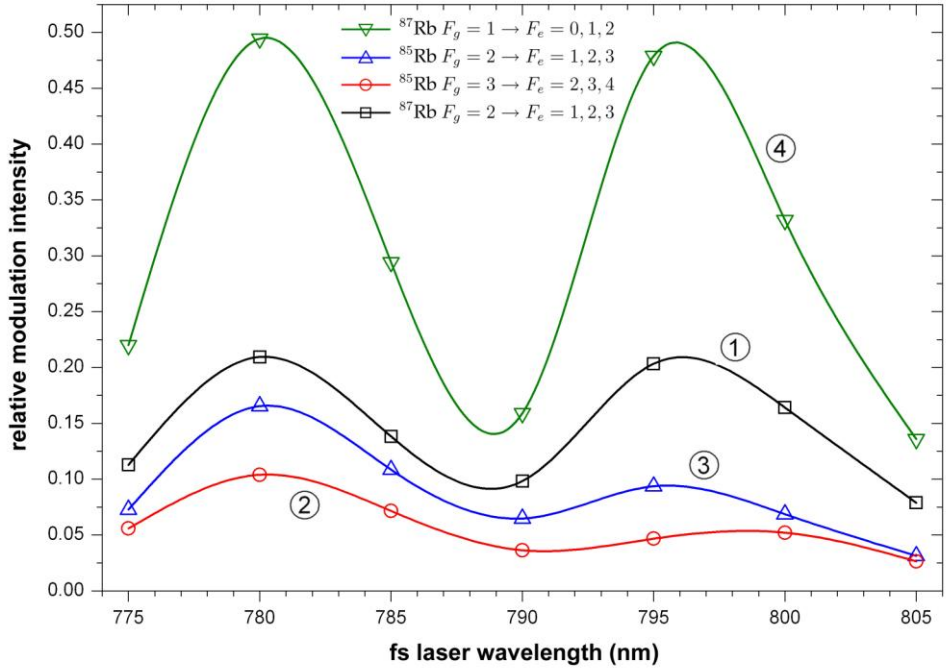

Since the optical pumping process is dependent upon hyperfine energy-level splittings and relative transition dipole moments, mapping of the frequency comb spectrum onto the velocity distribution of hyperfine level populations is not straightforward and a full time-dependent theoretical modeling of atom-laser field interaction is needed for interpretation of the observed phenomena.

Theoretical modeling of the interaction

- resonant excitation of Doppler broaded Rb atoms (room temperature) by a train of fs pulses
- probe laser intensity is small and can be neglected
- idea: **calculate ground state populations** and then use them to construct the absorption spectra of the probe laser

$$E_T(t) = \left[\sum_{n=0}^{N} \mathcal{E}(t - nT_R) e^{in\Phi_R} \right] e^{i\omega_\ell t} = \mathcal{E}_T(t) e^{i\omega_\ell t}$$

Density matrix formalism

- diagonal elements ρ_{nn} represent level populations
- nondiagonal elements ρ_{nm} represent coherences
- starting point: OBE

$$\frac{d\rho_{nm}}{dt} = \frac{-i}{\hbar} [\widehat{H}, \widehat{\rho}]_{nm} - \gamma_{nm}\rho_{nm} \qquad n \neq m$$

$$\frac{d\rho_{nn}}{dt} = \frac{-i}{\hbar} [\widehat{H}, \widehat{\rho}]_{nn} + \sum_{E_m > E_n} \Gamma_{nm}\rho_{mm} - \sum_{E_m < E_n} \Gamma_{mn}\rho_{nn}$$

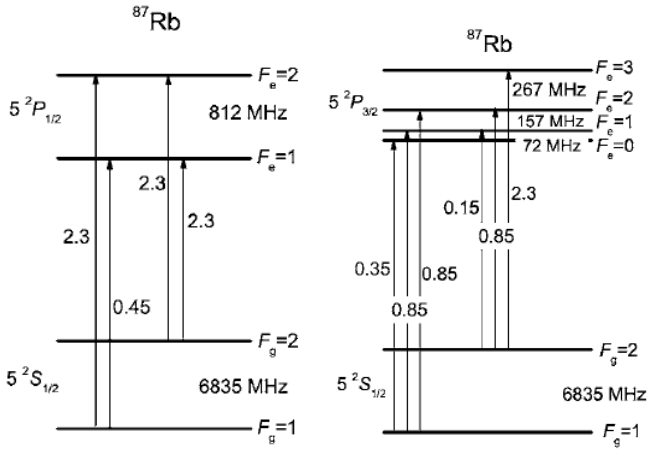

10 coupled DE for 795 nm excitation (4-levels)

21coupled DE for 780 nm excitation (6-levels)

$$\widehat{H} = \widehat{H}_0 + \widehat{H}_{int} \qquad \widehat{H}_{int} = -\mu_{kl} E_T(t) |k\rangle\langle l| \qquad \Gamma_n = \sum_{n' \ (E_{n'} < E_n)} \Gamma_{n'n} \qquad \gamma_{nm} = \frac{1}{2}(\Gamma_n + \Gamma_m) + \gamma_{nm}^{\text{sud}}$$

Coherence accumulation in 4-level Rb atoms

Time evolution of ^{87}Rb ($5S_{1/2}$, $5P_{1/2}$) hyperfine level populations

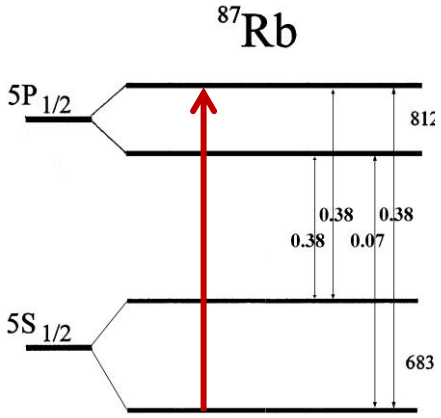

795 nm excitation

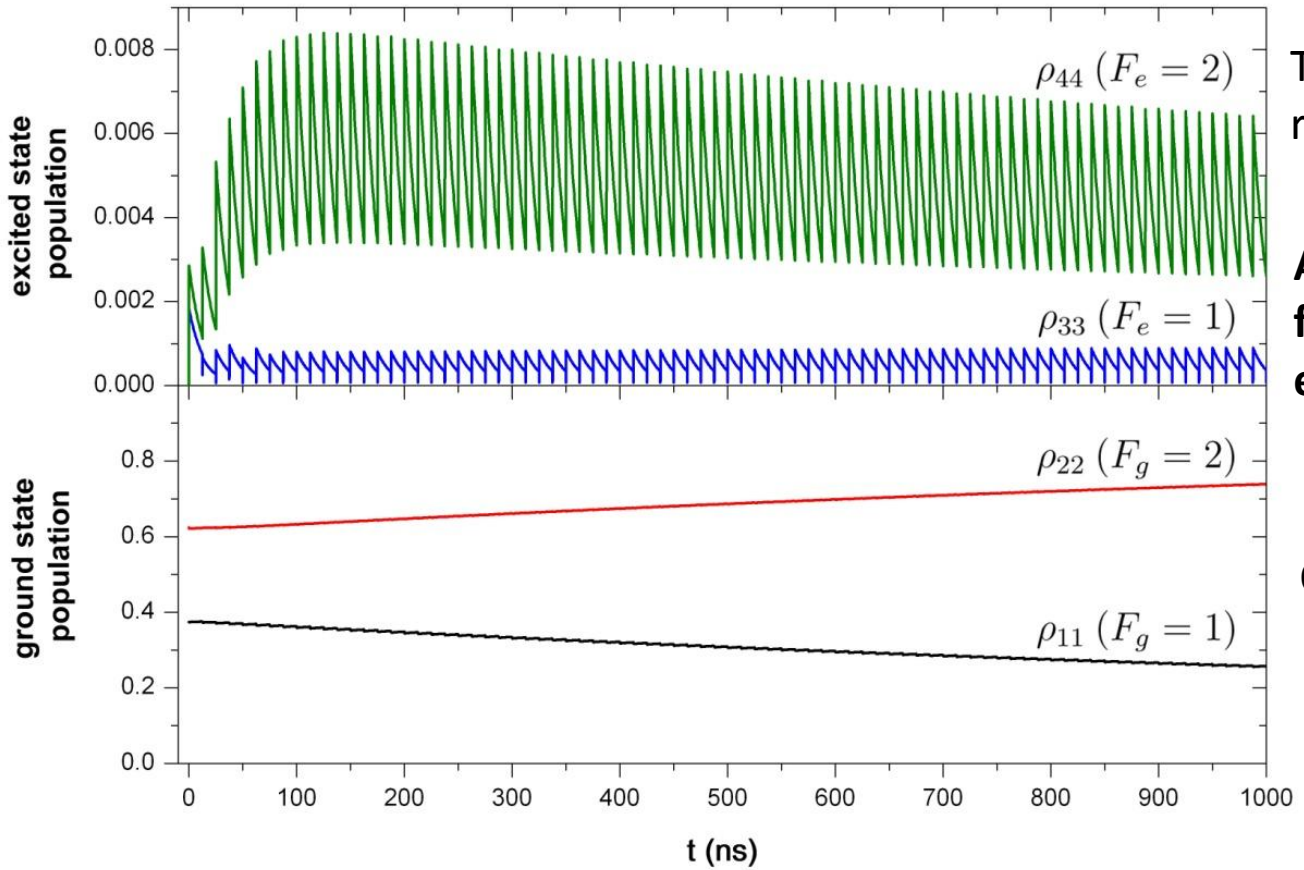

The system can never completely relax between two consecutive pulses

↓

Accumulation of excitation in the form of coherence and excited state population

Optical pumping in ground levels

Time evolution of ^{87}Rb ($5S_{1/2}$, $5P_{1/2}$) hyperfine level populations

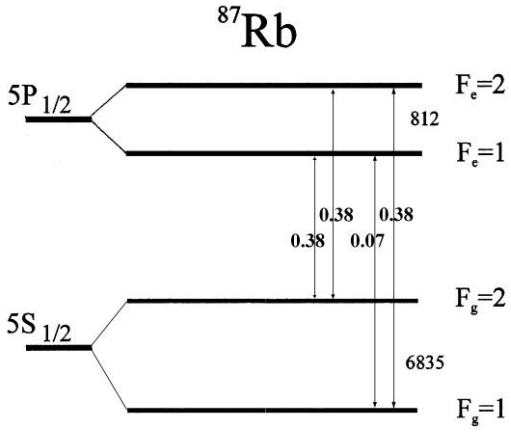

795 nm excitation

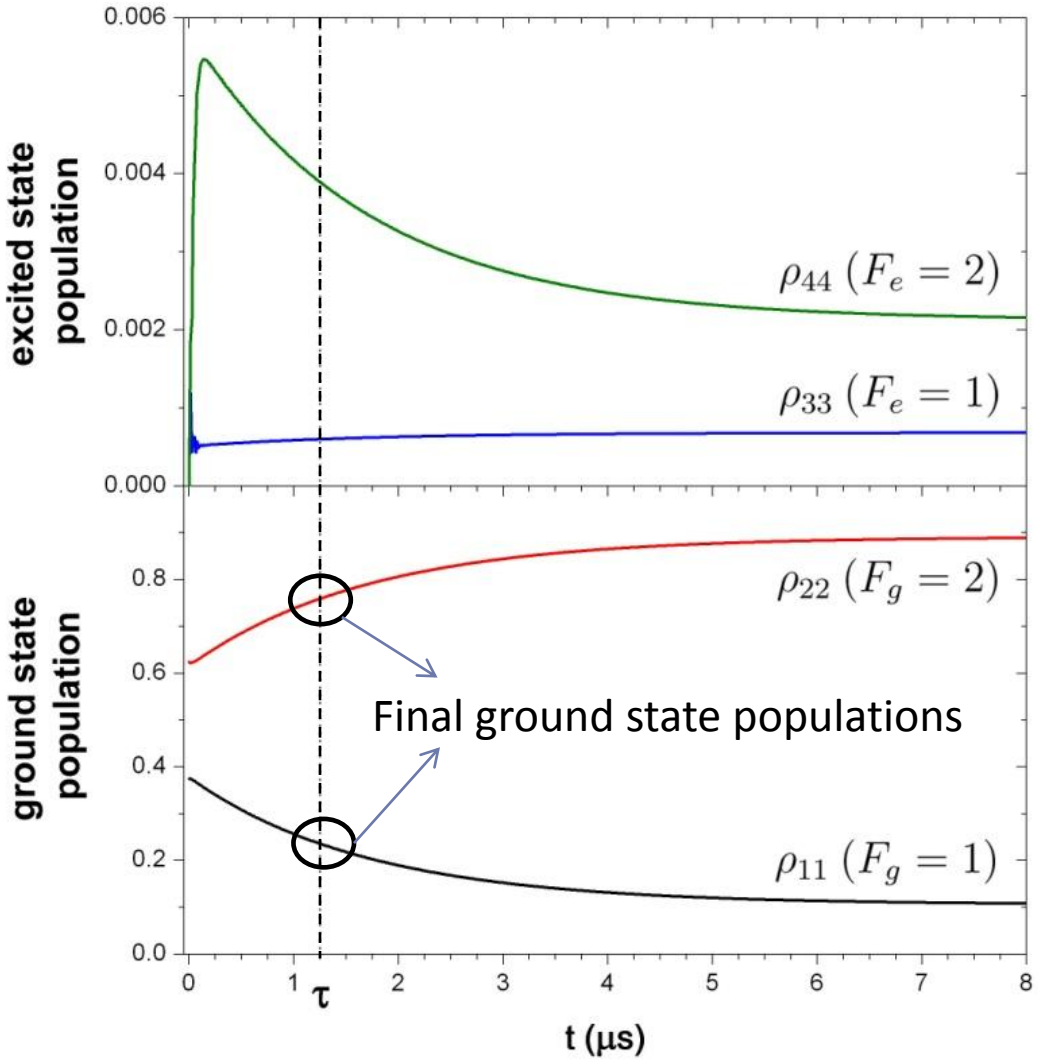

Stationary state –
low excited level
population due to optical pumping.

τ - average interaction time
of atoms with the fs laser.

Optical pumping

FC excitation of the Doppler-broadened atomic transition

Rb vapor at room temperature – Doppler brodening of about 500 MHz

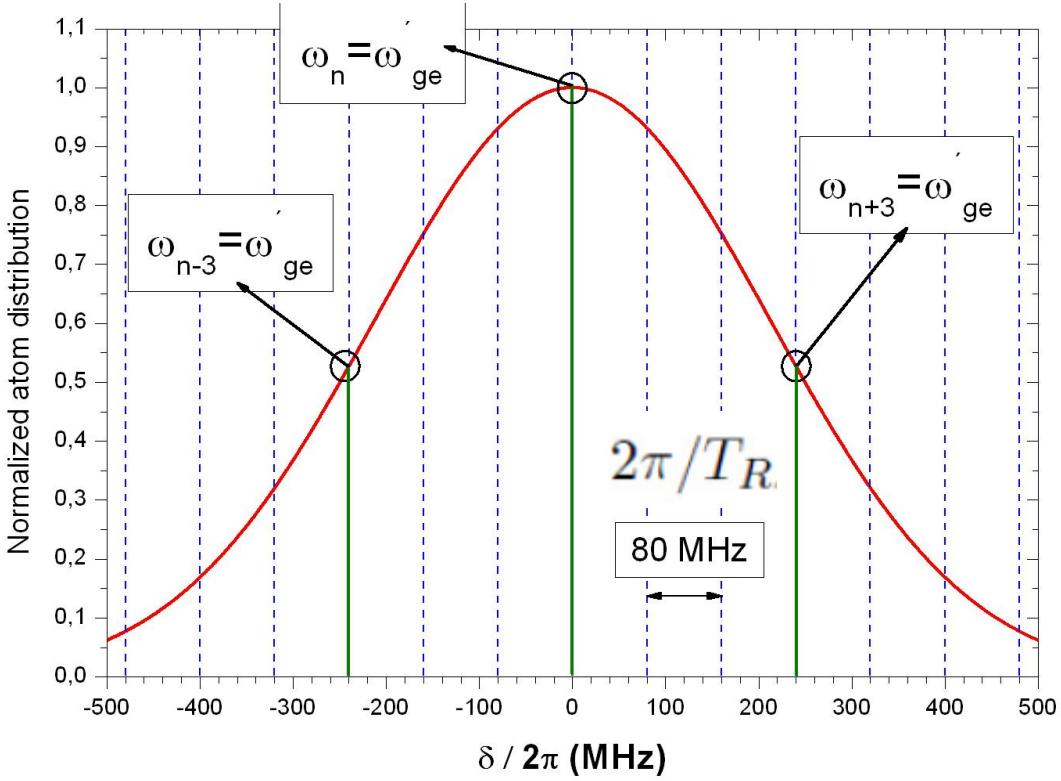

Atoms with different velocities "see" different laser frequency.

$$\omega'_{ge} = \omega_{ge} + \vec{k} \cdot \vec{v}$$

Modified atomic transition frequency

Different velocity groups correspond to different detuning $\delta = \vec{k} \cdot \vec{v}$

They are in different situations with respect to the excitation (accumulation) process.

Resonance condition $\omega_n = \omega'_{ge}$

is satisfied for velocity groups with $\delta = \delta_n \pm 2\pi m/T_R$

Rb D_1 $5S_{1/2}$-$5P_{1/2}$ excitation @ 795 nm

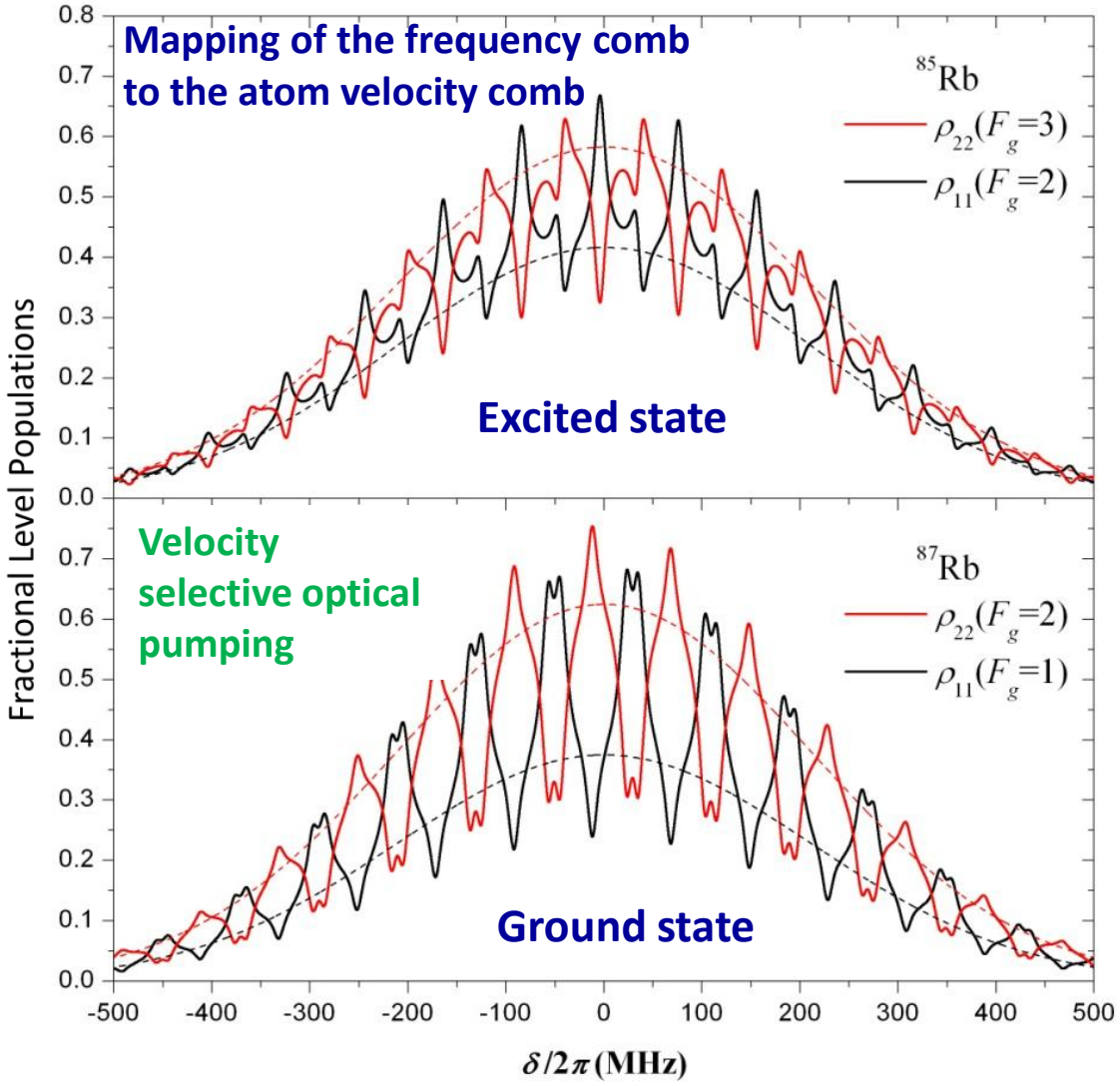

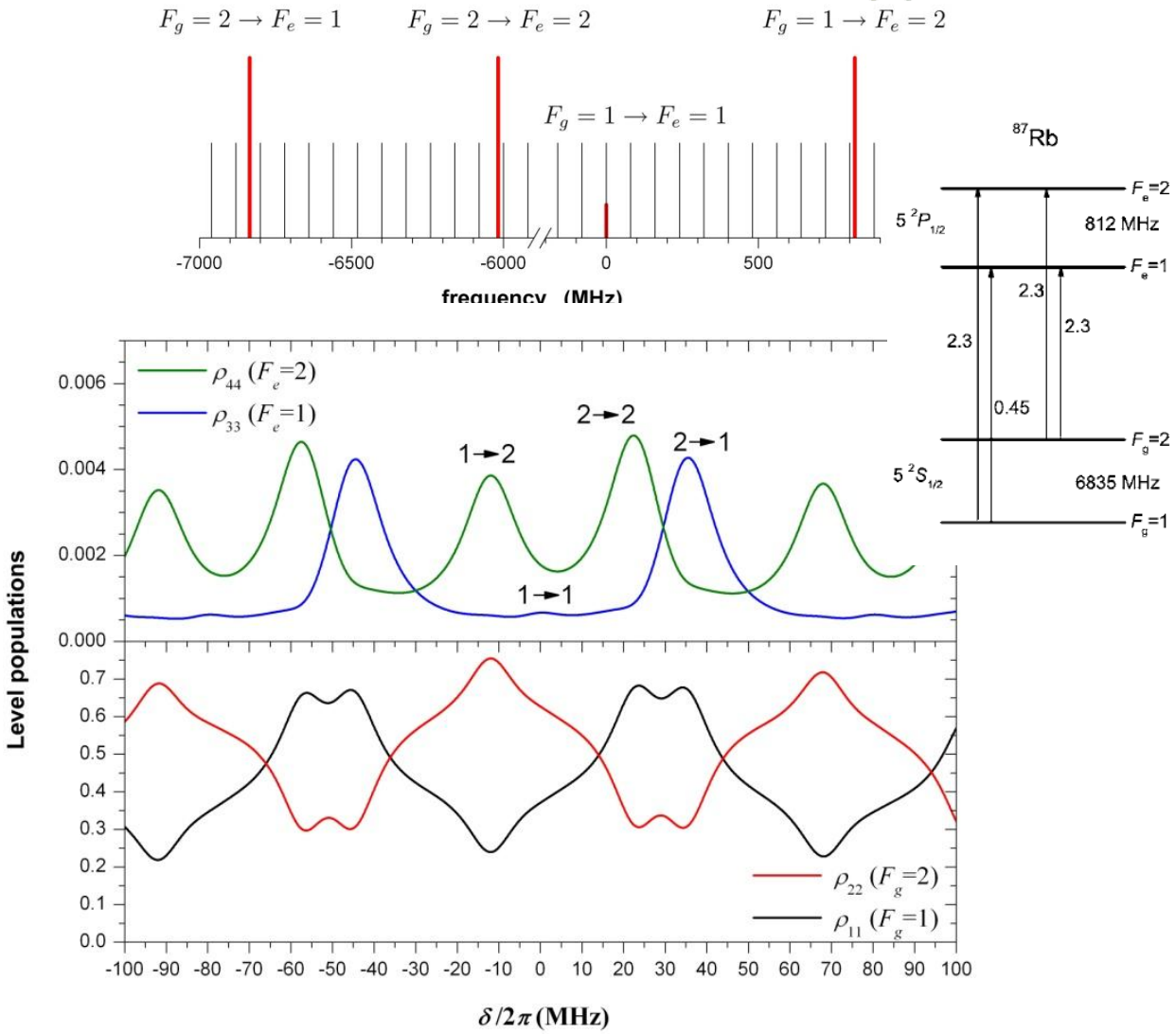

Rb D_2 $5S_{1/2}$-$5P_{3/2}$ excitation @ 780 nm

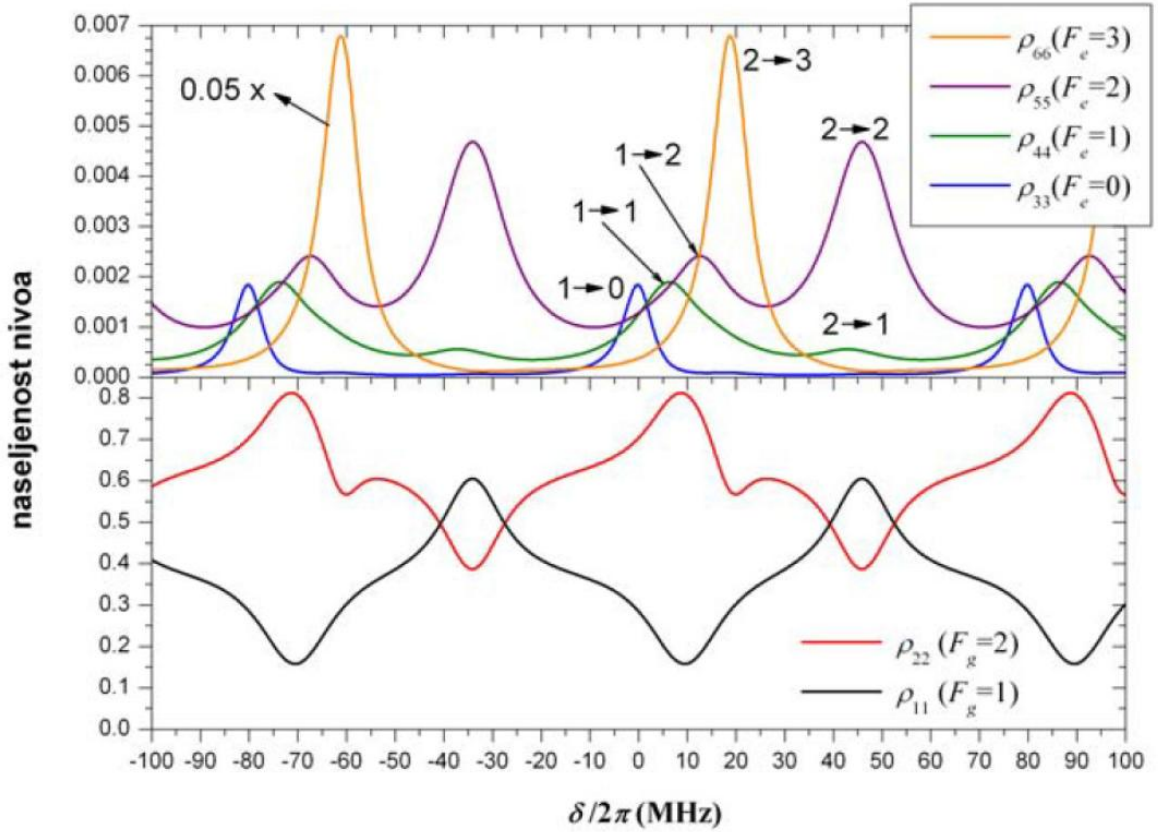

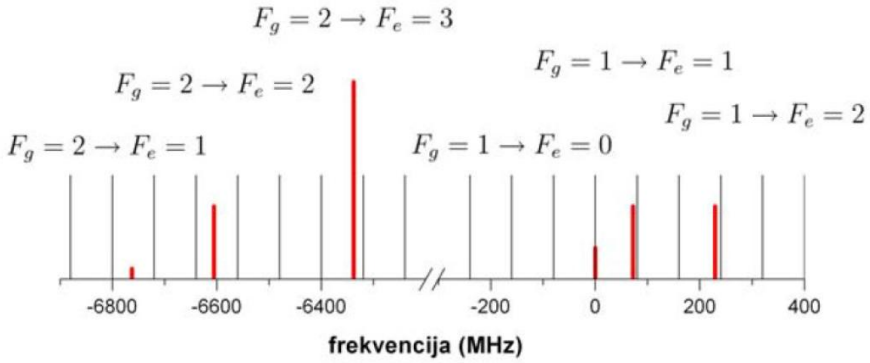

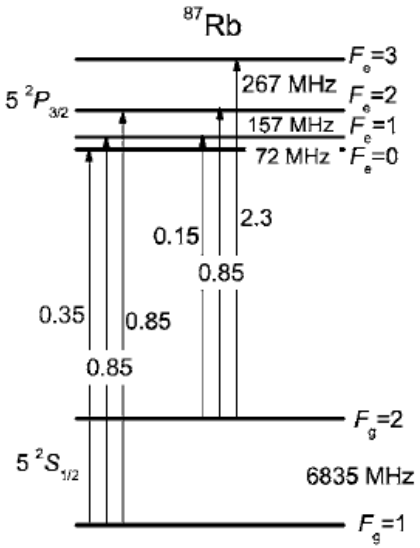

Simulation of $5S_{1/2}$-$5P_{3/2}$ line absorption spectrum (probe)

Hyperfine resolution absorption spectrum of Rb D_2 $5S_{1/2}$ - $5P_{3/2}$ line

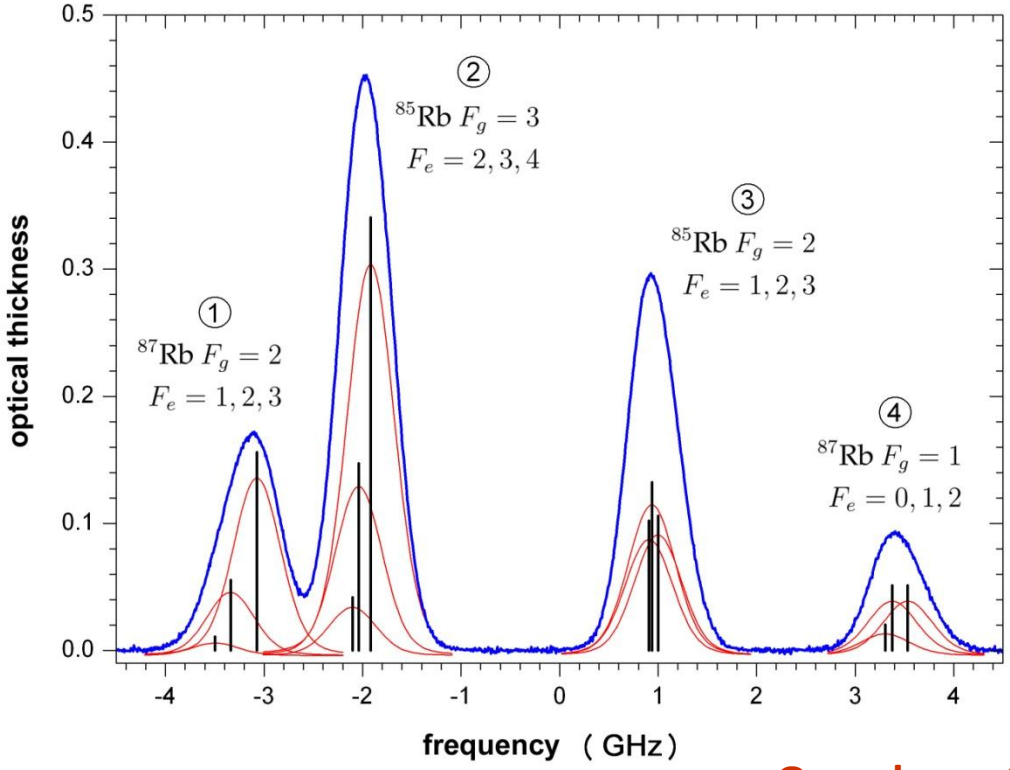

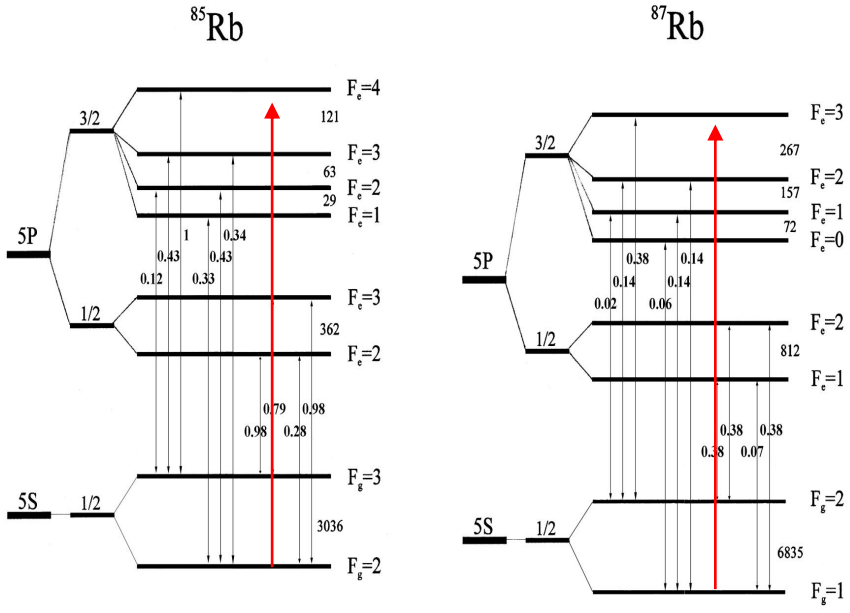

One absorption line – three hyperfine transitions

One hyperfine transition - convolution of the velocity distribution of the ground state population with the Lorentzian profile of natural linewidth

One absorption line - adding the contributions of three hyperfine components.

Simulation of $5S_{1/2}$-$5P_{3/2}$ line absorption spectrum (probe)

Simulation of absorption spectrum

^{87}Rb $5S_{1/2}$ (F_g=1) - $5P_{3/2}$ (F_e=0,1,2) hyperfine line

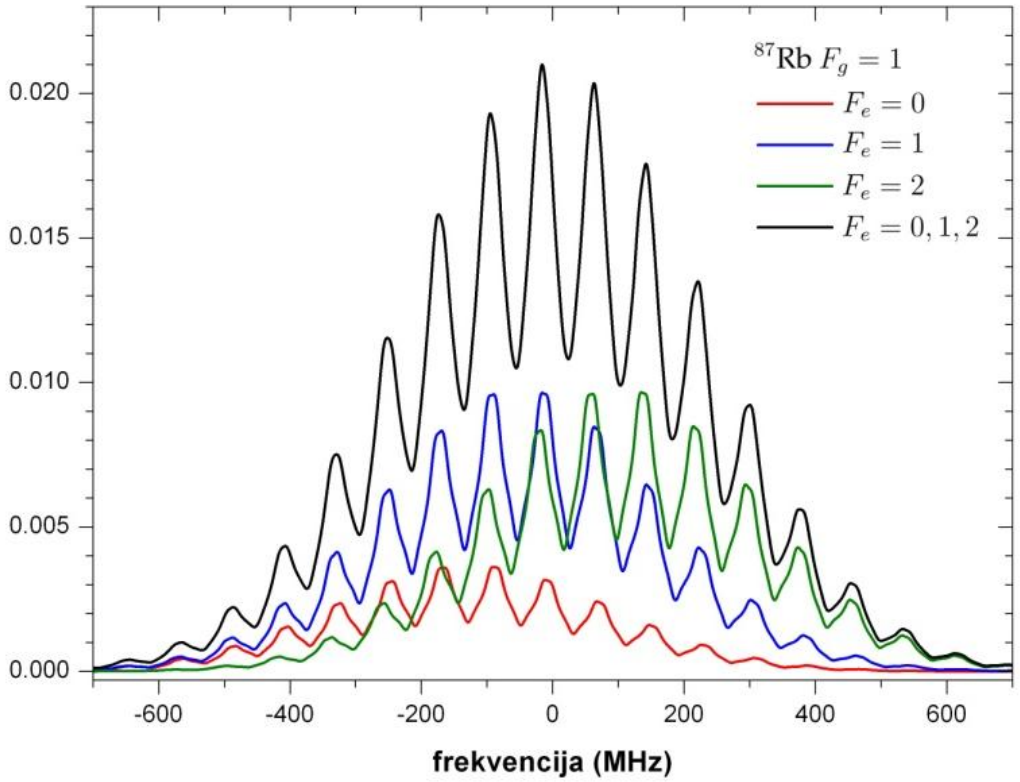

Simulation of absorption spectrum

^{85}Rb $5S_{1/2}$ (F_g=2) - $5P_{3/2}$ (F_e=1,2,3) hyperfine line

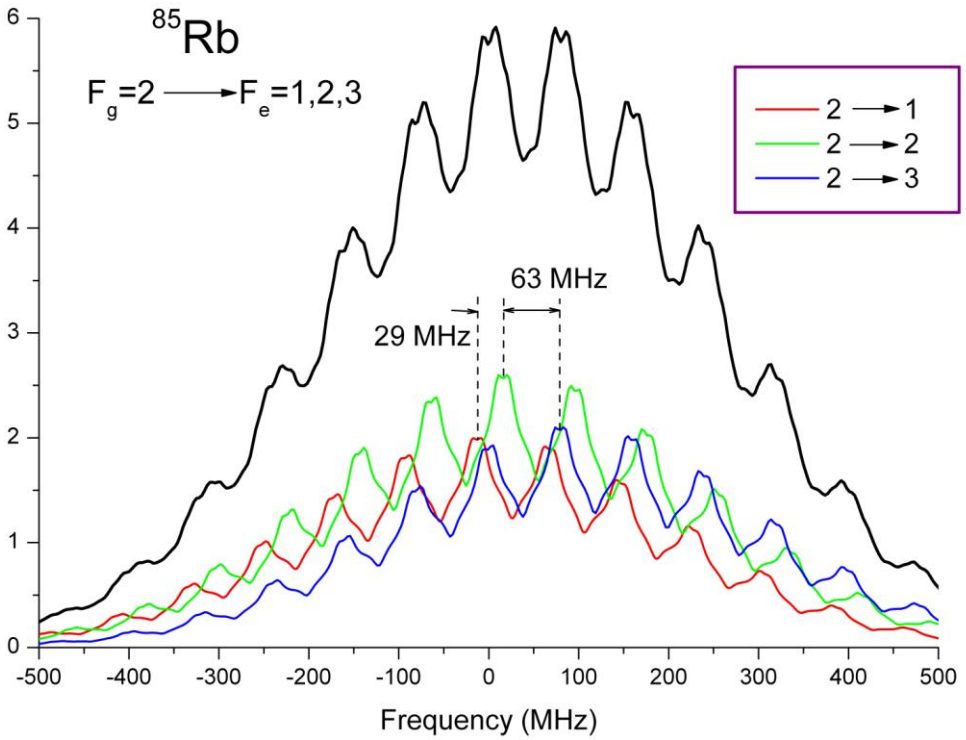

Rb ground and excited states hyperfine level populations are determined by the hyperfine energy splittings and relative transition probabilities with a periodic behavior given by the mode separation in the frequency comb.

Measured optical thickness is proportional to the ground states populations.

Experiment vs theory

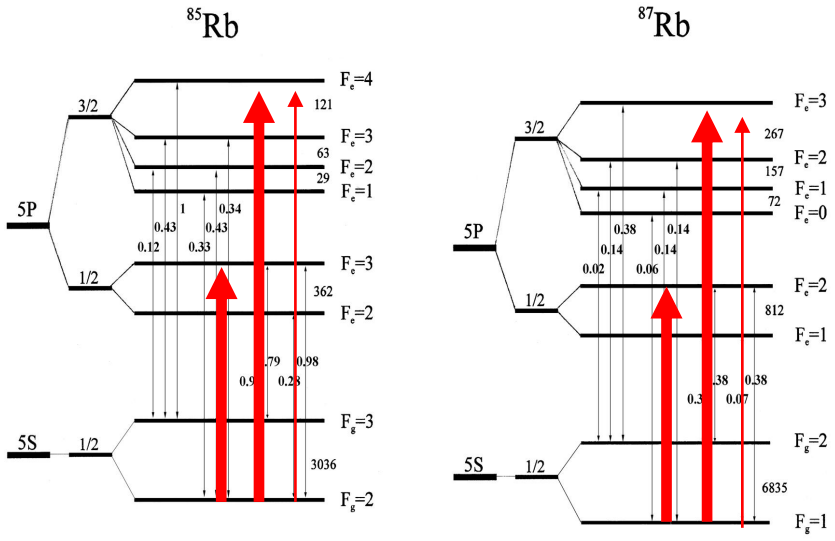

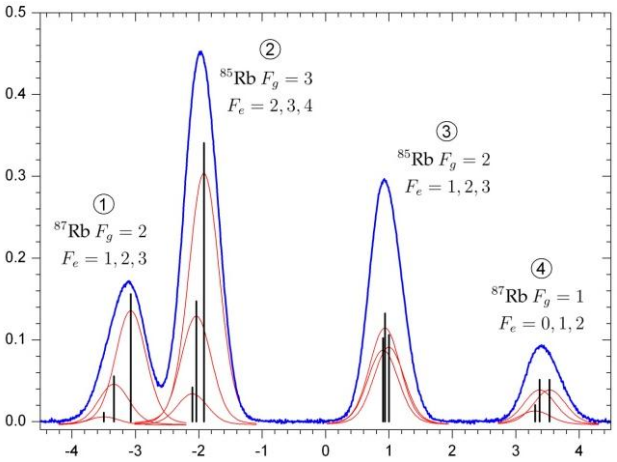

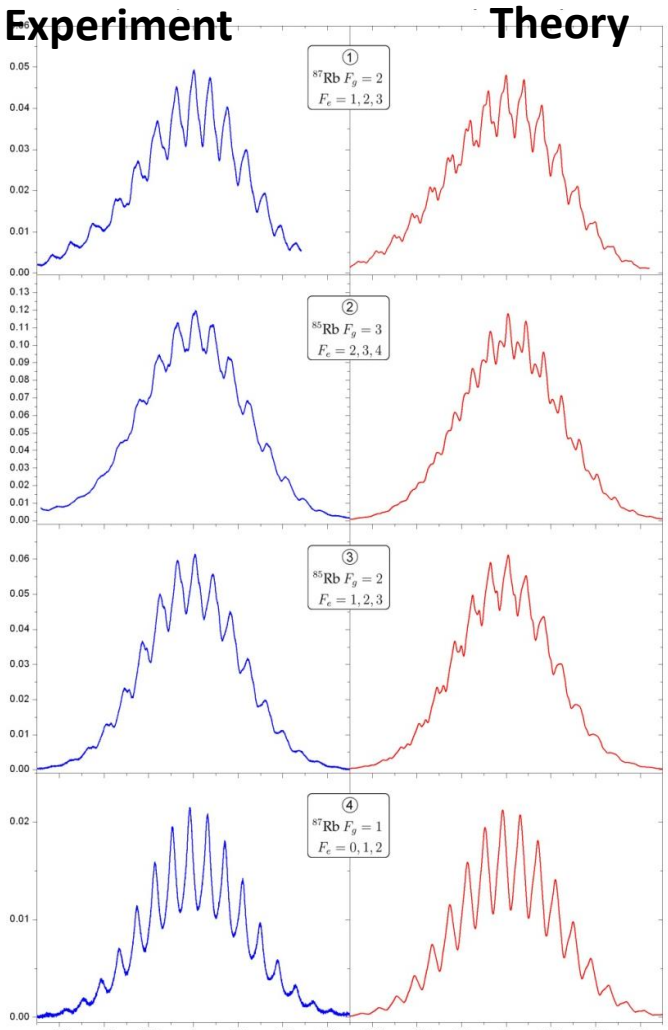

$5S_{1/2}$ - $5P_{1/2}$ fs excitation @ 795 nm

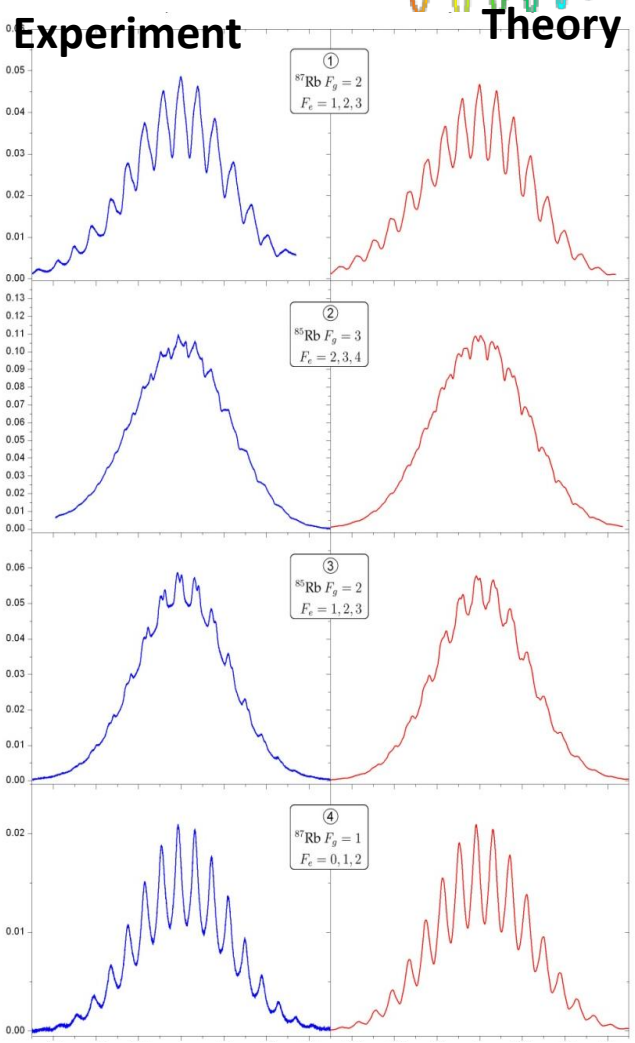

$5S_{1/2}$ - $5P_{3/2}$ fs excitation @ 780 nm

Experiment - lock-in detection

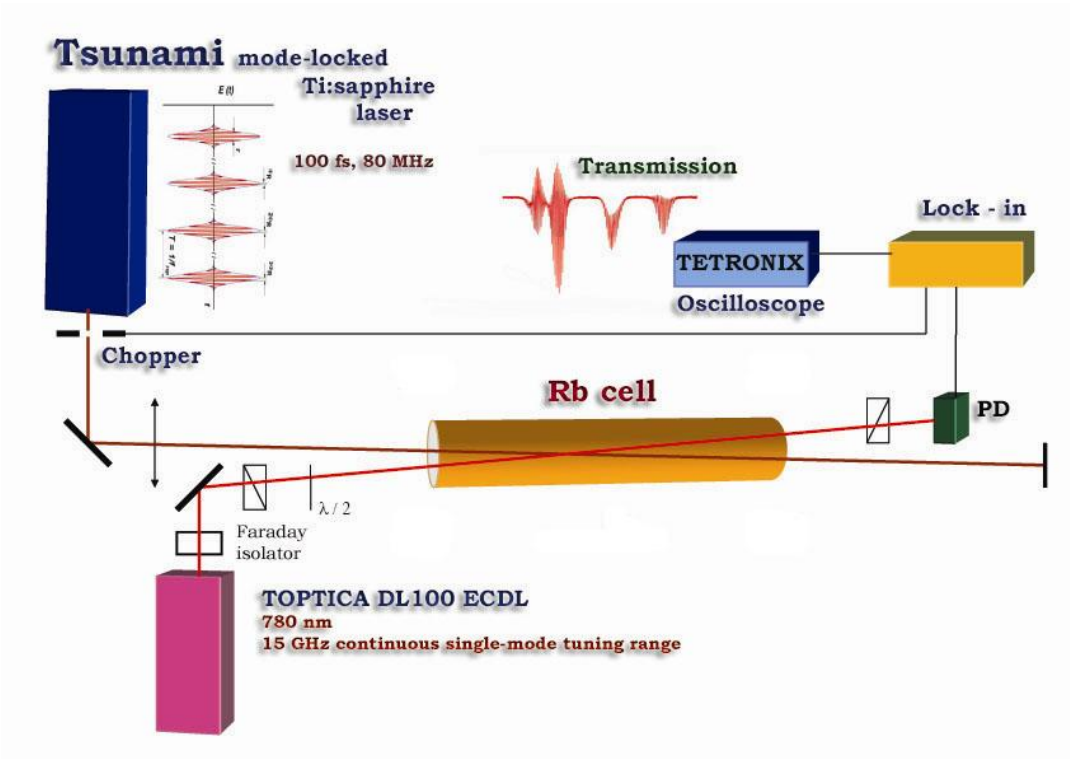

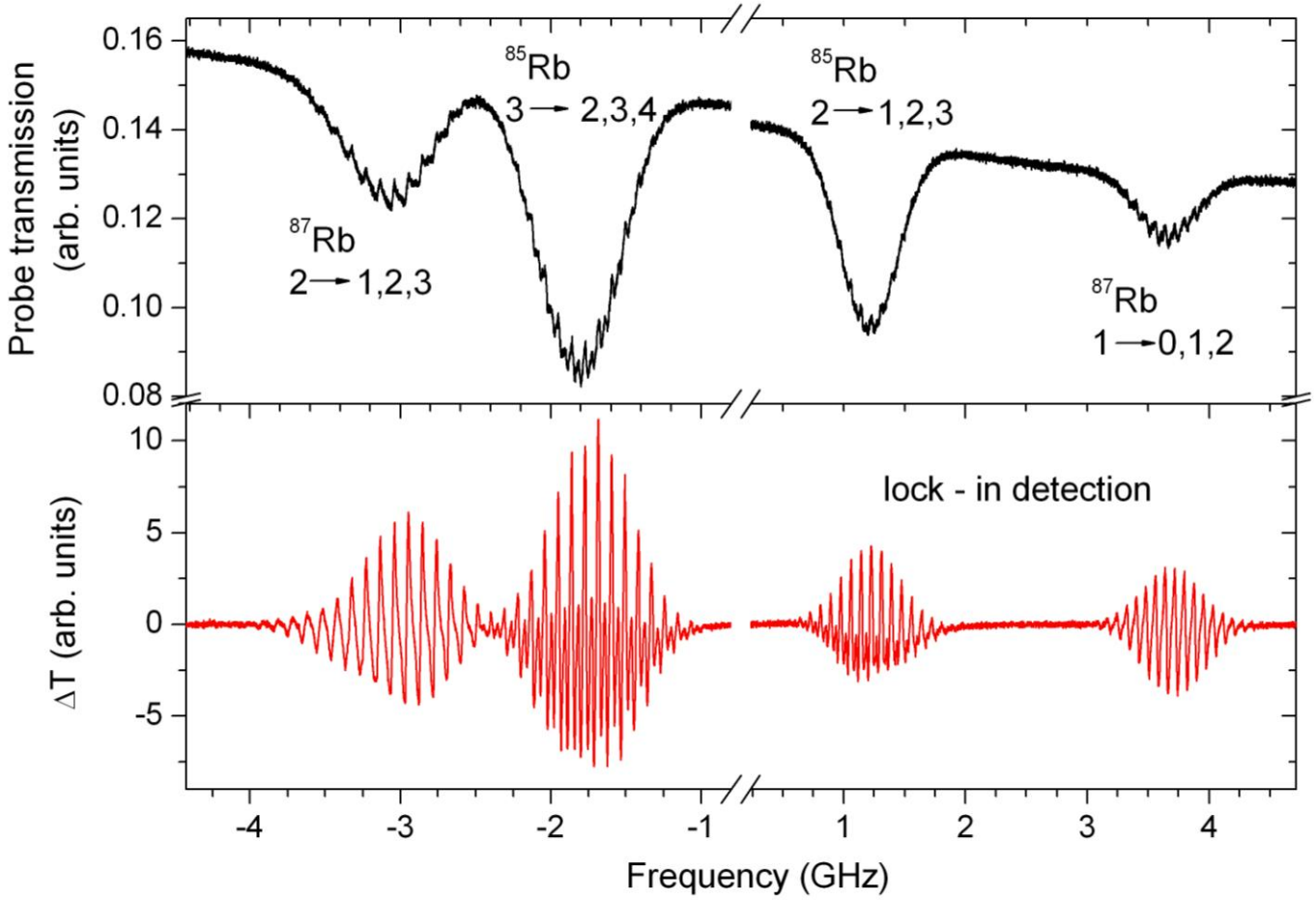

Experiment - fs laser wavelength dependence

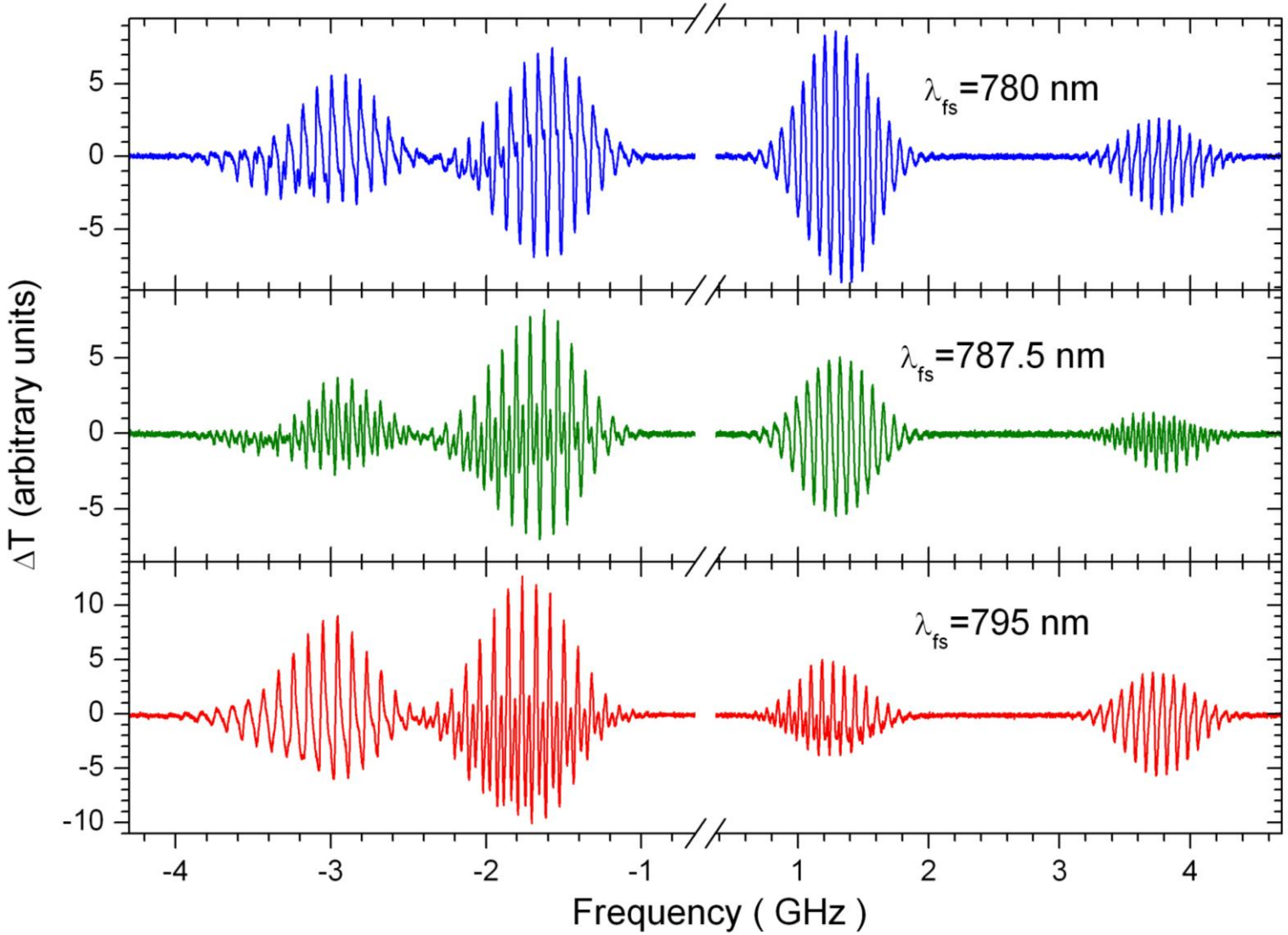

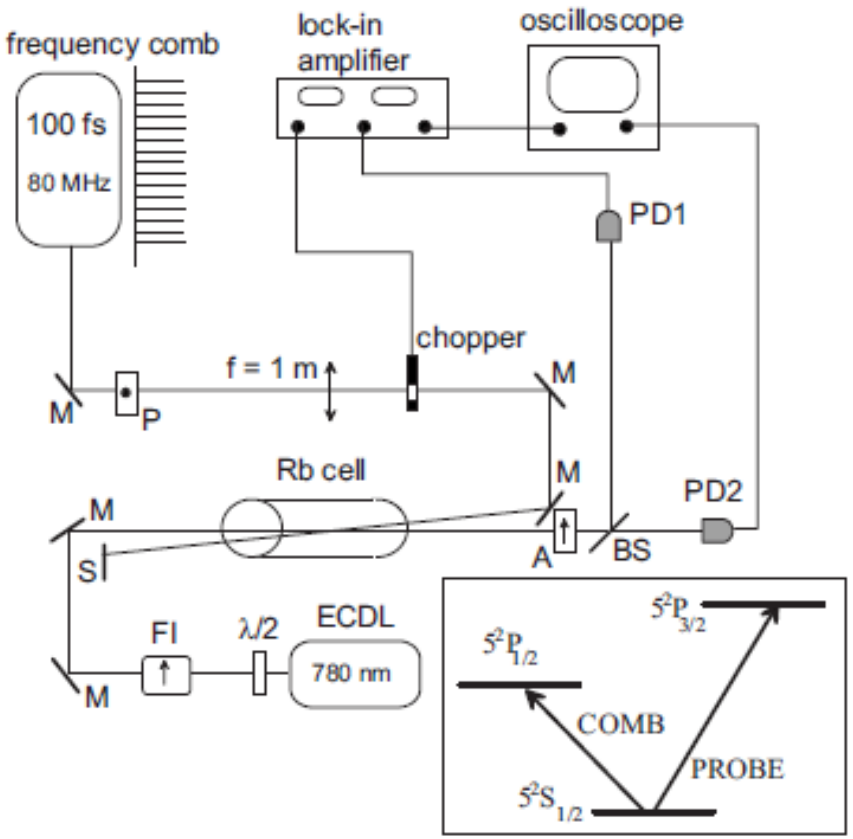

probe laser power dependence

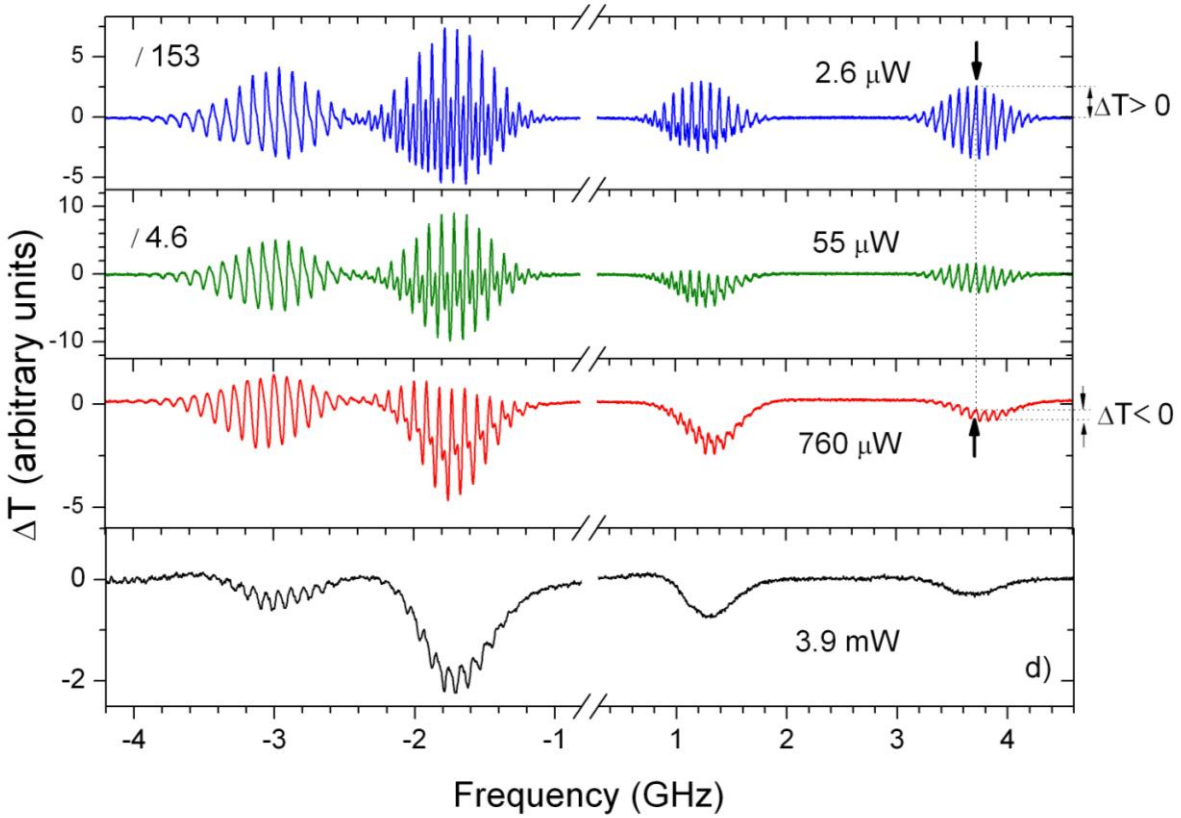

high power probe - cancellation of coherence accumulation effects!

1. Cancellation of the coherent accumulation

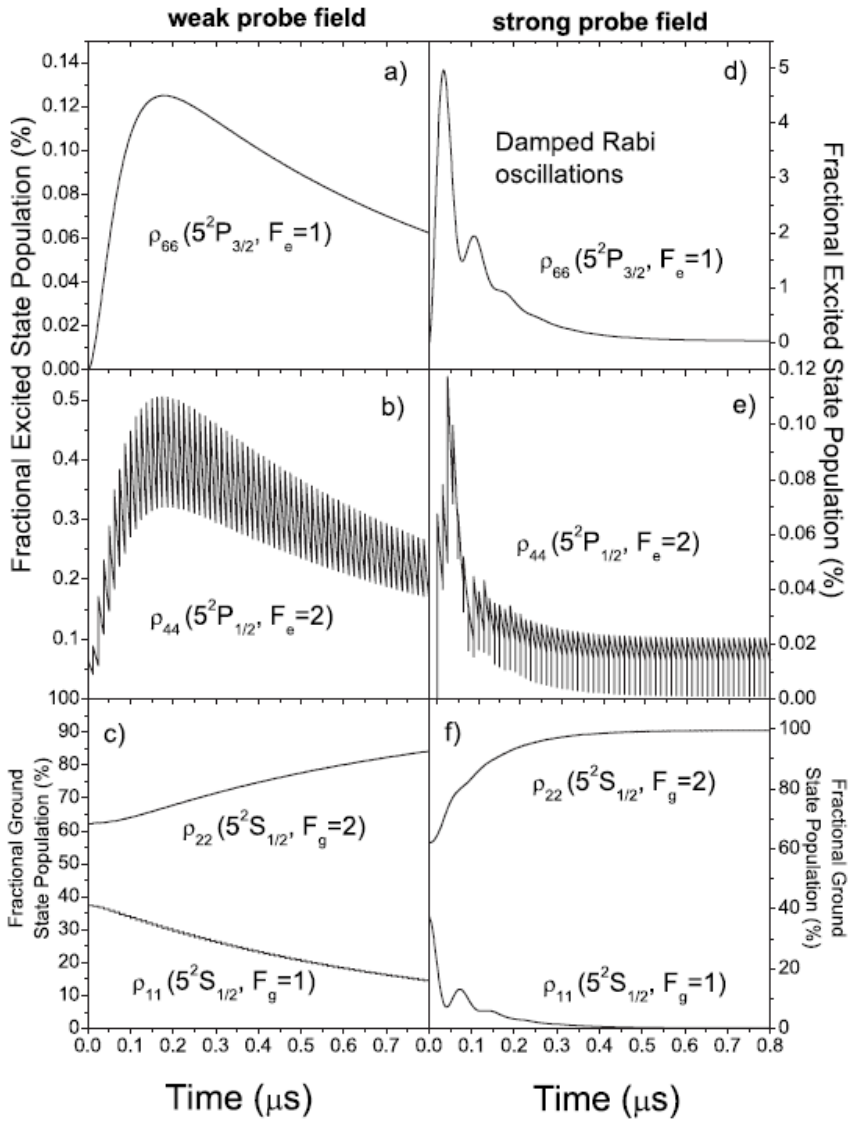

Strong cw laser serve as a switch from the pulse-train to pulse-by-pulse type of interaction.

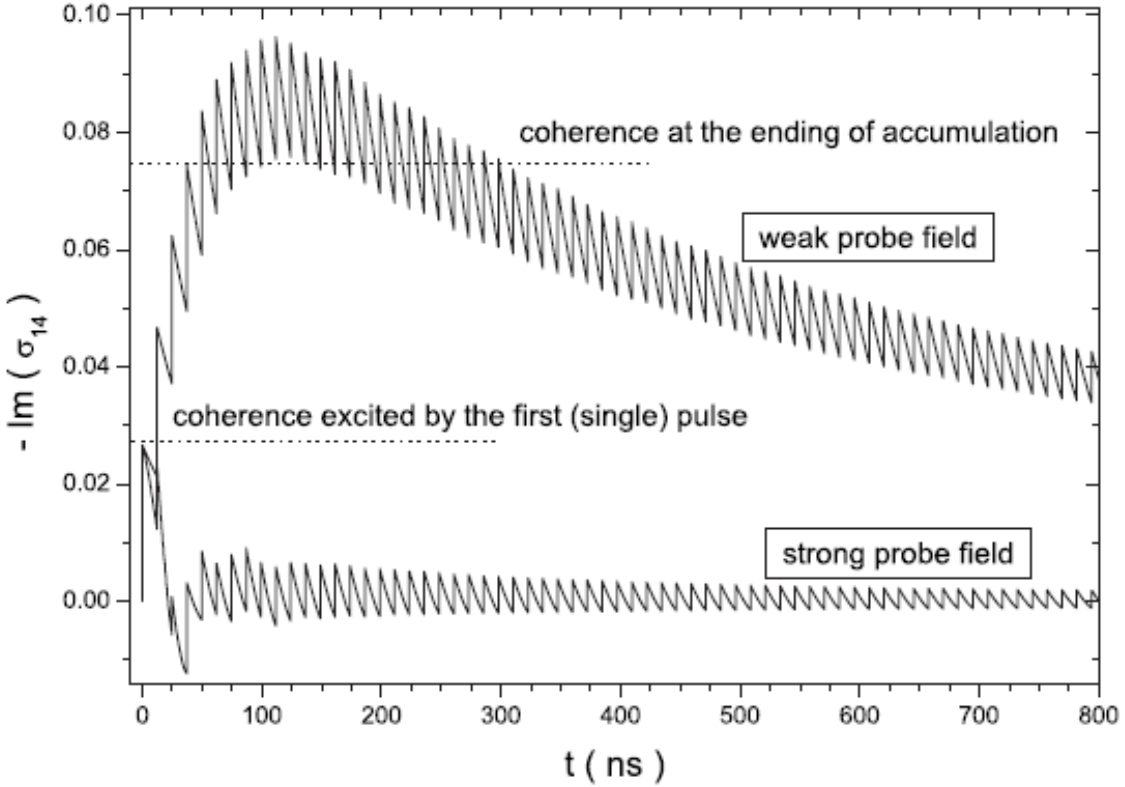

T. Ban, D. Aumiler, H. Skenderović, S. Vdović, N. Vujičić, and G. Pichler PRA 76, 043410 (2007).

2. Characterization of an frequency comb

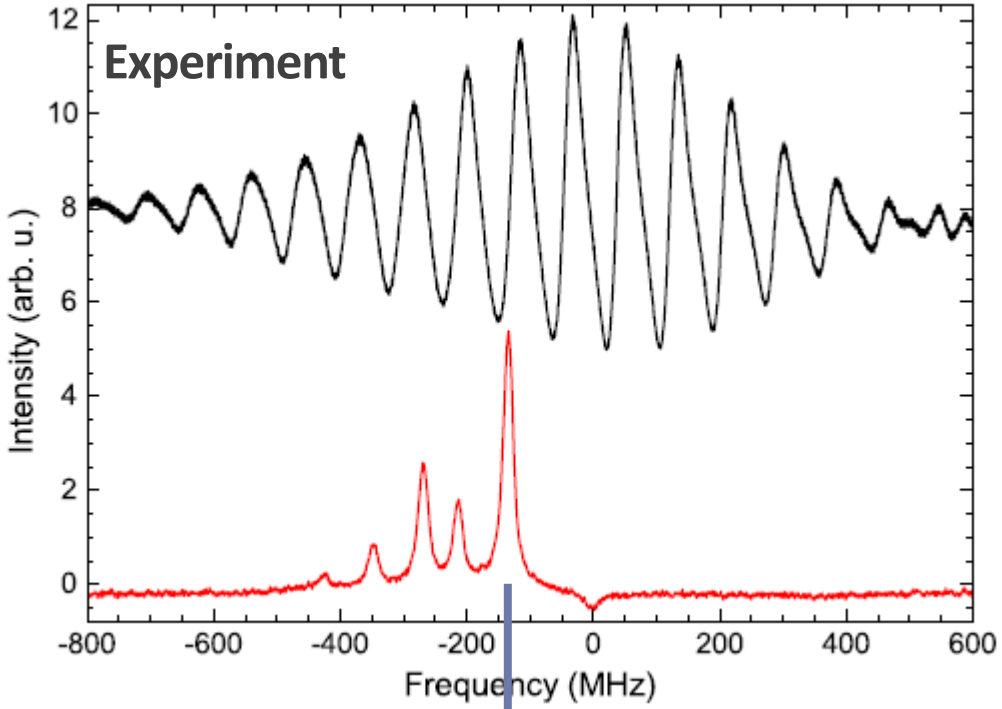

Rb saturation spectroscopy
accurate calibration of the absolute frequency scale.

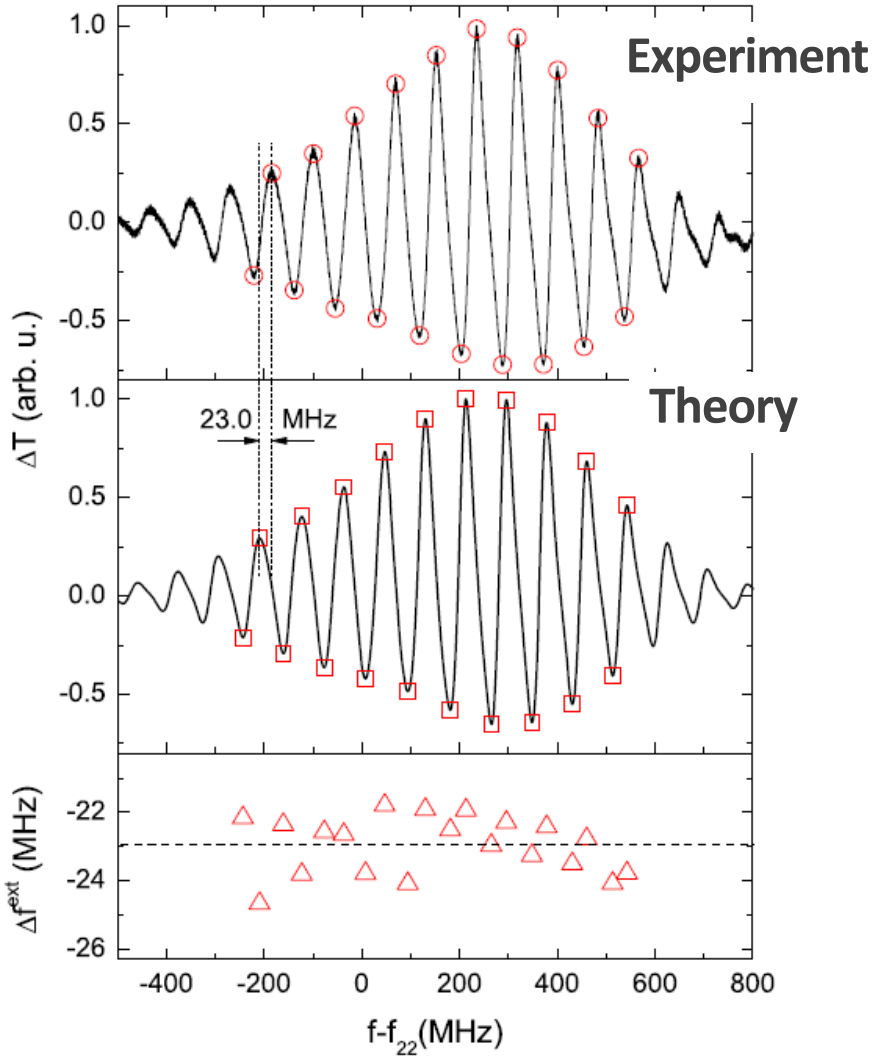

D. Aumiler, T. Ban, N. Vujičić, S. Vdović, H. Skenderović, and G. Pichler
Appl. Phys. B 97, 553 (2009).

3. Excitation by a train of 0π pulses

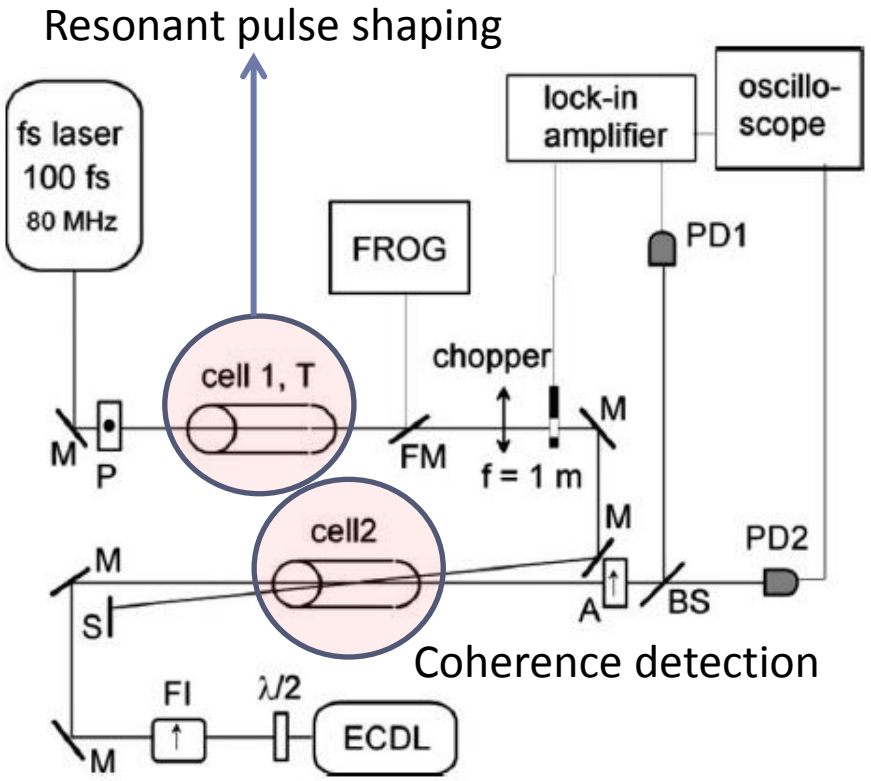

The 0π pulse shaping is achieved as a result of the natural fs pulse reshaping induced by linear dispersion of the absorption line by propagation of resonant weak fs pulses through the rubidium vapor.

Excitation: train of resonantly shaped 0π pulses
Characterization: frequency-resolved optical gating FROG
Interaction monitoring: modified DFCS

T. Ban, D. Aumiler,, S. Vdović, N. Vujičič, H. Skenderović, and G. Pichler PRA 80, 023425 (2009).

Pulse shaping

Phase, intensity and polarization

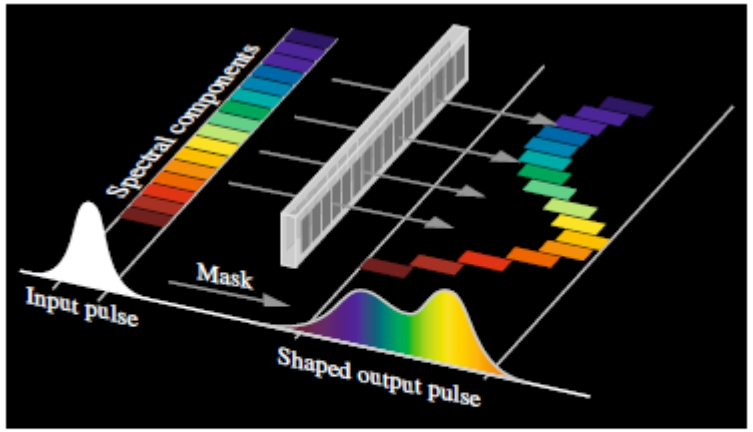

Fig. 12.13 Schematic illustration of shaping the temporal profile of an ultrashort laser pulse by retardation of the spectrally dispersed individual wavelength components in a phase only LC-SLM. The LC-SLM is located in the Fourier plane of the setups displayed in Figs. 12.10 and 12.11

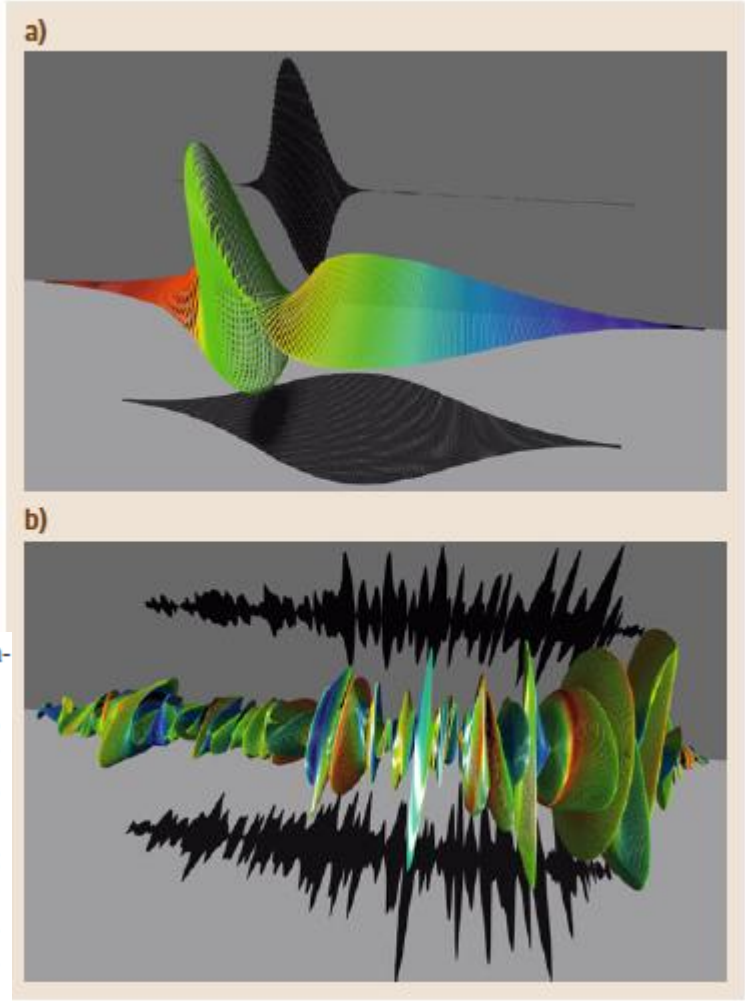

Fig. 12.14a, b Electric field representation for a polarization-modulated laser pulse. Time evolves from *left* to *right*, and electric field amplitudes are indicated by the sizes of the corresponding ellipses. The momentary frequency can be indicated by *colors*, and the *shadows* represent the amplitude envelopes of the orthogonal electric field components. **(a)** A Gaussian-shaped laser spectrum supporting 80 fs laser pulses is taken for an illustrative theoretical example. **(b)** A complex experimentally realized polarization modulated laser pulse is shown. The width of the temporal window is 7.5 ps. (After [12.78])▶

Evolutionary algorithm

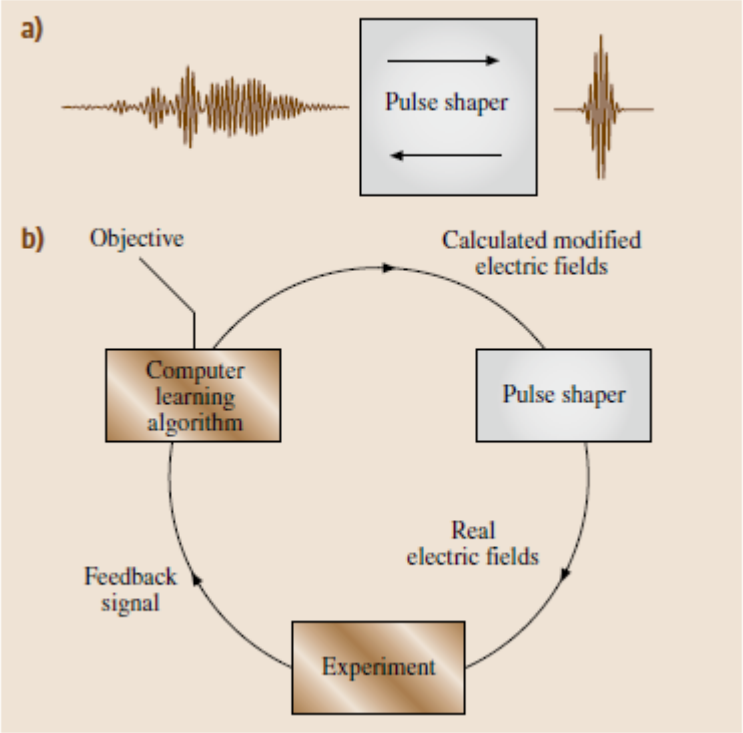

M. Wollenhaupt, A. Assion, T. Baumert, Short and Ultrashort Laser Pulses, Springer Handbook of Lasers and Optics pp 1047-1094, 2012.

Propagation of an fs pulse through the resonant rubidium vapor

Propagation in the frequency domain

$$\tilde{E}(\omega,z) = \tilde{E}(\omega,0)e^{-ik(\omega)z}$$

$$k(\omega) = \frac{\omega}{c}n(\omega)$$

complex Fourier transform of the pulse electric field, taken as a real hyperbolic-secant function

FT $^{-1}$

The large extension of the pulse wing followed by the oscillatory structure of the electric field Envelope at higher Rb atom number densities (ringing in the pulse tail).

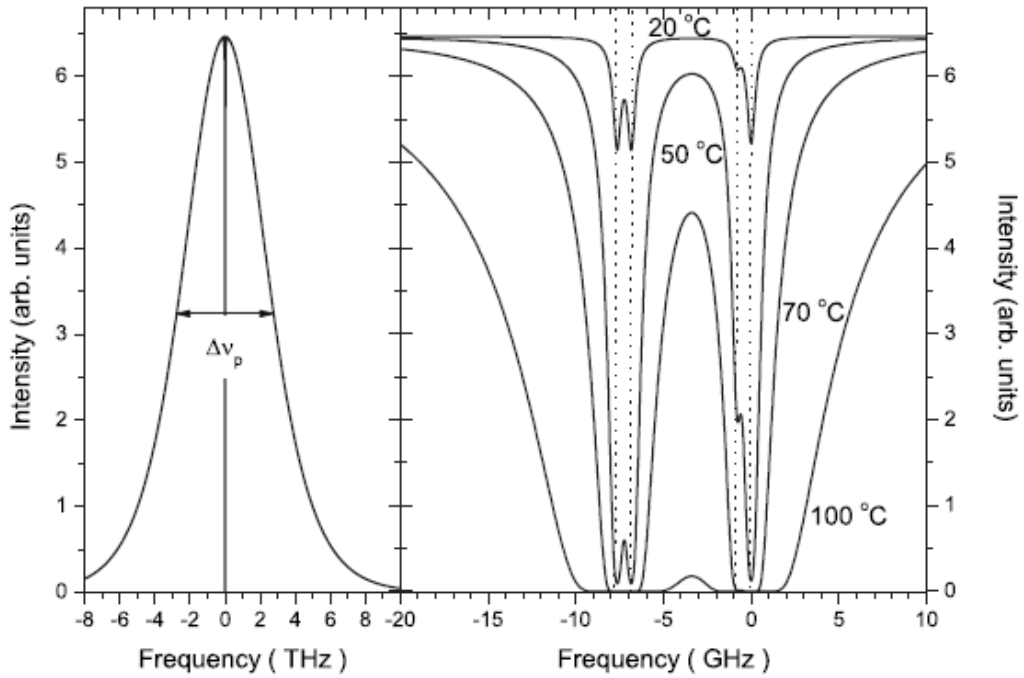

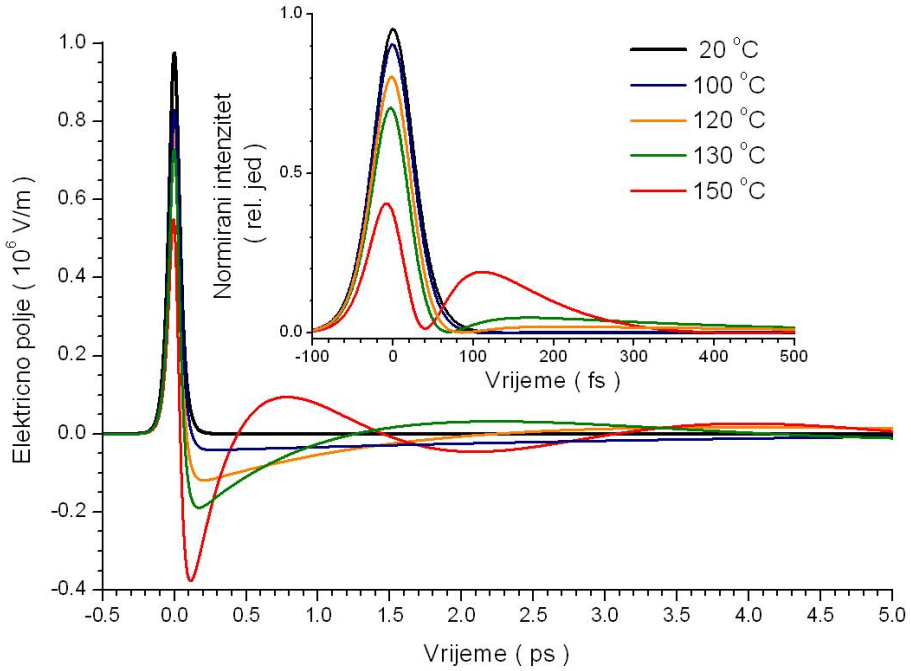

Electric field in the time domain

Low energy pulses, low density vapour

FROG - frequency-resolved optical gating

SHG FROG

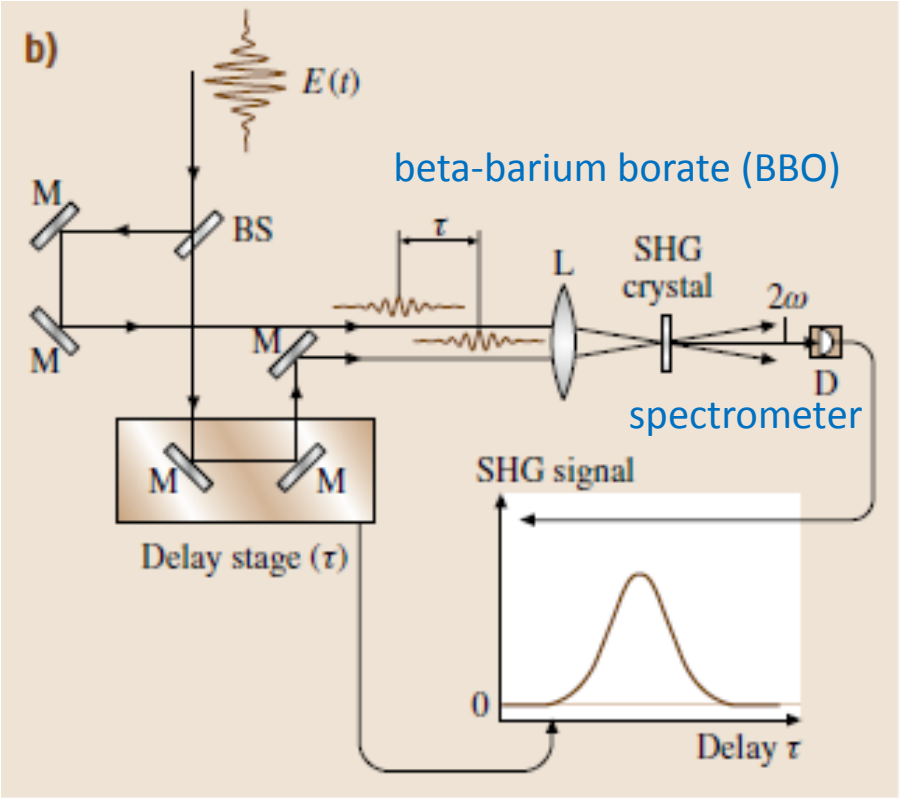

Intensity autocorrelation

Measuring the spatial overlap of the two pulses requires a nonlinear process to generate a detection signal proportional to the intensity product.

The intensity autocorrelation provides only limited information on the pulse shape, because there are infinitely many symmetric and asymmetric pulse shapes that lead to very similar symmetric autocorrelation traces.

Second-Harmonic-Generation (SHG) FROG.

$$I_{\mathrm{FROG}}^{\mathrm{SHG}}(\omega,\tau) = \left| \int_{-\infty}^{\infty} E_c(t) E_c(t-\tau) e^{-i\omega t}\, dt \right|^2$$

FROG - examples

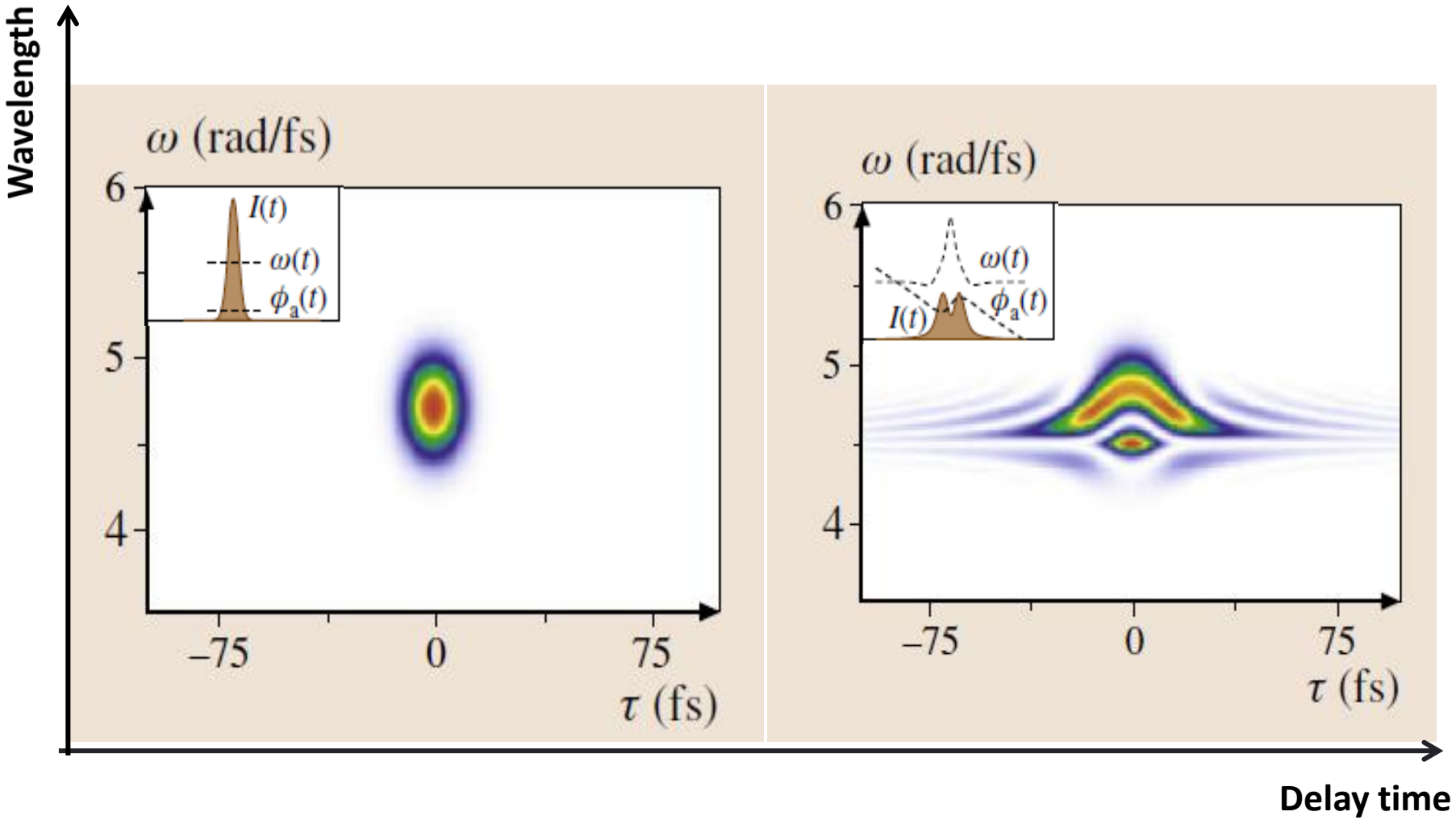

FROG – 0π pulses

Experimental set-up

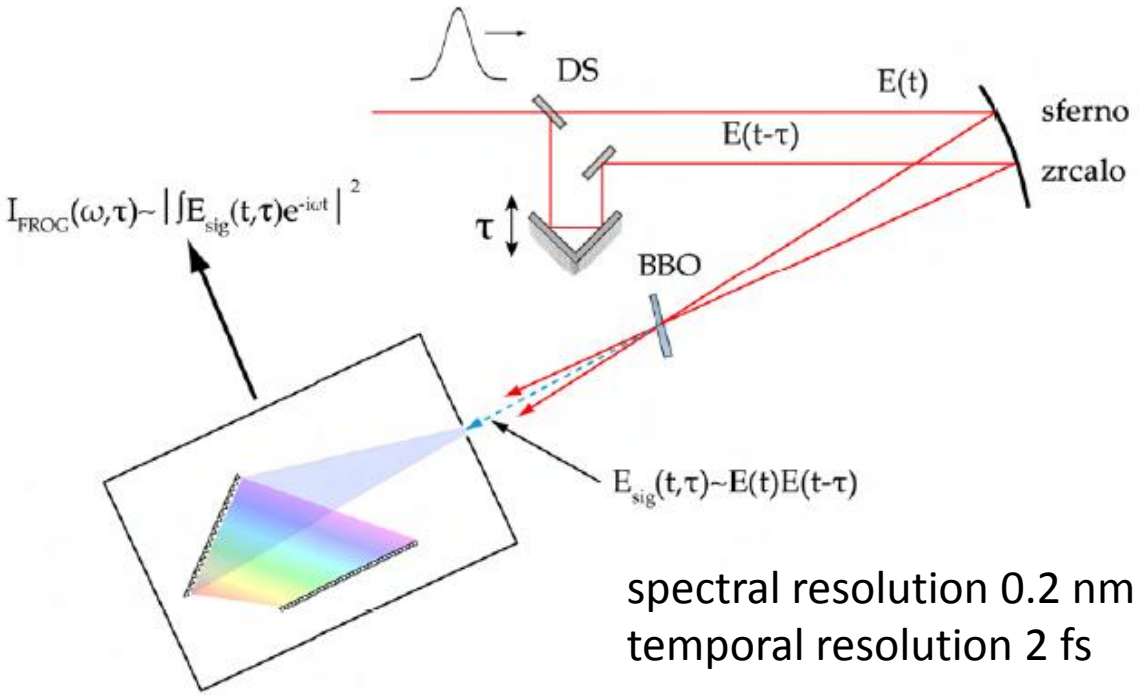

spectral resolution 0.2 nm
temporal resolution 2 fs

Ocean Optics HR2000

FROG

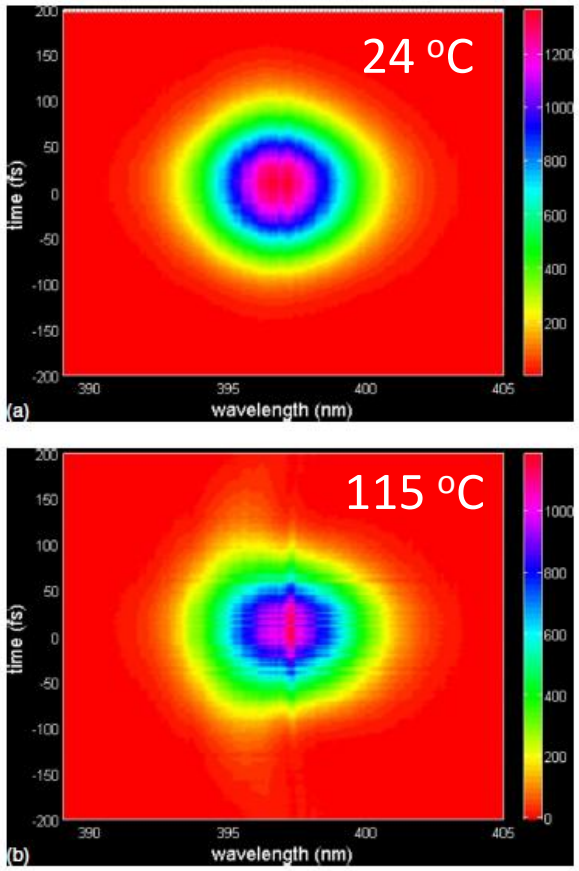

Effect of weak shaping could not be observed in FROG traces

Coherent accumulation effects - OBE

Time domain

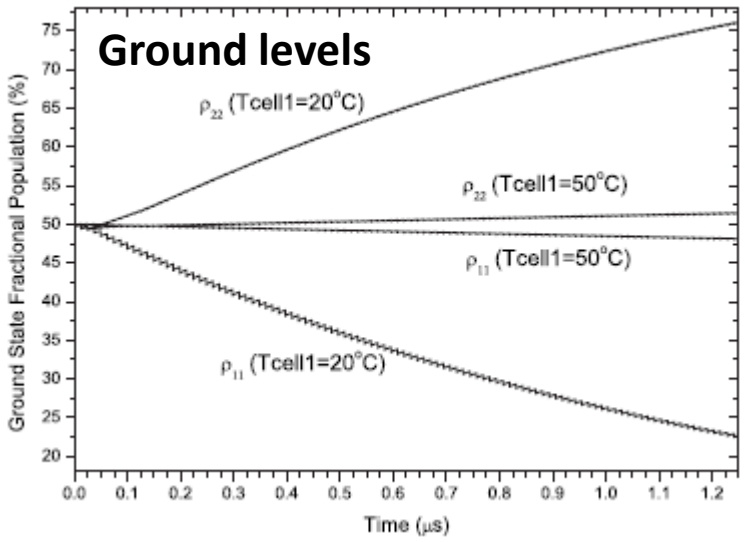

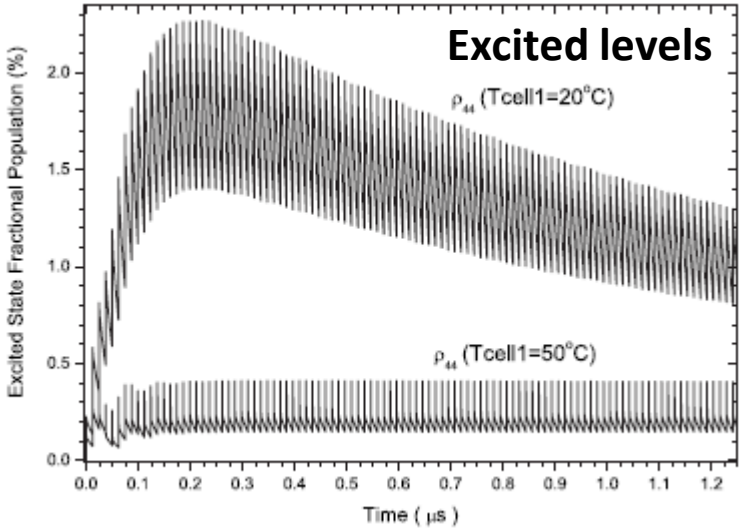

Frequency domain

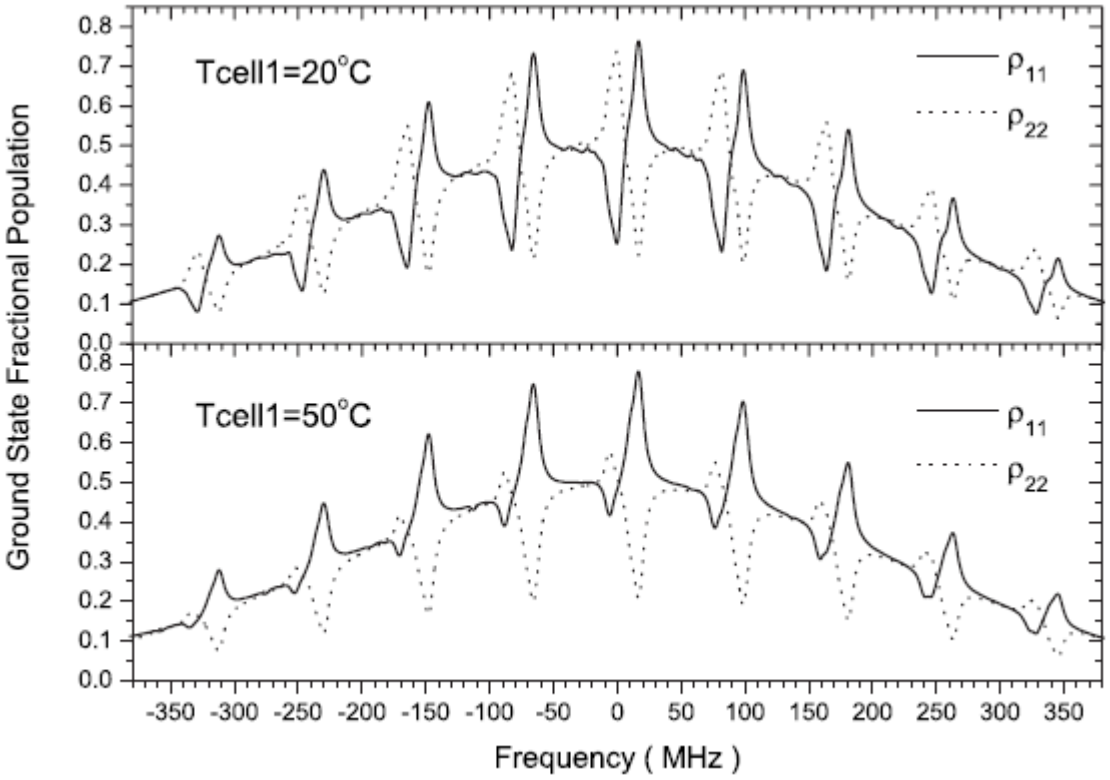

Coherent accumulation effects - experiment

MDFCS: exceptional sensitivity on the pulse shape

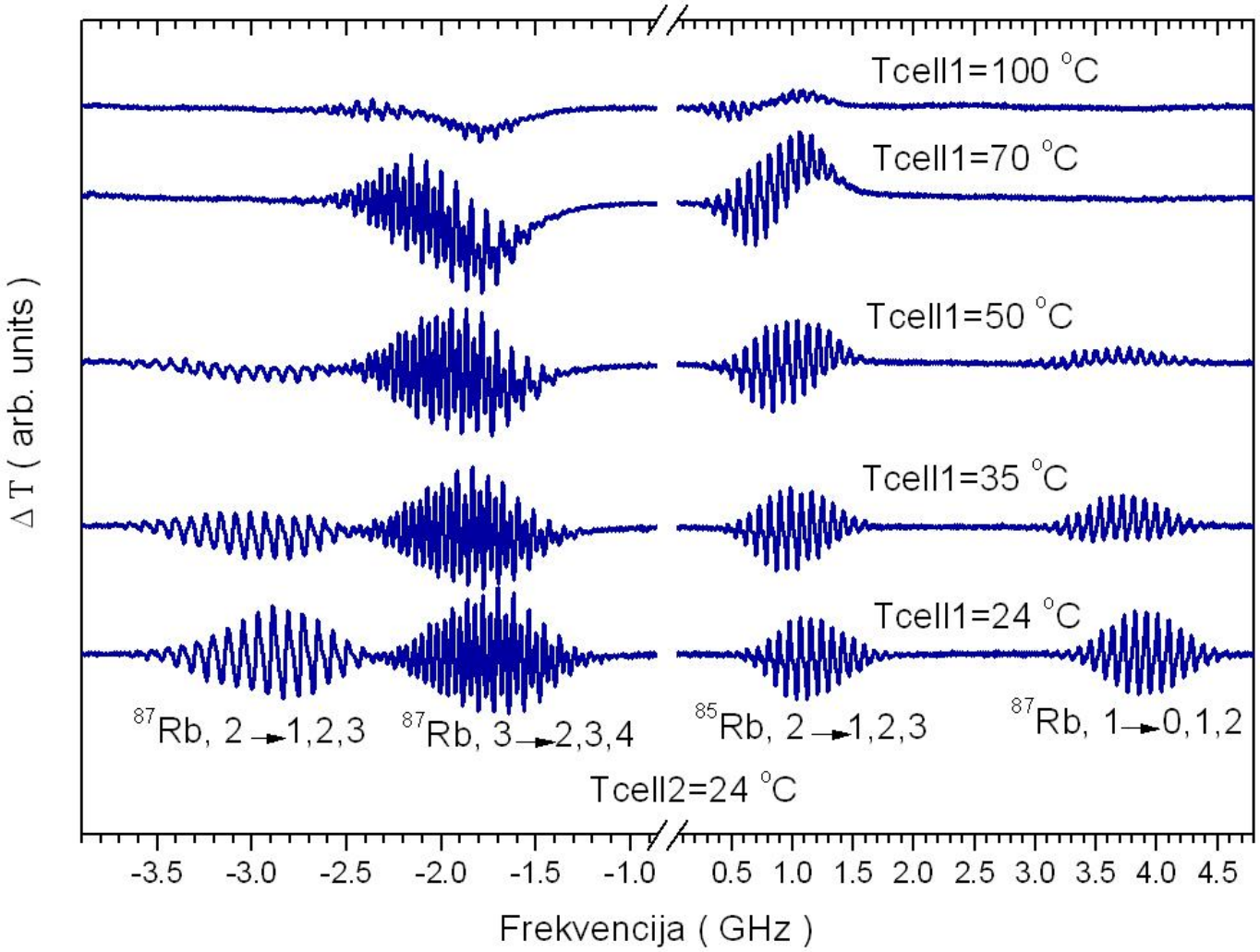

4. Velocity-selective double resonance - experiment

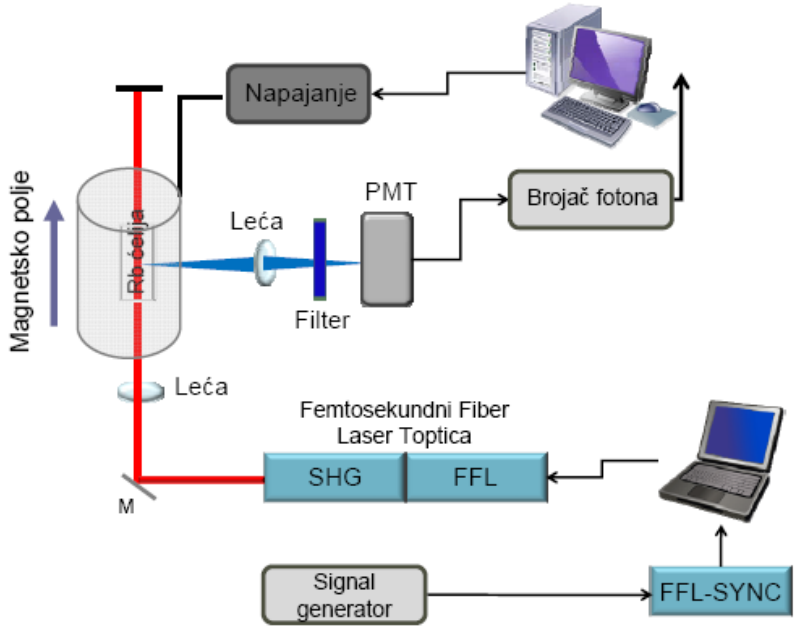

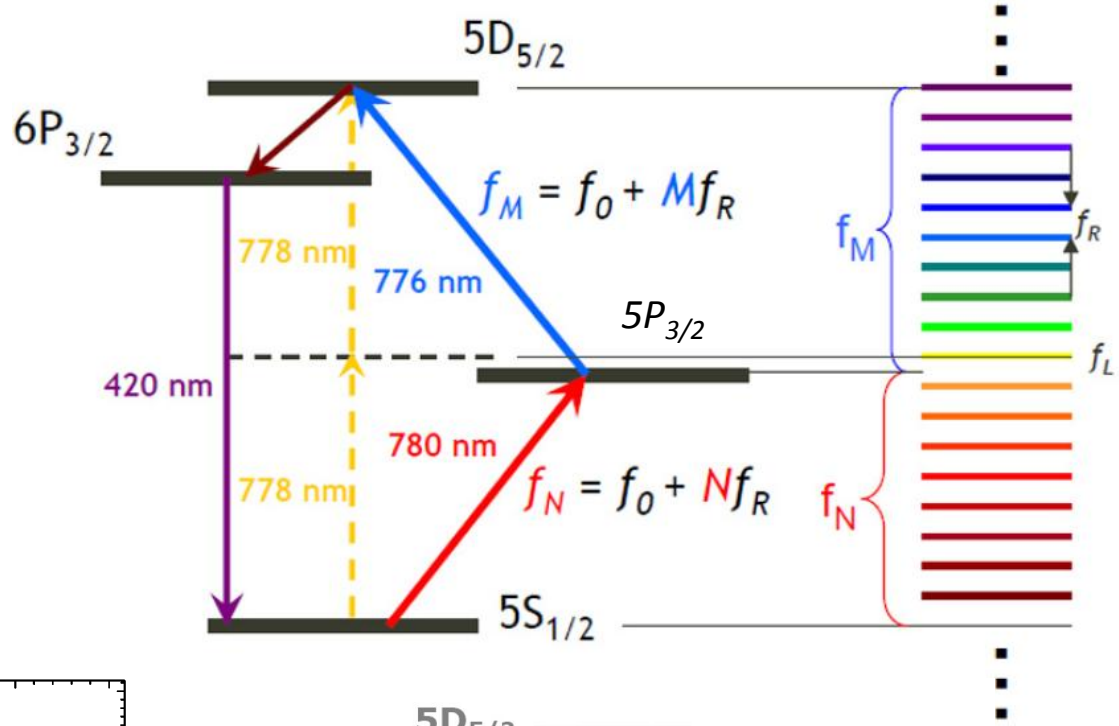

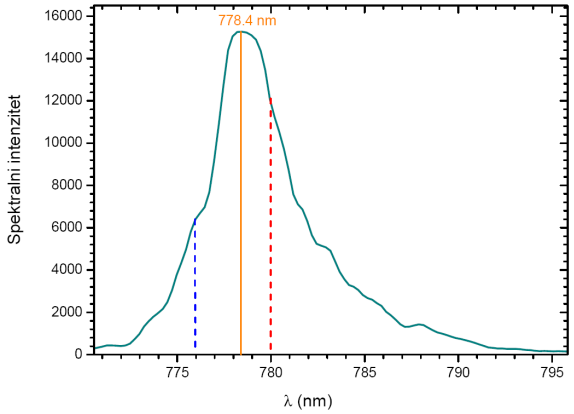

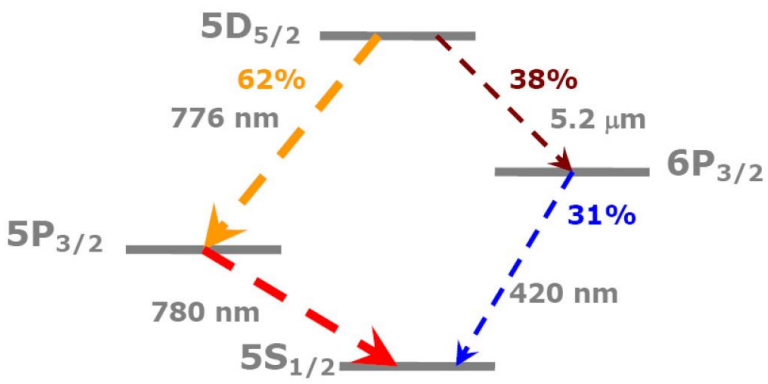

4. Velocity-selective double resonance

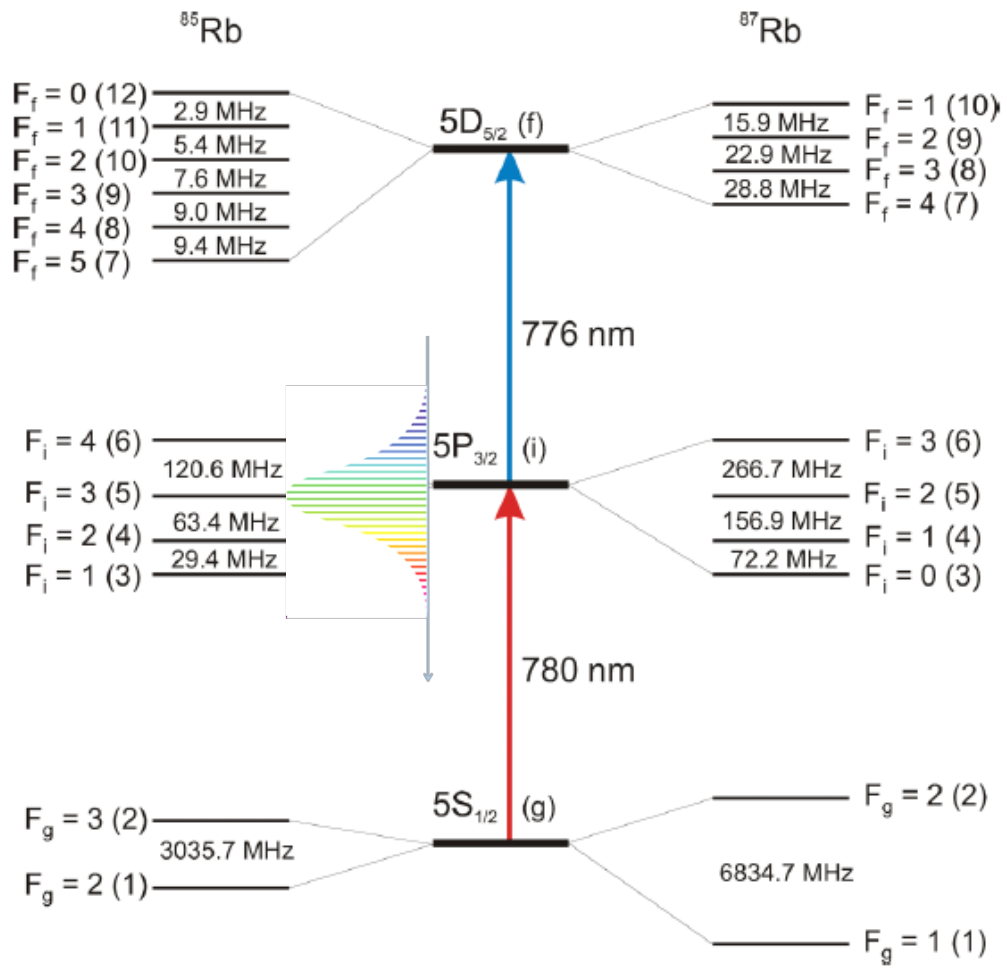

Two-step two-photon excitation induced by FC

Calculated fractional hyperfine-level populations

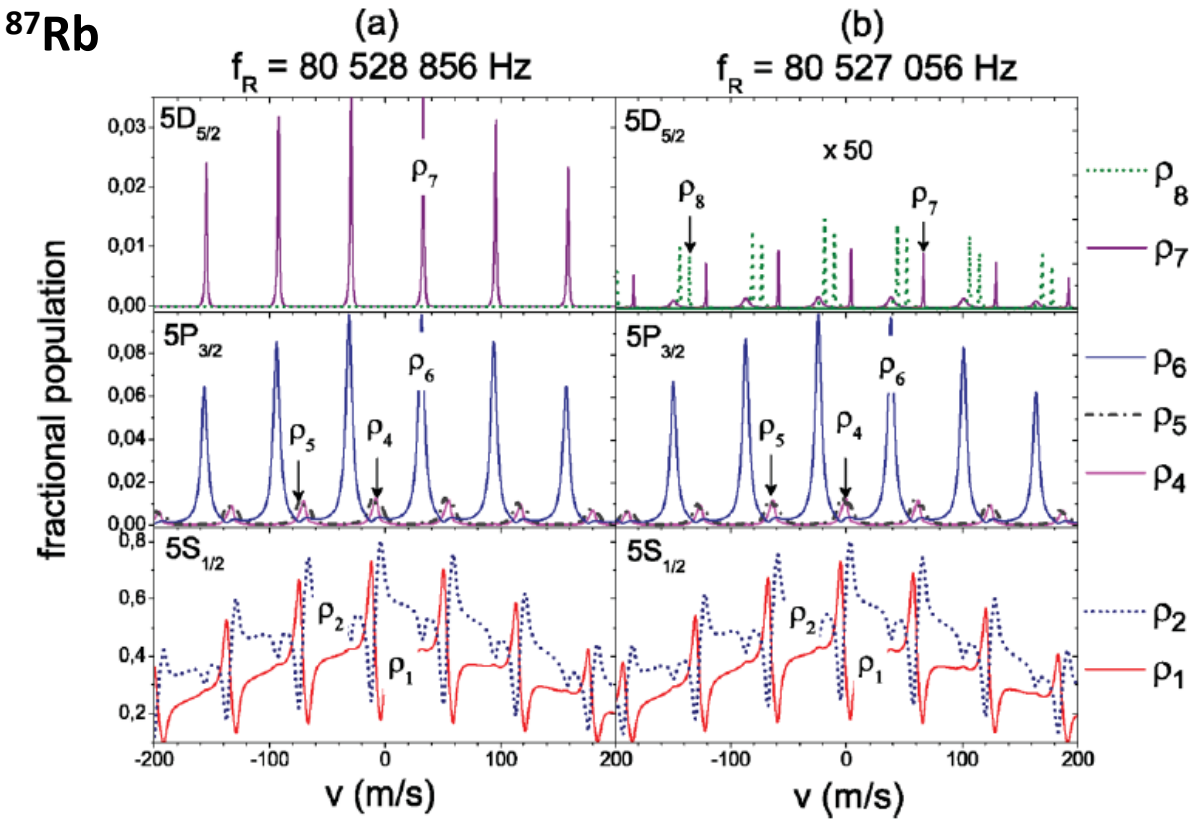

N. Vujičić, T. Ban, G. Kregar, D. Aumiler, and G. Pichler
PRA 87, 013438 (2013).

Two-photon spectra obtained with a frequency scan of f_{rep}

ROOM TEMPERATURE VAPOUR

Calculated $5D_{5/2}$-state population

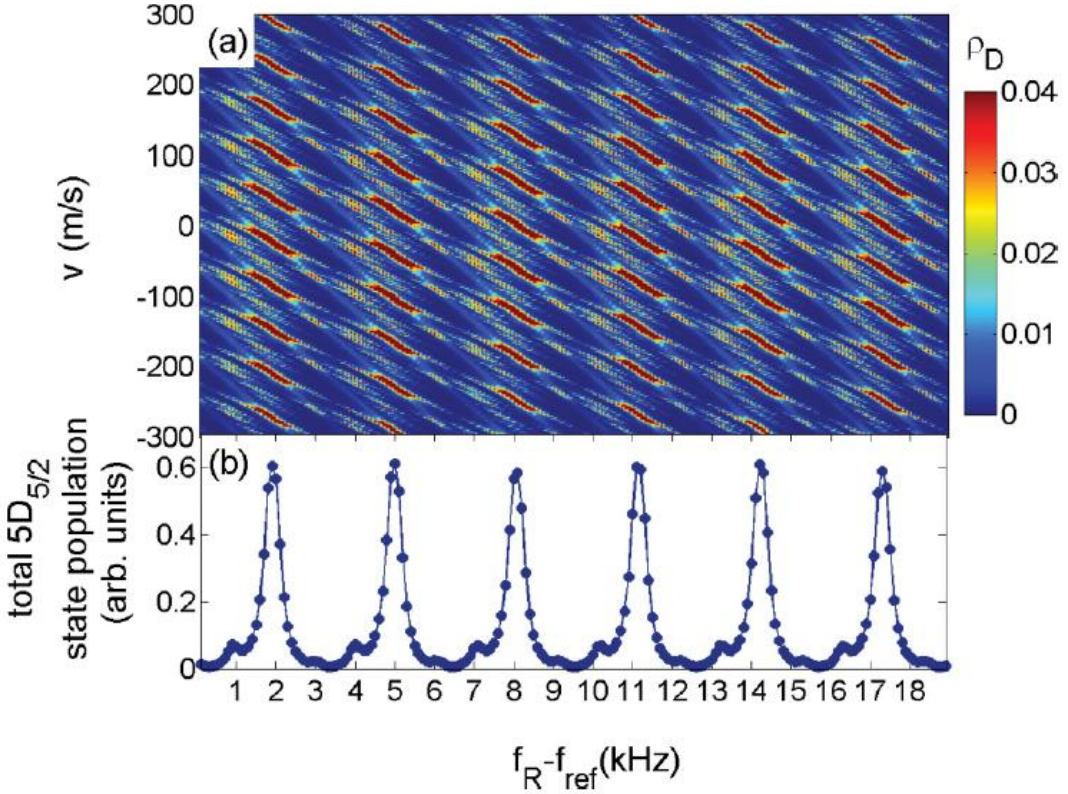

Enhanced $5D_{5/2}$-state population due to velocity-selective double resonance.

Experiment vs theory

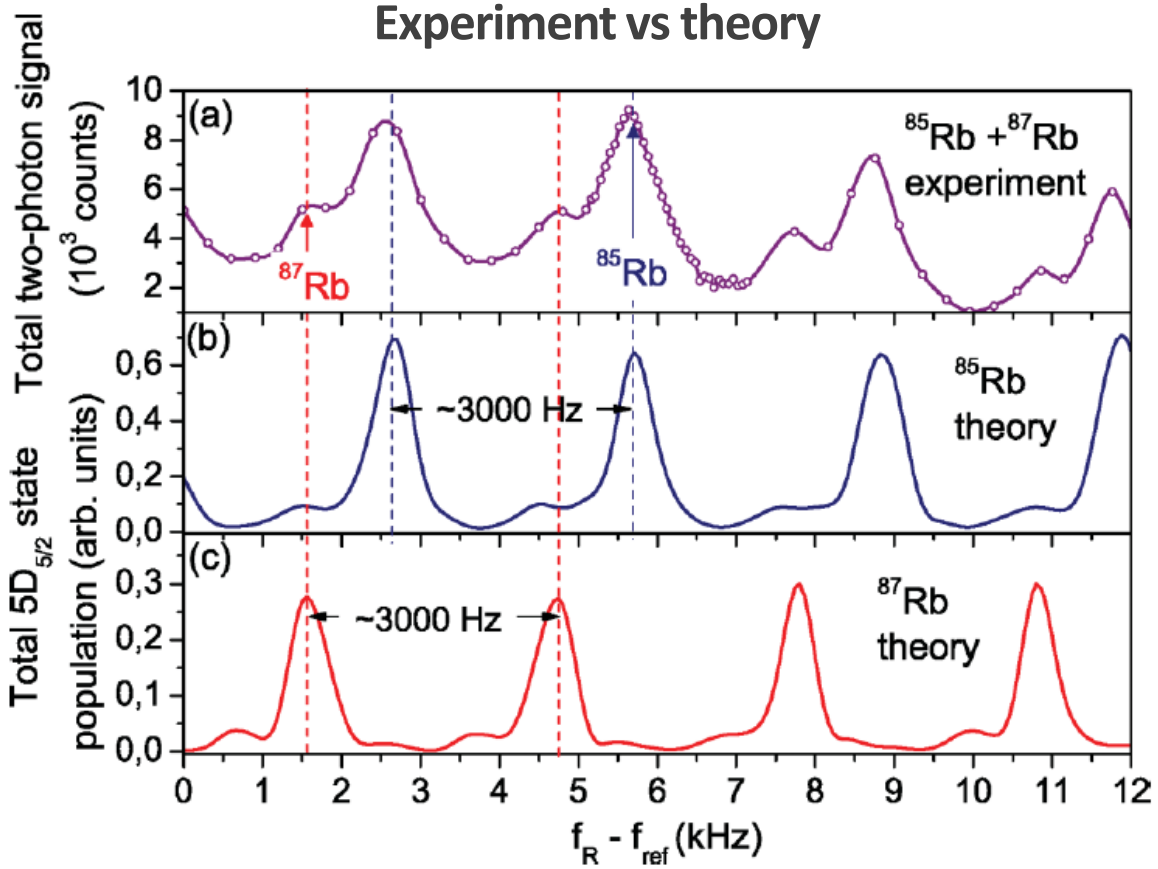

Isotope-selective two-photon excitation

High-resolution two-photon spectra obtained with a frequency scan of f_{rep}

LASER COOLED ATOMS

The coherent effects become more pronounced in atomic systems at low and ultralow temperatures
(no Doppler broadening and no dephasing due to collisions).

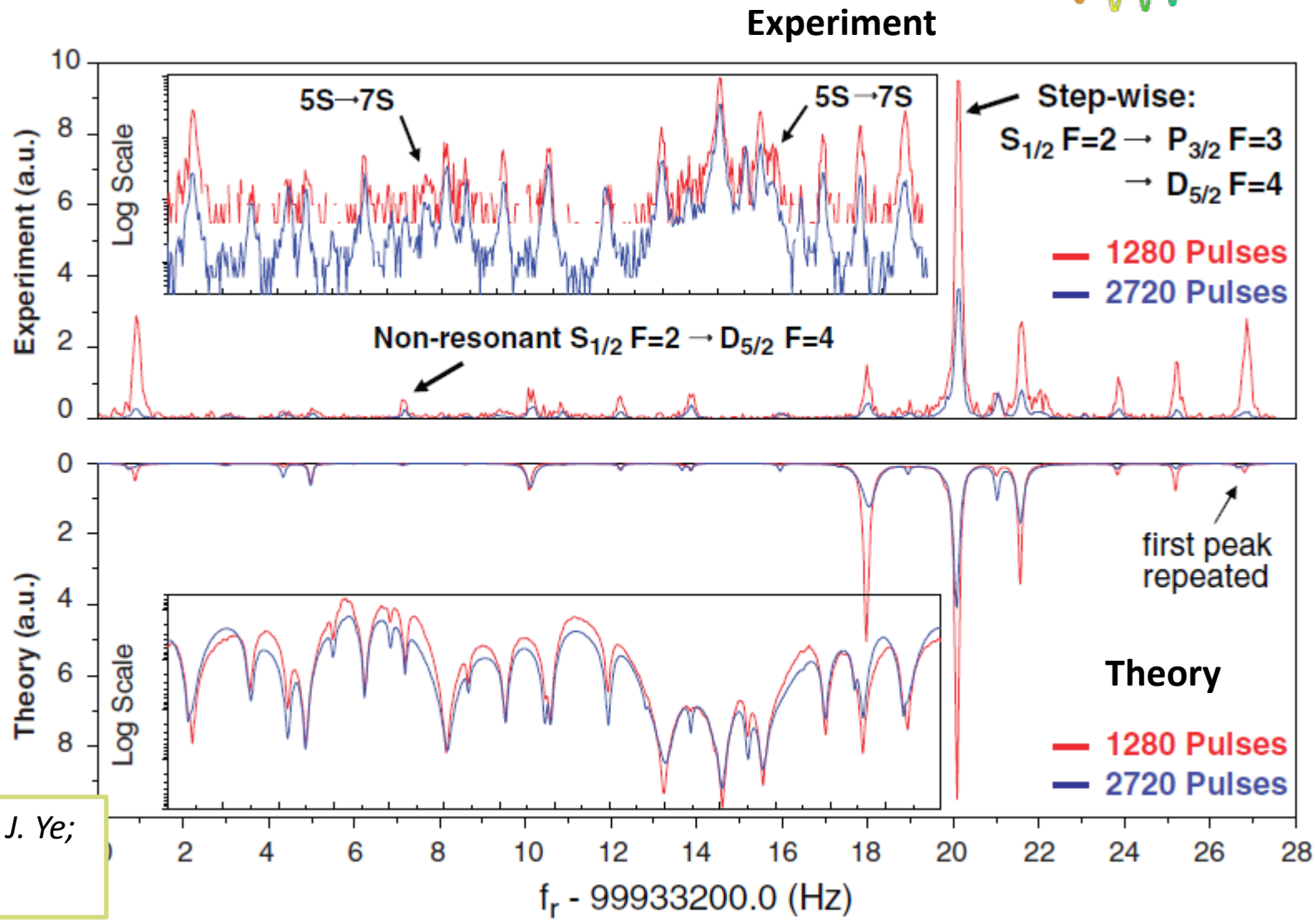

A. Marian, M.C. Stowe, J.R. Lawall, D. Felinto, and J. Ye; Science 306, 2063 (2004).

Two-photon DFCS

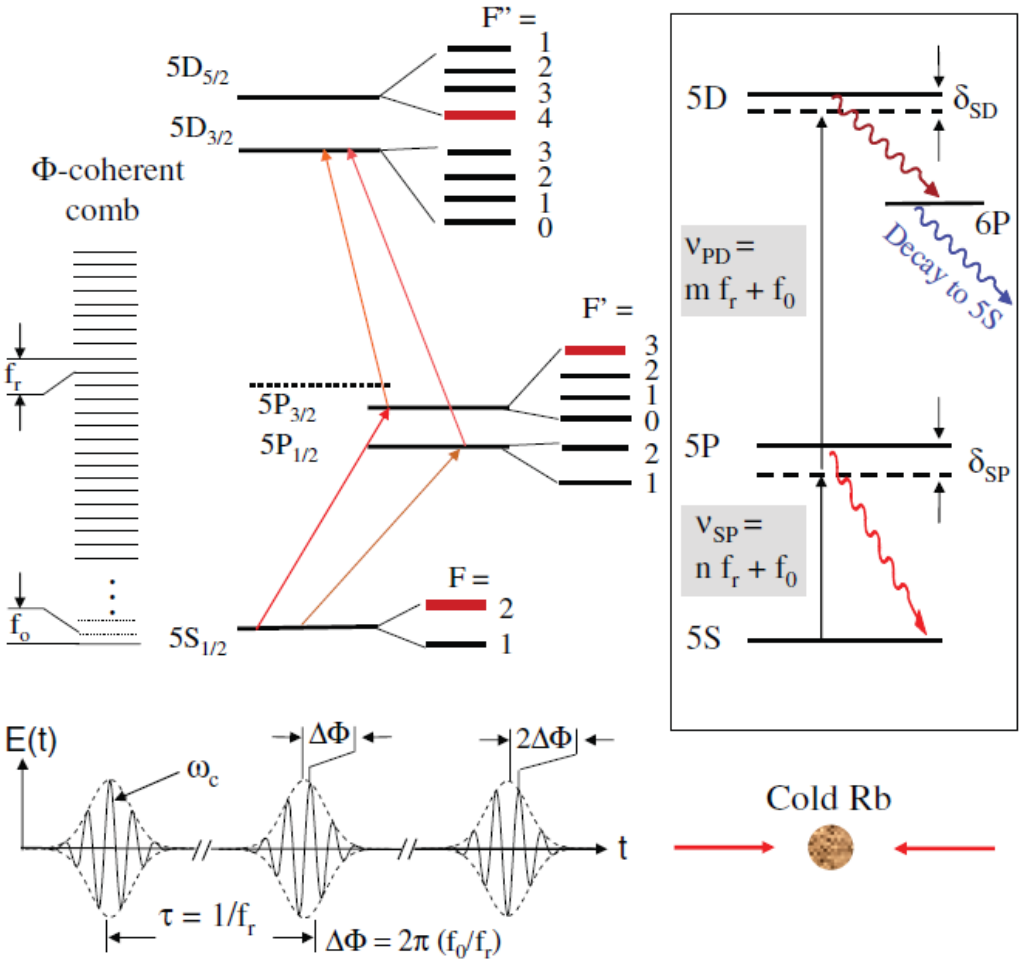

A. Marian, M.C. Stowe, J.R. Lawall, D. Felinto, and J. Ye; Science 306, 2063 (2004).

Calculated 5D population and linewidth

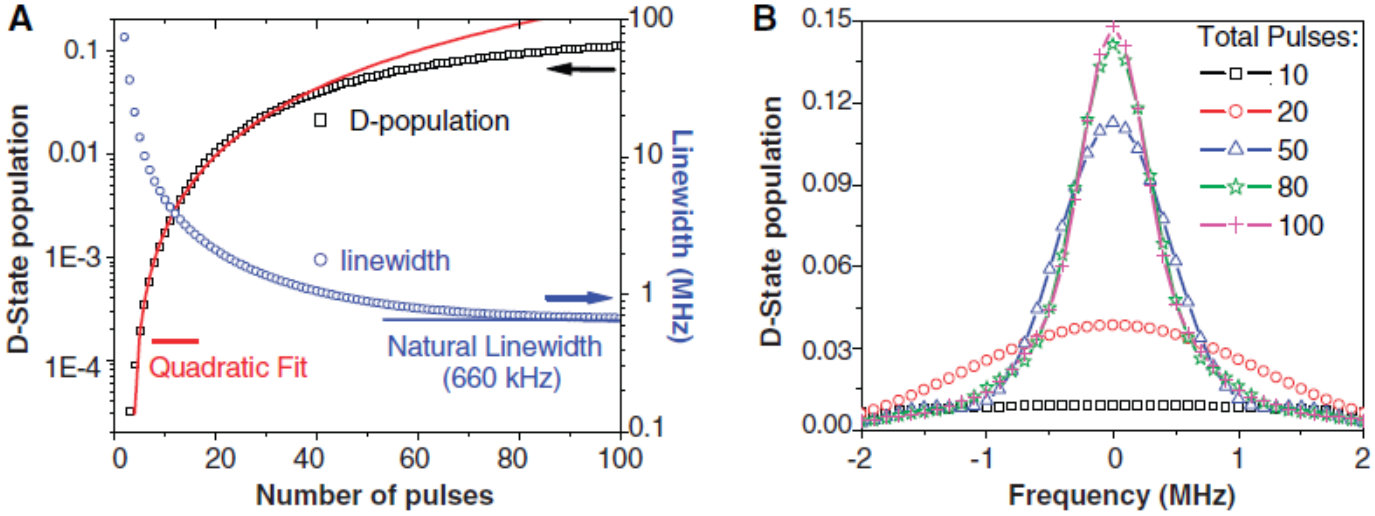

DFCS resolution is limited only by the 5D natural linewidth

DFCS for measurements of absolute optical frequencies

absolute atomic transition frequencies anywhere within the comb bandwidth, for one- and two-photon processes.

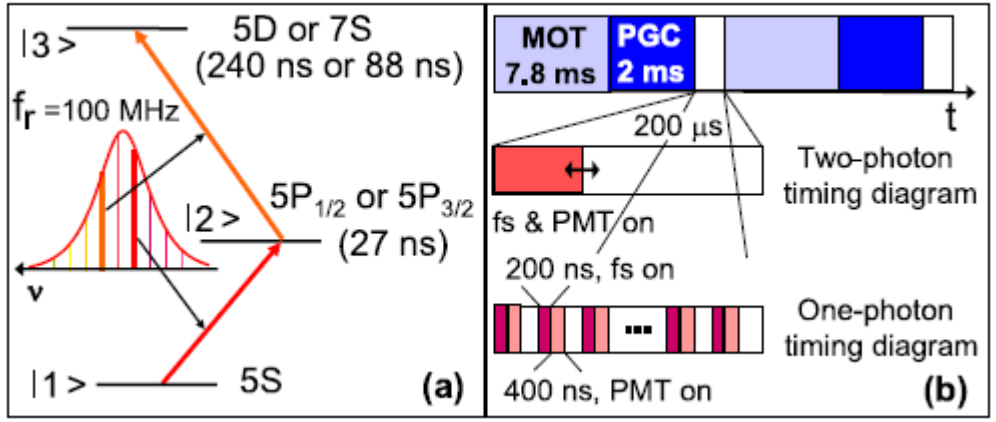

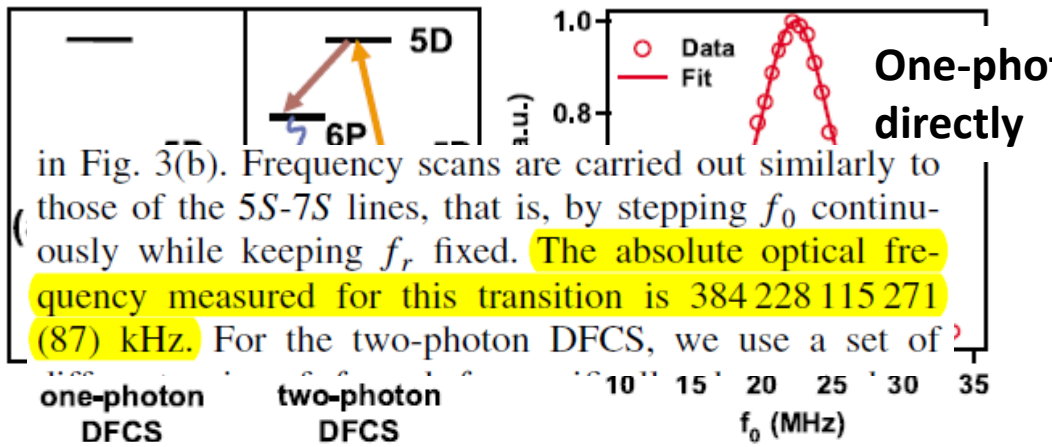

One-photon directly

in Fig. 3(b). Frequency scans are carried out similarly to those of the 5S-7S lines, that is, by stepping f_0 continuously while keeping f_r fixed. The absolute optical frequency measured for this transition is 384 228 115 271 (87) kHz. For the two-photon DFCS, we use a set of

Two-photon

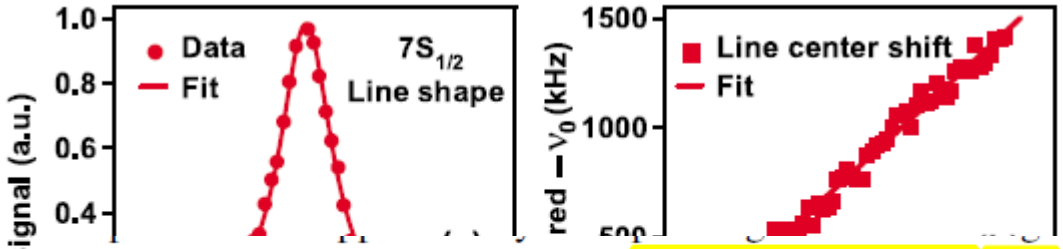

tion time, as shown in Fig. 2(b). We determine for the $5S_{1/2}$ $F=2 \rightarrow 7S_{1/2}$ $F''=2$ and the $5S_{1/2}$ $F=1 \rightarrow 7S_{1/2}$ $F''=1$ two-photon transitions in ^{87}Rb the absolute optical frequencies of 788 794 768 921 (44) and 788 800 964 199 (122) kHz, respectively. The excited state hyperfine inter-

One-photon indirectly

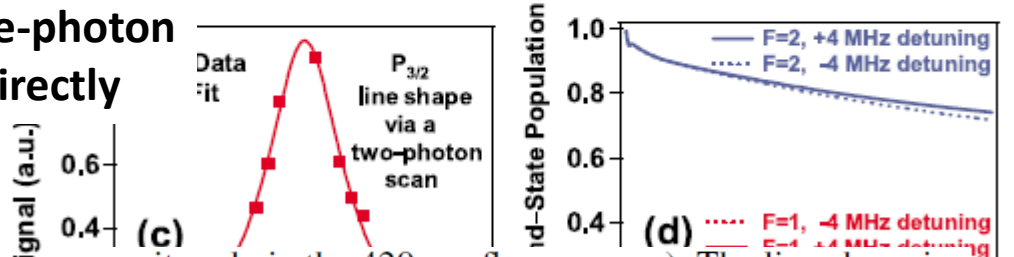

monitored via the 420 nm fluorescence). The line shape in Fig. 3(c) is retrieved by detecting the 420 nm signal as a function of 5P state detuning and the optical frequency measured by this two-photon DFCS is 384 228 115 309 (63) kHz, in agreement with the result obtained from one-photon DFCS within the standard deviation. It is im-

A. Marian, M.C. Stowe, D. Felinto, and J. Ye; PRL 95, 023001 (2005).

Comb + Cold @Institute of Physics, Zagreb

- **Expertise in coherent accumulation effects and laser cooling and trapping**

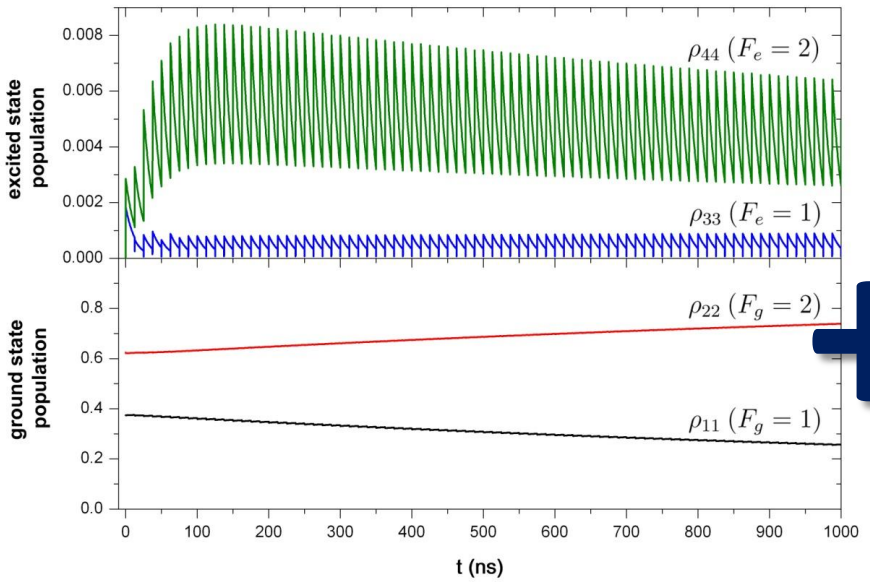

+

WHY ? → In order to explore novel phenomena that arise when the mechanical action on cold atoms is induced by frequency comb (FC) excitation.

Hrvatska zaklada za znanost

Frequency-Comb-induced OptoMechanics (MeCombO)

- FC-induced cooling
- Entanglement and decoherence
- Cavity cooling and self-organization

FC-induced radiative force on 2-level atom _ model

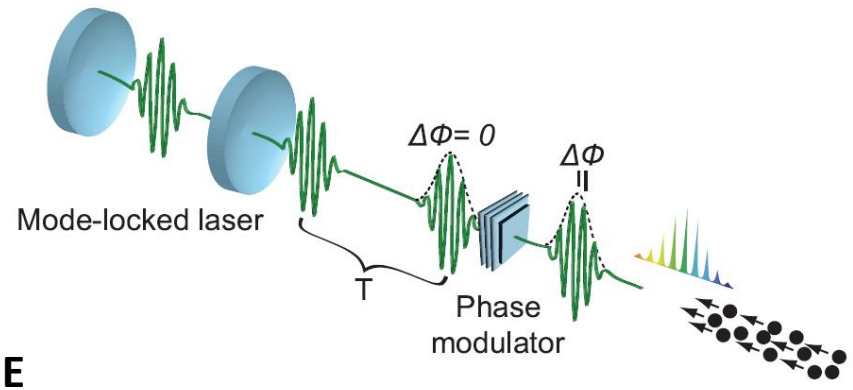

OBE

$$\dot{\rho}_{ee} = -\gamma\rho_{ee} + \frac{i}{2}(\rho_{ge}\Omega_{eg}(z,t) - \rho_{eg}\Omega_{ge}(z,t)),$$

$$\dot{\rho}_{eg} = -\left(\frac{\gamma}{2} - i\delta_{\text{eff}}\right)\rho_{eg} + \frac{i}{2}\Omega_{eg}(z,t)(\rho_{gg} - \rho_{ee}),$$

$$F = \langle \mathcal{F} \rangle = \frac{d}{dt}\langle p \rangle = \frac{i}{\hbar}\langle [H,p] \rangle$$ **Ehrenfest theorem**

$$F = -\left\langle \frac{\partial H}{\partial z} \right\rangle \quad , \left\langle \frac{\partial H}{\partial z} \right\rangle = Tr(\rho \frac{\partial H}{\partial z})$$

$$F_z = -p_r \,\mathrm{Im}[\rho_{eg}\Omega^*_{eg}]$$ Radiative force

$$p_r = \hbar k_c$$ Photon momentum

The laser field is present only during the pulse, so we deal with a **sum over instantaneous forces**.

The change in the atomic momentum due to a single pulse is

$$\frac{-\Delta \mathbf{p}_m}{p_r} = [(\rho^m_{ee})_r - (\rho^m_{ee})_l]\hat{\mathbf{k}}_c \qquad F_{\text{train}} = \Delta p_s / T$$

a laser pulse imparts a fractional momentum kick equal to the difference of populations before and after the pulse

E. Ilinova, M. Ahmad, and A. Derevianko,
PRA 84, 033421 (2011).

internal atomic dynamics + CM motion of the atom

Optical Bloch Equations (OBEs) - QUANTUM

Linear momentum - CLASSICAL

SMOOTH TRANSITION BETWEEN QUANTUM AND CLASSICAL MECHANICS

$$F = \langle \mathcal{F} \rangle = \mathrm{d} \langle p \rangle / \mathrm{d}t$$

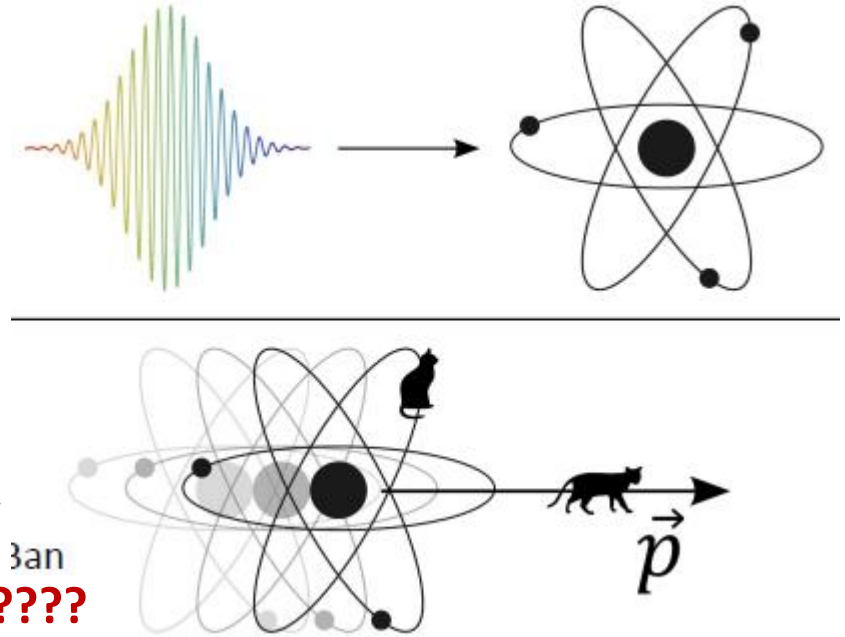

CM motion classically

Momentum transfer (kick) after each pulse

$$\Delta \mathbf{p}_n = \Delta \rho_{n,ee} \hbar \mathbf{k}$$

CM motion quantum mechanically

What is the expetation value for the momentum transfer after each pulse?

For how many pulse kicks should we treat CM motion quantum mechanically, before transferring this information to the velocity (in the classical world)?

Entanglement ?????

How to measure the FC-induced radiative force_ 1

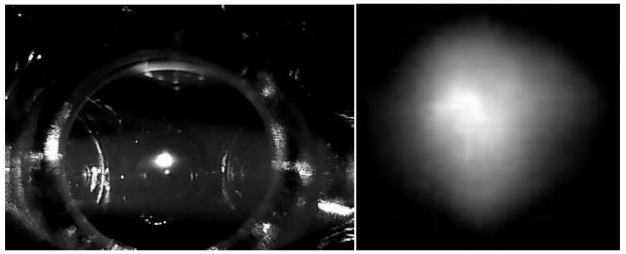

$8x10^8$ ^{87}Rb atoms in a cloud of (0.9±0.1) mm radius @ 50 mK

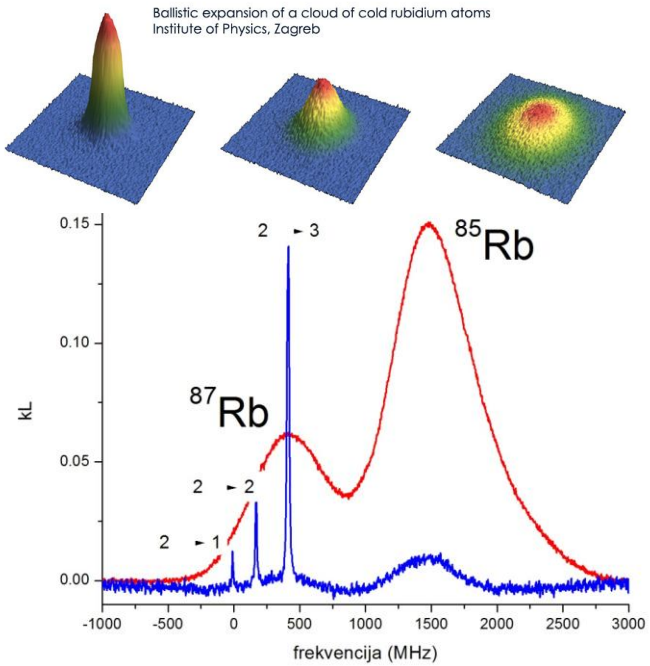

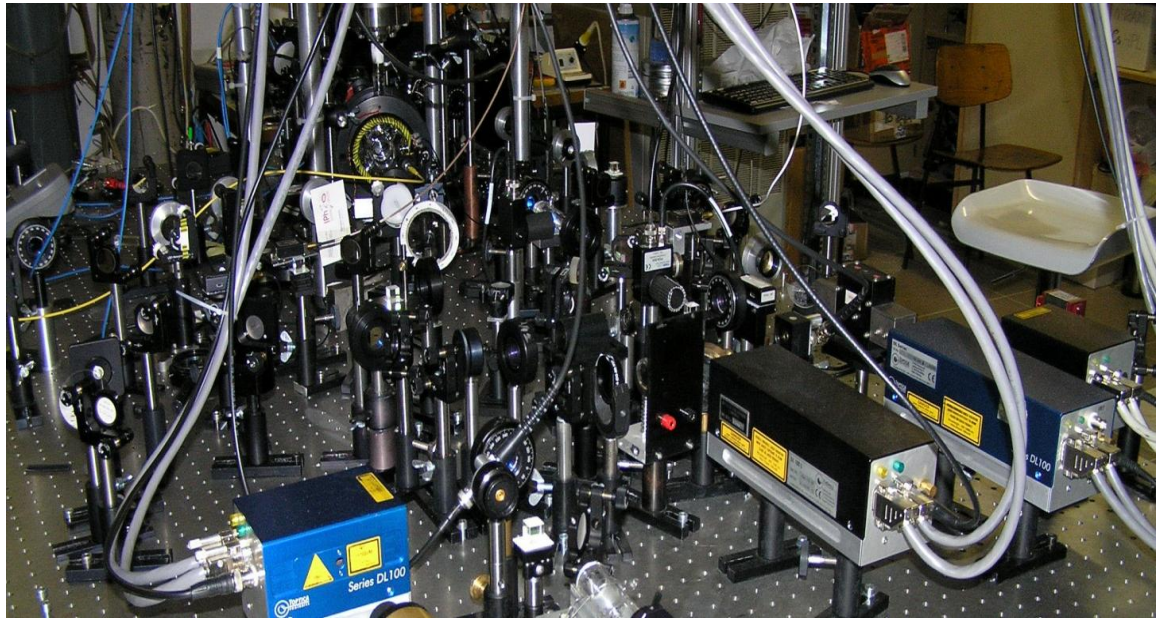

Measure the displacement of the CM of the cold cloud

*G. Kregar, N. Šantić, D. Aumiler, H. Buljan and T. Ban, PRA **89**, 053421 (2014).*

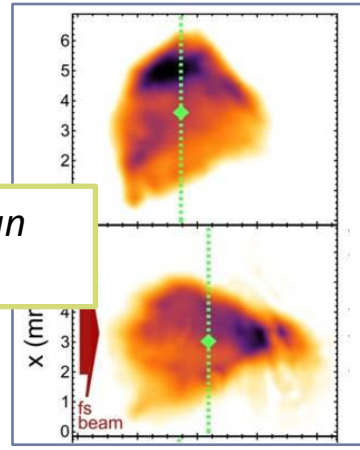

fs beam @ 795 nm

$$F = \kappa \Delta x$$

ΔX = (0.92±0.06) mm

F = (4.9±0.4)x10^{-23} N

How to measure the FC-induced radiative force_ 2

PRL 116, 043002 (2016) PHYSICAL REVIEW LETTERS week ending 29 JANUARY 2016

Doppler Cooling Trapped Ions with a UV Frequency Comb

Josue Davila-Rodriguez,* Akira Ozawa,† Theodor W. Hänsch, and Thomas Udem
Max-Planck-Institute for Quantum Optics Hans-Kopfermann-Straße 1, Garching 81789, Germany
(Received 8 October 2015; published 26 January 2016)

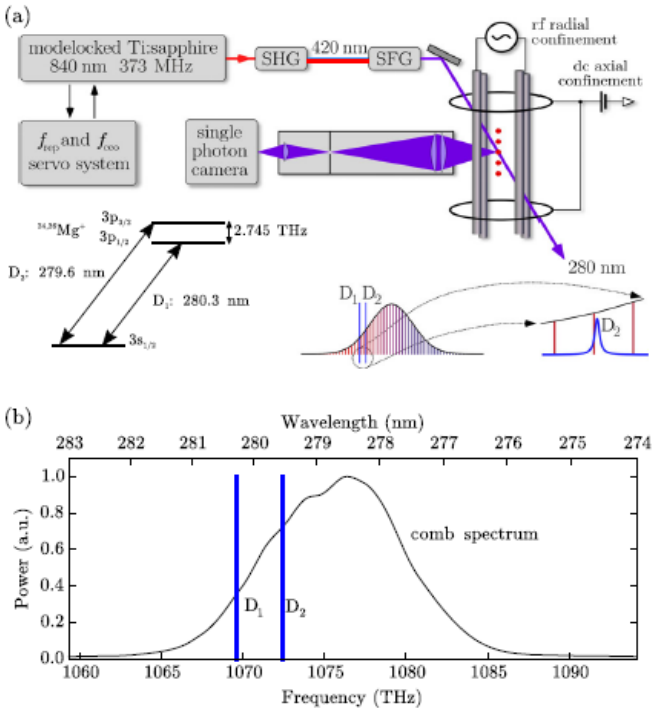

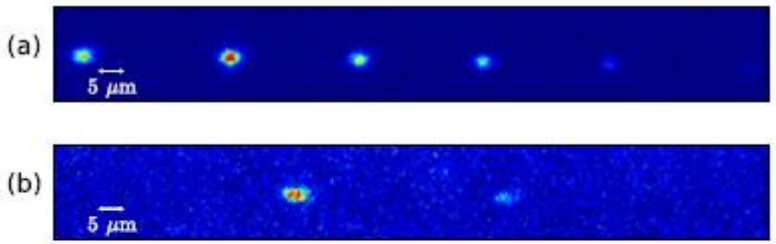

FIG. 2. (a) Image of a pure $^{26}Mg^+$ ion crystal integrated during 300 s exposure while illuminated only with the frequency comb. The ions remain clearly crystallized for the entire time. (b) Two $^{25}Mg^+$ ions cooled by the frequency comb. The scale bars on the images are 5 μm long.

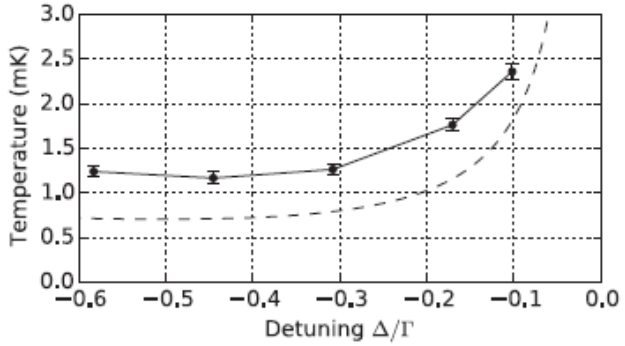

FIG. 4. Spatial thermometry measurement of a single ion while cooled with the frequency comb. The ion's temperature is measured by carefully quantifying its spatial extent in a trap with relaxed axial potential. The error bars indicate the statistical uncertainty from fitting a Gaussian profile to the ion image. The solid line joining the data points is shown as a guide for the eye. The dashed line indicates the Doppler-limited temperature as a function of laser detuning for a saturation parameter of 10^{-2}.

What is the force on atoms induced by two counterpropagating combs?

What happens when we shine two counterpropagating beams of a frequency comb on room-temperature Rb atoms?

*D. Aumiler and T. Ban, PRA **85**, 063412 (2012).*

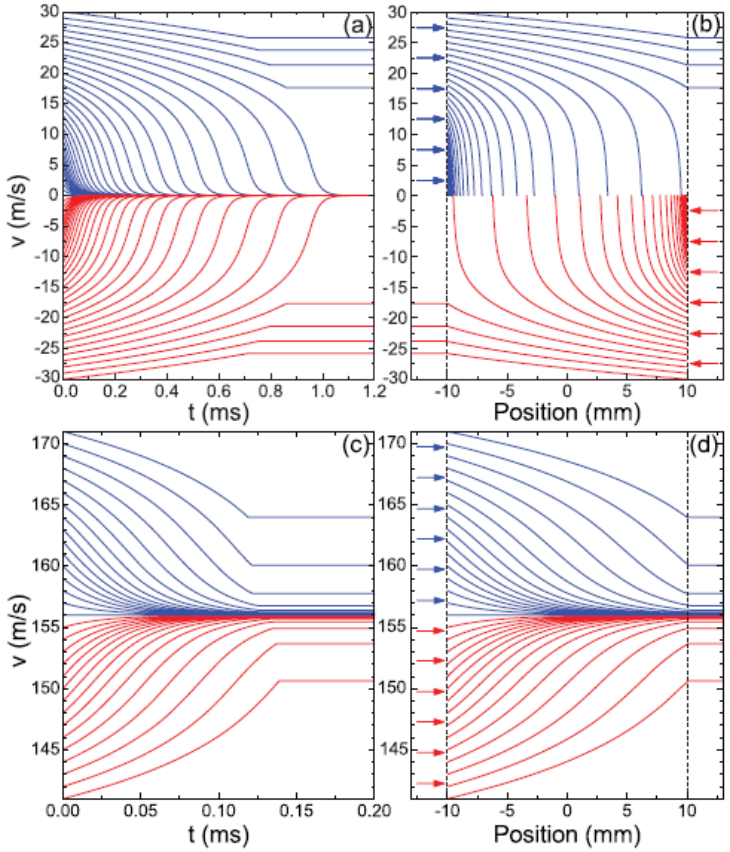

FIG. 5. (Color online) Simulation of the capture process for ^{85}Rb-like atoms that enter the interaction region with different initial velocities. The atoms are assumed to interact with two counterpropagating pulse trains with the same parameters as in Fig. 2,

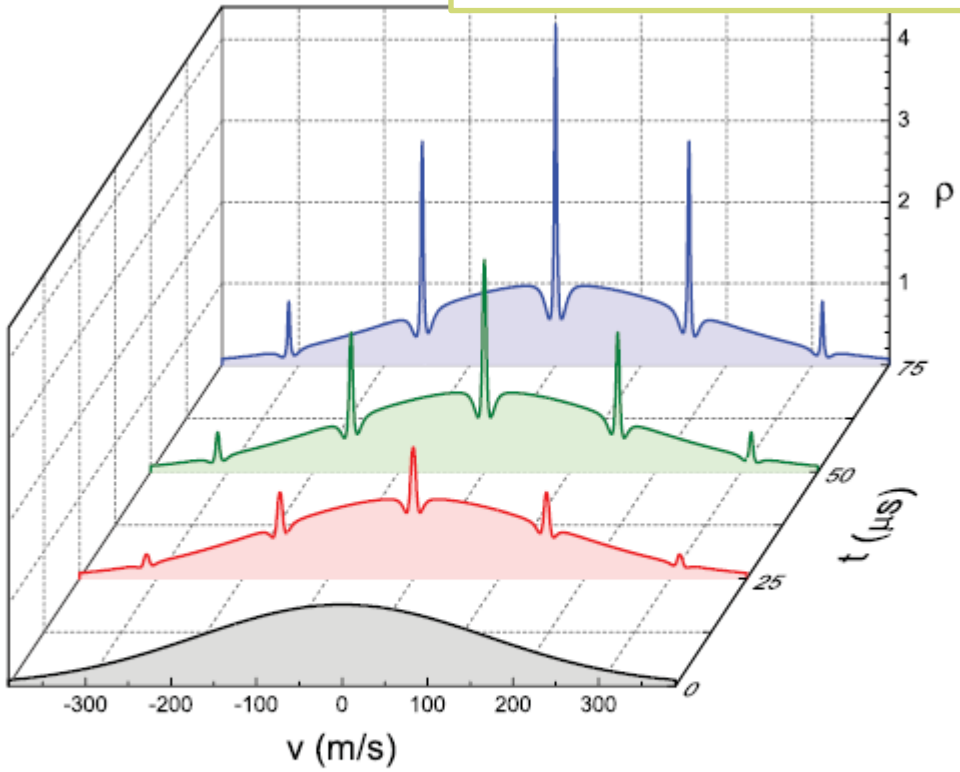

FIG. 2. (Color online) Time evolution of the atomic velocity distribution for room-temperature ^{85}Rb-like atoms excited by two counterpropagating pulse trains. Pulse-train parameters are the same as in Fig. 1 with $\theta = \pi/10$.

The prospect ...

Simultaneous laser cooling of multiple atomic species using an optical frequency comb which holds potential for preparation of coherent ultracold atomic mixtures.

*D. Aumiler and T. Ban, PRA **85**, 063412 (2012).*

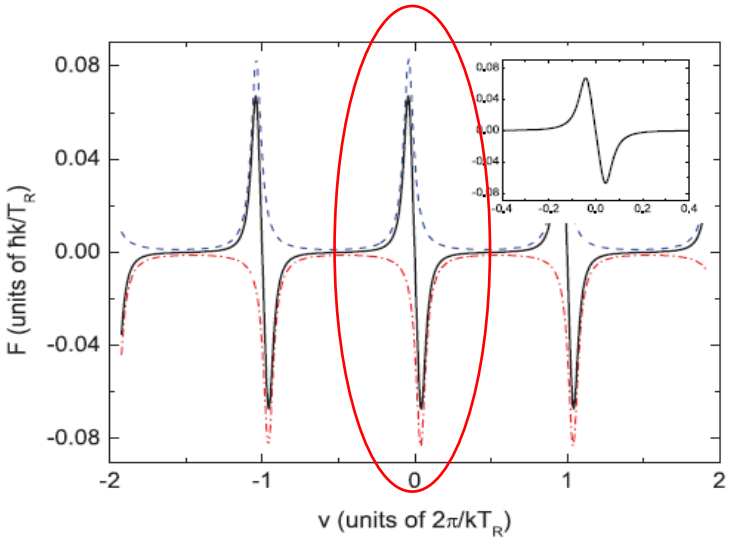

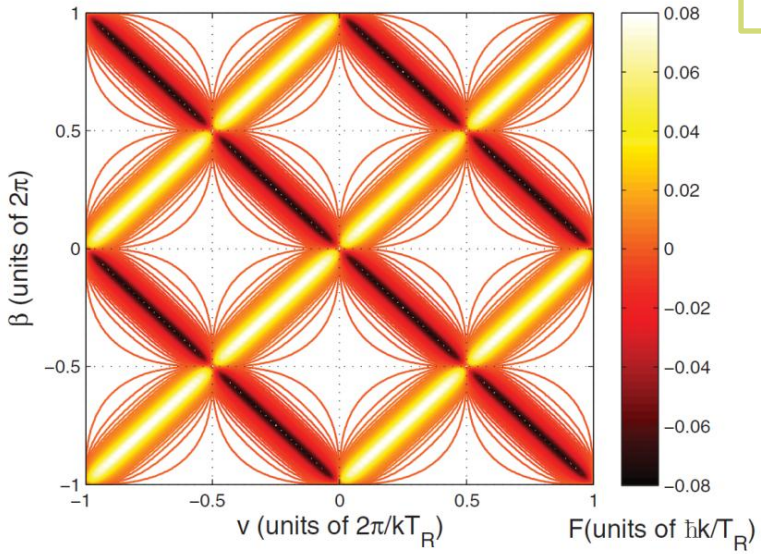

- preparation of coherent ultracold atomic mixtures
- homo- and heteronuclear cold collisions

		Transition	N	$f_N - f$ (units of $\Gamma/2\pi$)
^{40}K	Cooling	$4\,^2S_{1/2}(F=9/2) \rightarrow 4\,^2P_{3/2}(F=11/2)$	280 1803	−0.9
	Repumper	$4\,^2S_{1/2}(F=7/2) \rightarrow 4\,^2P_{3/2}(F=9/2)$	280 1794	−3.3
^{85}Rb	Cooling	$5\,^2S_{1/2}(F=3) \rightarrow 5\,^2P_{3/2}(F=4)$	275 3167	−2.9
	Repumper	$5\,^2S_{1/2}(F=2) \rightarrow 5\,^2P_{3/2}(F=3)$	275 3188	−0.3
^{87}Rb	Cooling	$5\,^2S_{1/2}(F=2) \rightarrow 5\,^2P_{3/2}(F=3)$	275 3159	−1.2
	Repumper	$5\,^2S_{1/2}(F=1) \rightarrow 5\,^2P_{3/2}(F=1)$	275 3205	0.2

Testing the FC-induced radiative force in different beam geometries

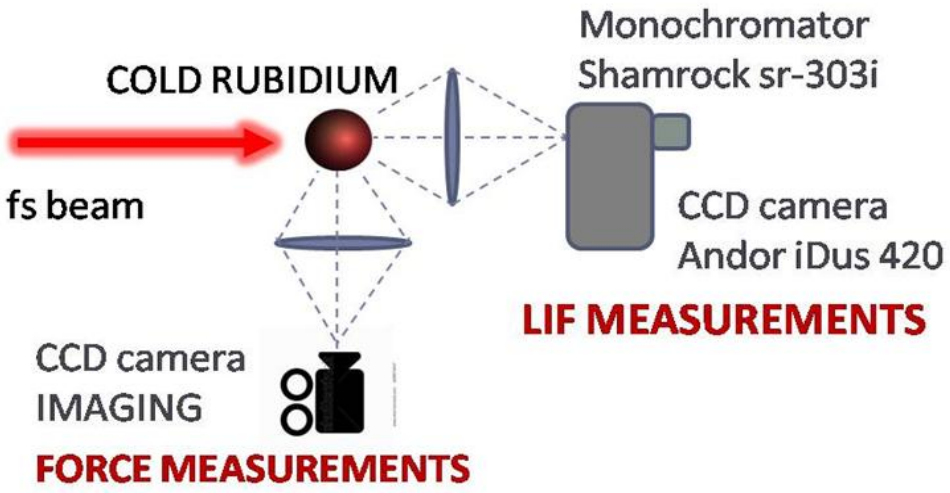

SINGLE BEAM CONFIGURATION

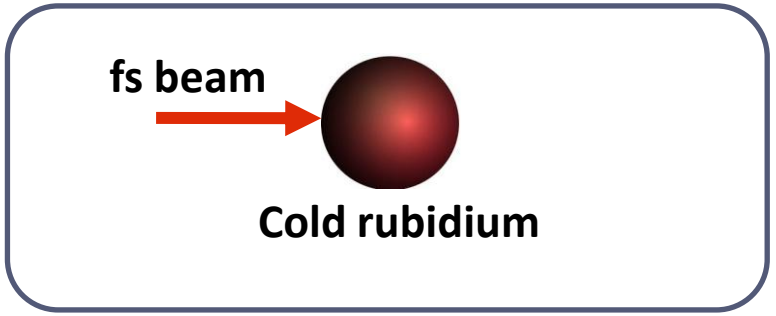

Plan of the experiment

TWO COUNTERPROPAGATING BEAMS CONFIGURATIONS

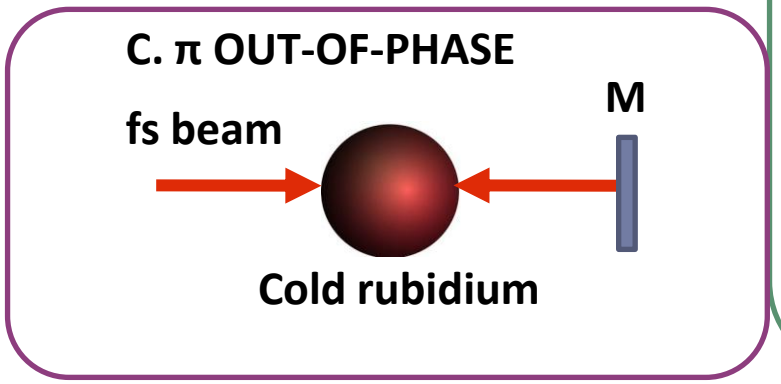

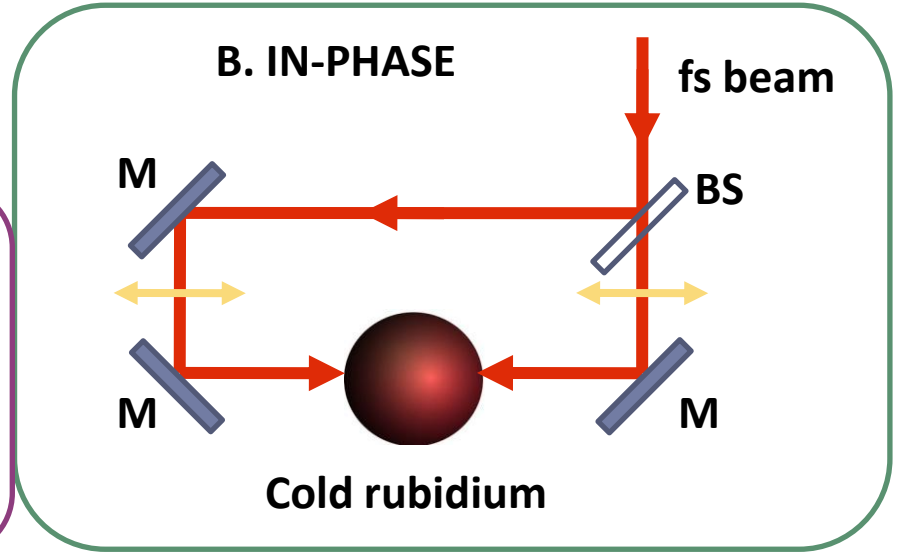

Testing the FC-induced radiative force in different beam geometries

$$\Delta \mathbf{p}_n = \Delta \rho_{n,ee} \hbar \mathbf{k}$$

The FC radiative force:

$$\mathbf{F}_r = \frac{\Delta \mathbf{p}_n + \Delta \mathbf{p}_{n+1}}{\Delta t_{n,n+1}}$$

Force: instantaneous momentum kicks

E.Ilinova *et al.*, PRA **84**, 033421 (2011)

What the theory tells us?

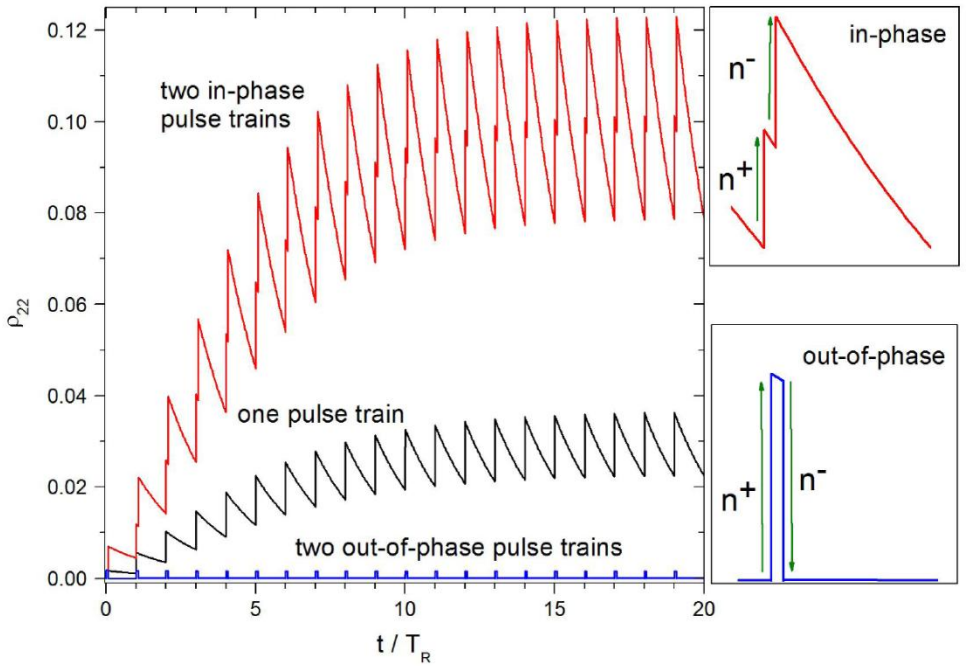

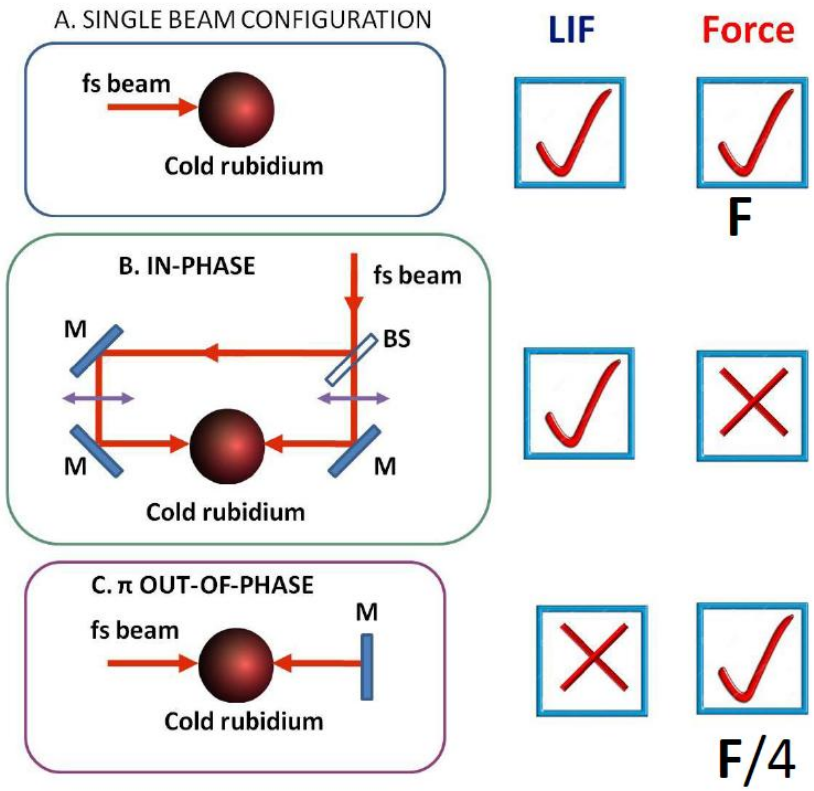

FC-induced radiative force in retro-reflected configuration

1. Frequency stabilization of Er:doped frequency comb
2. Measure the FC force on cold Rb atoms as a function of the system coherence
3. Develop the quantum mechanical (QM) model for the FC force calculation

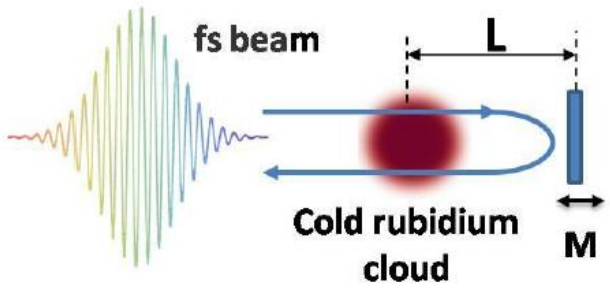

Figure 4

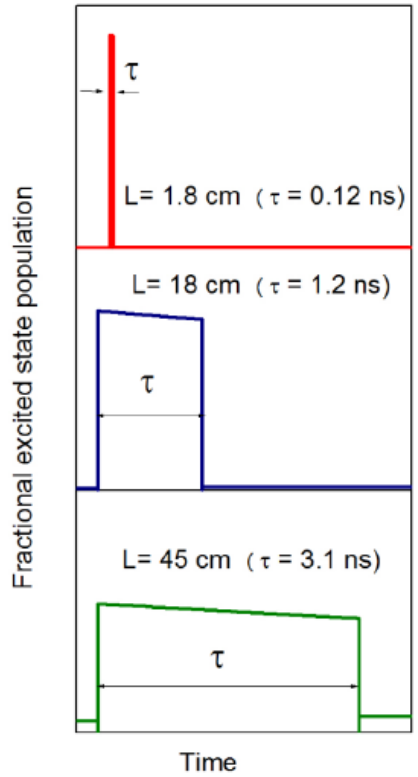

Figure 5